THE UNIVERSITY OF MANITOBA

SOME APPLICATIONS OF PARAMETER ADAPTIVE TECHNIQUES IN POWER SYSTEM CONTROL

by

YOUSSEF LOTFY ABDEL-MAGID

A Thesis

Submitted to the Faculty of Graduate Studies

in Partial Fulfilment of the Requirements for the Degree

of Doctor of Philosophy

DEPARTMENT OF ELECTRICAL ENGINEERING

WINNIPEG, MANITOBA R3T 2N2

February 1976

"SOME APPLICATIONS OF PARAMETER ADAPTIVE TECHNIQUES IN POWER SYSTEM CONTROL"

by

YOUSSEF LOTFY ABDEL-MAGID

A dissertation submitted to the Faculty of Graduate Studies of the University of Manitoba in partial fulfillment of the requirements of the degree of

DOCTOR OF PHILOSOPHY

To my parents .....

For many years of encouragements.

To my wife .....

For the understanding and support that permit a thesis to be done.

ABSTRACT

The purpose of the research described herein was to investigate the possibility of applying parameter adaptive control techniques to the design of power system controllers in order to eliminate some of the compromise normally involved in the design of these controllers. Two different power system problems were considered, and in each case a different adaptive technique was suggested.

The first problem deals with the design of adaptive stabilizers to supplement generator static excitation systems. Eigen-value techniques were used to determine the influence of the generator static excitation on its small perturbation stability for a wide range of loading. A variable structure power stabilizer that will adapt to changes in system dynamics caused by load changes was then synthesized in such a way as to make the overall system optimum with respect to a prescribed criterion. A direct approach to the problem was taken, employing the state-space point of view and an open-loop adaptive technique based on measurements of the system operating conditions. Analog computer tests showed the effectiveness of the variable structure power stabilizer.

The second problem deals with the variation of incremental speed deviation with loading. A closed-loop adaptive controller was introduced to compensate for these variations.

Computer simulations showed that the adaptive loop is capable of maintaining satisfactory performance.

ACKNOWLEDGEMENTS

The author wishes to express his deep gratitude to Professor Glen W. Swift for suggesting the research area as well as for his valuable guidance, supervision and encouragement during the course of this research. The author is also indebted to Professor Swift for reading the thesis and offering many helpful suggestions for its improvement.

The financial support provided by the University of Manitoba, the National Research Council of Canada and Manitoba Hydro is greatly appreciated.

The author also wishes to thank his colleagues and staff members of the Department of Electrical Engineering for their cooperation. Special appreciation is due to Mrs. Shirley Clubine for her untiring effort in expertly typing the thesis.

Above all, the author acknowledges the faithful patience and constant encouragement of his wife, Azza.

TABLE OF CONTENTS

		PAGE
ABSTRACT		i
ACKNOWLEDGEMENT		iii
TABLE OF CONTENTS		iv
LIST OF FIGURES		vi
LIST OF TABLES		x
LIST OF SYMBOLS		xi
chapter one	INTRODUCTION	1
chapter two	EFFECT OF STATIC EXCITATION SYSTEM ON THE SMALL SIGNAL SYNCHRONOUS MACHINE DYNAMICS UNDER WIDELY VARYING LOADING CONDITIONS	6
2.1	Relation of Excitation System to the Stability Problem	7
2.2	Semiconductor Fast Acting Excitation System	9
2.3	Types of Electronic Excitation Systems	10
2.4	Adverse Effects Associated with the use of Fast Acting Electronic Excitation System	12
2.5	Power System Model and Assumptions	15
2.6	Eigen-Value Analysis of the Effect of Static Exciter on Machine Dynamic Stability	22
2.7	Correlation between the Eigen-Value Technique and the Synchronizing/Damping Torques Technique	32
chapter three	VARIABLE STRUCTURE POWER STABILIZER TO SUPPLEMENT STATIC EXCITATION SYSTEM	41
3.1	Review of Stabilizing Signals	41

3.2 Problem Description and Approach 46

3.3 Performance Criterion and Parameter Optimization 49

3.4 Adaptive Stabilizing Signals Design 52

3.5 Analog Computer Tests and Results 58

chapter four A MODEL-REFERENCE ADAPTIVE CONTROLLER TO COMPENSATE FOR VARIATIONS IN THE INCREMENTAL SPEED REGULATION 78

4.1 Problem Description 78

4.2 Model Reference Adaptive Technique 80

4.3 Theory of Adaptation Mechanisms 83

4.3.1 M.I.T. Design Rule 83

4.3.2 Dressler's Design Rule 85

4.3.3 Lyapunov Design Rule 87

4.4 Power System Model 90

4.5 Computer Simulation and Results 93

4.5.1 Adaptive Laws Based on M.I.T. Rule 93

4.5.2 Adaptive Laws Based on Dressler's Method 95

4.5.3 Adaptive Laws Based on Lyapunov's Method 99

chapter five SUMMARY AND CONCLUSION 109

BIBLIOGRAPHY 113

APPENDIX A 118

APPENDIX B 121

LIST OF FIGURES

		PAGE
Fig. 2.1	Rotating A.C. exciter with diode rectifier "Brushless" (After Heeley[2])	11
Fig. 2.2	Static exciter thyristor converter and electronic regulator (After Heeley[2])	13
Fig. 2.3	External impedance system configuration for single machine against infinite bus	16
Fig. 2.4	Block diagram of the single machine infinite bus system including the effects of voltage regulator excitation system (*stabilizing input to be introduced later)	21
Fig. 2.5a	Variation of K_1 with real and reactive loading	25
Fig. 2.5b	Variation of K_2 with real and reactive loading	26
Fig. 2.5c	Variation of K_4 with real and reactive loading	27
Fig. 2.5d	Variation of K_5 with real and reactive loading	28
Fig. 2.5e	Variation of K_6 with real and reactive loading	29
Fig. 2.6	Constant real-power lines and constant reactive-power lines in the complex frequency plane (T_e = 0.05 secs)	31
Fig. 2.7	Boundary constant real-power lines and constant reactive-power lines in the complex frequency plane (T_e = 2.0 secs)	33
Fig. 2.8	Reduction of linearized small perturbation model for the single machine infinite bus system	35
Fig. 2.9	The load-loop showing synchronizing and damping torque	37
Fig. 2.10	Variations of synchronizing torque coefficient with real and reactive loading	38
Fig. 2.11	Variation of damping torque coefficient with real and reactive loading	39

List of Figures cont.

		Page
Fig. 3.1	Block diagram of the open-loop adaptive technique (q_1, q_2, ... q_m represent the adjustable parameters)	48
Fig. 3.2	Linearized small-perturbation block diagram of the single machine infinite bus system with the power stabilizer	53
Fig. 3.3	Computational flow graph for optimization procedure	57
Fig. 3.4	Speed deviation for the fixed structure stabilizer design point: P=1.0, Q = -0.3 following a step disturbance in mechanical torque	62
Fig. 3.5	Speed deviation following a small step disturbance in mechanical torque. Loading : P = 1.0 , Q = 1.0	63
Fig. 3.6	Speed deviation following a small step disturbance in mechanical torque. Loading: P = 0.1 , Q = -0.3	64
Fig. 3.7	Speed deviation following a small step disturbance in mechanical torque. Loading: P = 0.1, Q = 1.0	65
Fig. 3.8	Speed deviation following a small step disturbance in mechanical torque. Loading: P = 0.1 , Q = 0	66
Fig. 3.9	Speed deviation following a small step disturbance in mechanical torque. Loading: P = 0.1 , Q = -0.2	67
Fig. 3.10	Speed deviation following a small step disturbance in mechanical torque. Loading: P = 0.5 , Q = 0	68
Fig. 3.11	Speed deviation following a small step disturbance in mechanical torque. Loading: P = 0.3 , Q = -0.1	69

List of Figures cont.

		Page
Fig. 3.12	Speed deviation following a small step disturbance in mechanical torque Loading: P = 1.0 , Q = 0.6	70
Fig. 3.13	Speed deviation following a small step disturbance in mechanical torque Loading: P = 0.4 , Q = -0.2	71
Fig. 3.14	Speed deviation following a small step disturbance in mechanical torque Loading: P = 0.5 , Q = 0.5	72
Fig. 3.15	Speed deviation following a small step disturbance in mechanical torque Loading: P = 0.7 , Q = 0.	73
Fig. 3.16	Speed deviation following a small step disturbance in mechanical torque Loading: P = 1.0 , Q = 0.	74
Fig. 3.17	Speed deviation following a small step disturbance in mechanical torque Loading: P = 0.3 , Q = -0.3	75
Fig. 3.18	Speed deviation following a small step disturbance in mechanical torque Loading: P = 0.7 , Q = -0.3	76
Fig. 3.19	Speed deviation following a small step disturbance in mechanical torque Loading: P = 0.5 , Q = -0.3	77
Fig. 4.1	Typical speed-power output curves for different speed changer settings	79
Fig. 4.2	Block diagram representation of a single isolated area with transfer functions for steam turbine and governor.	91
Fig. 4.3	Block diagram representation of the adaptation mechanism based on the M.I.T. design	94
Fig. 4.4a	Output deviations following a step-change in load for a) the model b) the system with no adaptation 3) the system with adaptation. (M.I.T. design; μ = 0.162)	96

List of Figures cont.

		Page
Fig. 4.4b	Adaptive error with and without adaptation (M.I.T. design ; μ = 0.162)	97
Fig. 4.4c	Adaptive parameter variation (M.I.T. design ; μ = 0.162)	98
Fig. 4.5	Block diagram representation of the adaptation mechanisms based on Dressler method	100
Fig. 4.6a	Output deviations following a step change in load for a) the model b) the unadapted system c) the adapted system. (Dressler design ; μ = 0.39)	101
Fig. 4.6b	Adaptive error with and without adaptation (Dressler design ; μ = 0.39)	102
Fig. 4.6c	Adaptive parameter variation (Dressler method ; μ = 0.69)	103
Fig. 4.7	Block diagram representation showing the adaptation mechanism based on Lyapunov design	105
Fig. 4.8a	Output deviations following a step change in load for a) the model b) the unadapted system c) the adapted system (Lyapunov design ; μ = 4.03)	106
Fig. 4.8b	Adaptive error with and without adaptation (Lyapunov design : μ = 4.03)	107
Fig. 4.8c	Adaptive parameter variation (Lyapunov design ; μ = 0.69)	108
Fig. B.1	Nelder and Mead (Nelder algorithm) logic diagram	125

LIST OF TABLES

		PAGE
Table I	Variation of stabilizer gain K with real and reactive loading	59
Table II	Variation of stabilizer time constant T with real and reactive loading	60

LIST OF MOST-USED SYMBOLS

A, A_s	System matrices
A_m	Model system matrix
B_m	Model input matrix
C_m	Model output
C_s	System output
D	Damping coefficient
E	Infinite bus voltage (p.u.)
e	Adaptive error
E_{fd}	Generator field voltage (p.u.)
E_q	Internal voltage back of x_q (p.u.)
E'_q	Internal voltage on q-axis proportional to field flux linkage (p.u.)
F	Frequency (p.u.)
H	Inertia constant
i_d, i_q	Armature current, direct and quadrature axis components (p.u.)
j	Performance index
K	Stabilizer gain
$K_1 \ldots K_2$	Heffron-Phillips constants
K_e	Exciter gain
M	Inertia coefficient, $M = 2H$
P	Electrical power output from machine (p.u.)
P_c	Speed changer position
P_d	Operating load of the area
P_G	Power generated

P_m	Mechanical power input to machine (p.u.)
Q	Reactive power output from machine (p.u.)
R	Positive definite symmetrical matrix
r_e	Transmission line resistance (p.u.)
R_s	System incremental speed regulation
T	Stabilizer time constant
T_e	Exciter time constant
$T_{e\ell}$	Electrical torque output from machine (p.u.)
T_m	Mechanical torque input to machine (p.u.)
T'_{do}	Open circuit generator field time constant
T'_{dz}	Effective field time constant under load
T_G	Governor time constant
T_T	Turbine time constant
U	Disturbance vector
V	Lyapunov function
v_d, v_q	Armature voltage, direct and quadrature axis components (p.u.)
v_t	Machine terminal voltage (p.u.)
W	Positive-semi-definite real symmetrical matrix
X	State vector
$\dot{X}$	Time derivative of X
x_e	Transmission line reactance (p.u.)
x_d	Direct axis reactance (p.u.)
x'_d	Direct axis transient reactance (p.u.)
x_q	Quadrature axis reactance (p.u.)
Y	Model state vector

α	Adaptive parameter
Γ	Disturbance matrix
δ	Angle between q-axis and infinite bus
ΔT_d	Damping torque coefficient (p.u.)
ΔT_s	Synchronizing torque coefficient (p.u.)
μ	Adaptive gain
ω_o	Radian frequency
ω_{osc}	System oscillation frequency
$'$	Superscript denoting transpose
p	$\frac{d}{dt}$
$p\delta$	Speed deviation from synchronous (p.u.)

chapter one

INTRODUCTION

An electric power system consists basically of a set of generating units or sources with their associated prime moving, controlling and protective equipment, a set of energy absorbing elements or loads and the complex network of transmission lines, transformers, switches necessary to interconnect the energy sources and sinks satisfactorily. The prime function of the control system in a power network is to automatically maintain a balance between the real and reactive power supplies and demands in such a way as to maintain optimum system performance.

One of the problems associated with the control of power systems is the off-line analysis, design and optimization of settings of regulators and controllers. Due to the characteristics of the power system, which can be considered a high order interacting multivariable process, basically non-linear with time varying coefficients, it is not possible to specify an optimum set of controller parameters. Up to a few years ago, controllers were designed under the more or less explicit assumption of constant environmental conditions. In marked contrast to this assumption, power systems are characterized by the severe requirement that the system has to operate in a more or less rapidly changing environment, exerting an influence not only on the process to be controlled,

but in some instances also on the controller itself. Under such circumstances, the concept of adaptation seems to be an effective tool to eliminate some of the compromises normally required in controller design and system analysis of power systems.

In recent years, a great deal of effort has been devoted to the study of adaptive control systems. The interest in adaptive control systems has been largely motivated by a sizable class of problems for which conventional techniques for synthesizing the controller have proved inadequate. Specifically, a controller having fixed parameters may not be capable of achieving the desired system performance with a given plant. Such a situation may occur when the parameters that describe the plant vary over a wide range of values during the operation of the system (i.e., when the dynamic characteristics of the plant change markedly). To make the problem more complex, the entire system may be directly affected by an environment that varies drastically over the range of operation.

Essentially, there have been two distinct approaches to the adaptive control problem; each in turn, has given rise to a multiplicity of techniques for the implementation of the adaptation procedure. In both approaches, it is assumed that a performance criterion can be defined as a measure of the quality of control. One approach, termed "open-loop" with respect to the system performance, does not directly employ

the performance criterion in determining the adjustments of the adaptive controller parameters. The first step, which is generally referred to as the identification problem, is to obtain a description of the plant (e.g., pole-zero configuration, or differential equation). Based on the description of the plant, the adaptive controller is synthesized in such a way as to make the overall system optimum with respect to a prescribed criterion. That is, the adaptive parameters are set at those values according to some computational algorithm, that provide the optimum system performance. In this scheme, the adaptation is based on measurements of the operating environment that are directly related to the values of the plant parameters.

The second approach, on the other hand,is "closed-loop" with respect to the system performance - that is the performance criterion is periodically or continuously monitored and, using this information, the adaptive controller parameters are adjusted to extremize the performance measure. Among the techniques employing the philosophy of performance feed-back, the Model-Referenced adaptive control technique is the most popular. In such a scheme, the desirable dynamic characteristics of the system are specified in a model and the controllable parameters of the plant are adjusted continuously so that its response will duplicate that of the model as closely as possible. The identification of the plant dynamic performance is not necessary and hence a fast adaptation can be achieved.

It is the purpose of this thesis to investigate the application of the adaptive control concept, open-loop and closed-loop to some problems in the power system area. Two problems are considered. The first problem deals with the design of adaptive compensators to supplement static excitation systems. The second problem deals with the deviation of incremental speed regulation with load changes. In Chapter 2, the influence of a generator static excitation system upon the small-perturbation stability of a single machine-infinite system - under widely varying loading conditions - is closely scrutinized in a new way: The dominant eigenvalues of the system are plotted in the complex s-domain for different loading conditions and power factors. Constant real power and constant reactive power contours are shown. The tendency of an unsupplemented static exciter to degrade the system damping for medium and heavy loading is made clear.

In Chapter 3, the design of a variable-structure power stabilizer (i.e., variable parameters) which is altered to compensate for variations in the system active and reactive loading is discussed. An open-loop adaptive technique is adopted, and the optimum settings of the stabilizer parameters associated with a selected set of grid points in the real power-reactive power domain, are computed off-line by minimizing a performance criterion. Whereas a stabilizer with fixed parameters is of necessity a compromise, it is shown that one with variable parameters can offer improved dynamic performance

under widely varying load conditions.

In Chapter 4, the Model Reference adaptive control techniques are applied to a classical one-area system. An adaptive controller is introduced to compensate for variations of the speed regulation parameter with loading. The results demonstrate that the adaptive loop is capable of maintaining satisfactory performance.

chapter two

EFFECT OF STATIC EXCITATION SYSTEM ON THE SMALL-SIGNAL SYNCHRONOUS MACHINE DYNAMICS UNDER WIDELY VARYING LOADING CONDITIONS

Modern generators on a power system are invariably equipped with high speed continously acting excitation systems. These are feedback systems which regulate the terminal voltage of the machine. Such systems, using rotating or magnetic amplifiers, have been used for a number of years in the control of generator excitation, supplied by the rotating direct current exciter usually monitored on the generator shaft. The principal functions of excitation systems are[1] :

1. To preserve desired voltage at the terminals of generators and synchronous condensers
2. To retain the load reactive volt-ampere sharing between the paralleled operating generators
3. To prevent excessive reactive volt-ampere loading and loss of synchronisms by providing the suitable excitation requirements
4. To increase the system damping and raise the stability limits.

An historical review of the development of excitation systems, the criteria of exciter performance, and the various types of apparatus used in excitation systems is found elsewhere[2].

2.1 Relation of Excitation System to the Stability Problem

Increased speed of exciter response was one of the first means suggested and applied for improving power system stability. The excitation systems have an influence on the stability of power systems under both transient and steady-state conditions. This influence is clarified by recalling that the power transmitted in a two-machine system is, according to the approximate equation, proportional to the product of the internal voltages of the two machines, divided by the reactance. Therefore, the power is increased if either internal voltage is increased. These statements hold regarding the power at any particular value of angular separation between the two-internal voltages, and hence also for the maximum power. It is also true on a multimachine system that raising the internal voltages increases the power that can be transmitted between any two machines or groups of machines[3]. Therefore, it is apparent that raising the internal voltages increases the stability limits.

Under transient conditions, power is calculated with the use of transient reactances of the synchronous machines and the voltages behind transient reactance (which are proportional to flux linkages). Upon the occurrence of a fault, the flux linkages are initially the same as they were just before the fault occurred. During the fault, however, the flux linkages decay at a rate described by the short-circuit time

constant T'_d, which is least in the event of a three-phase short-circuit at the terminals of the machine and is somewhat greater for less severe types and locations of fault[3].

If the fault is sustained for a long time, a machine may survive the first swing of its rotor, but, because of the continued decrease of its field flux linkages, it may pull out of step on the second swing or on subsequent swings.

An excitation system controlled by an automatic voltage regulator causes the flux linkages first to decrease more slowly and then to increase. As a result, a machine which does not go out of step on the first few swings will not go out of step on subsequent swings of the same disturbance. On a more severe disturbance, however, it may pull out of step on one of the first few swings. Accordingly, the action of excitation system during a fault is an important factor in power system stability. The faster the excitation system responds to correct low voltage, the more effective it is in improving stability.

In the steady state, power is calculated with the use of saturated synchronous reactances and the voltages behind these reactances (which are proportional to the respective field currents). If the voltages are constant, the power limit is reached when the phase angle between the voltages becomes $\pi/2.0$ radians. An automatic voltage regulator tends to preserve the terminal voltage constant. If it were entirely

successful in doing so under all conditions, the power limit would depend upon the reactance of the circuits between machines, instead of upon this reactance plus the internal (synchronous) reactance. The power limit would be greatly raised by such ideal voltage regulation, particularly if the internal reactance was the major part of the total reactance.

Unfortunately, voltage regulators cannot raise the power limit to anything near the theoretical value just discussed. Due to the delay in the field circuit, the desired restoration of voltage can not always be obtained rapidly enough to increase the electric power in a way to match the mechanical power and thus to prevent power differentials that pull the machines out of synchronism.

It has been found by tests, however, that the use of fast-acting excitation systems does raise the steady-state stability limit a substantial amount[4].

2.2 Semiconductor Electronic Fast-acting Excitation System

As early as 1946[2], a practical experiment was made in the use of a high power electronic device as a utility generator exciter. The device was a mercury arc rectifier. Because of the trouble associated with the use of mercury arc rectifiers (e.g. cooling systems, arc backs, cost), they were not used on a large scale.

With the advent of reliable semiconductor high power

devices such as silicon diodes and controlled rectifiers during the 1960's, semiconductor electronic excitation systems have found a significant place in the industry. Consequently, rotating exciters have been replaced by electronic exciters, in which the generator supplies its own excitation through rectifiers supplied from a transformer connected to generator terminals. The exciter voltage is controlled by the use of controlled rectifiers using a signal derived from the generator potential transformers. This type of excitation is a significant advance over previously used excitation systems, in its possible effects on transient and steady-state stability limits, because of its ability to change generator field voltage almost instantaneously. In addition to the basic requirements of a voltage and reactive volt-ampere control on a generator, electronic exciters have a fast speed of response and a high ceiling voltage.

2.3 Types of Electronic Excitation Systems

Basically, two types of systems have been developed using semiconductor devices: the "brushless system" and the "static system".

2.3.1 The Brushless Excitation System

The brushless system shown in Figure 2.1 has so far been confined to thermal turbine generator units. It consists of: (1) a small 3-phase pilot exciter with a permanent

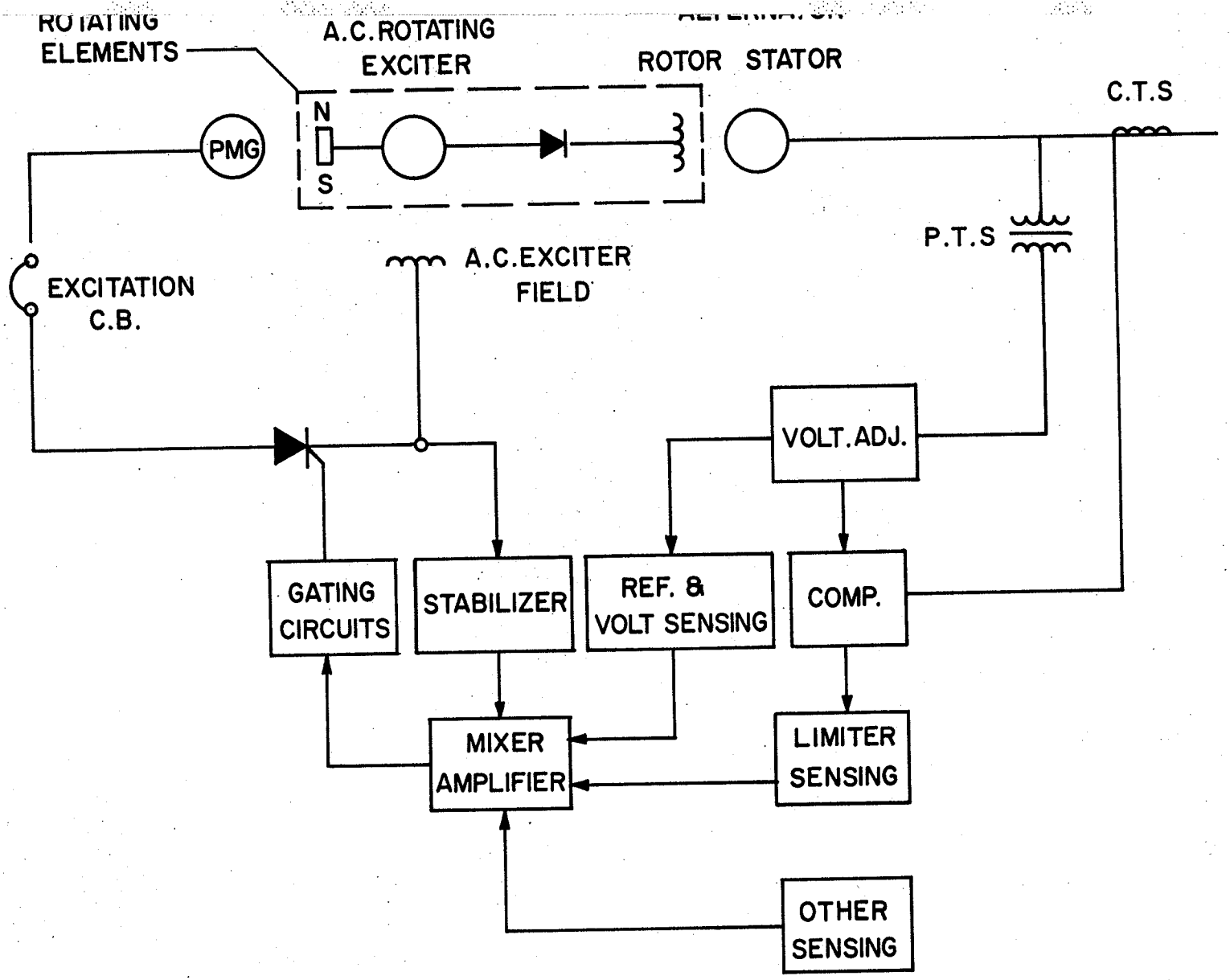

Fig. 2.1 Rotating A.C. exciter with diode rectifier "Brushless" (After Heeley[2])

magnet rotor; (2) a rotating exciter with a 3-phase rotor and a stationary field structure; (3) a 3-phase diode rectifier set which rotates with the rotating exciter structure.

The alternator field structure rotates with the exciter rotor and diode rectifier assembly. The power flow from the pilot exciter to the stationary field of the alternating current rotating exciter is controlled by a thyristor converter, thereby allowing control of the alternator field voltage.

2.3.2 The Static Excitation System

Static excitation systems of the type shown in Figure 2.2 are in service or under design for the majority of the hydraulic turbine generators under development at the present time. The static excitation system is a stationary controlled rectifier to provide the required direct current energy for the alternator field. A self-excited alternating current generator or an alternating current power supply tapped off the alternator terminals may be used to energize the alternator field.

2.4 Adverse Effects Associated with the use of Fast-acting Electronic Excitation System

It has been stated before that it is sometimes convenient to treat the excitation control system as effectively reducing the generator impedance. In fact, an ideal excitation

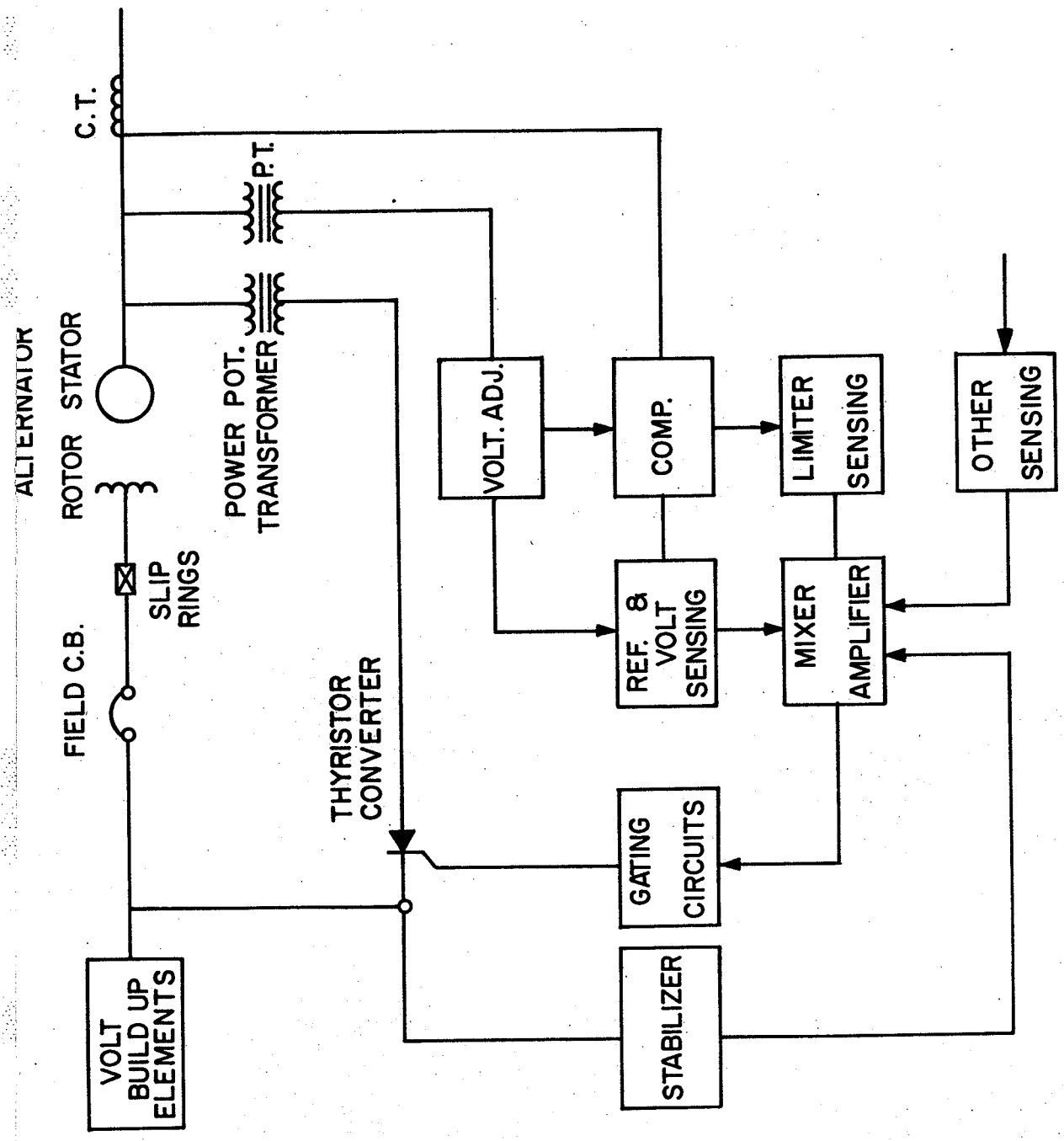

Fig. 2.2 Static exciter thyristor converter and electronic regulator (After Heeley[2])

would be able to maintain a constant generator terminal voltage at all times and the apparent generator impedance would be effectively zero. Stability limits would then normally be a function of system elements external to the generator.

Under conditions of large transient disturbances (e.g. faults), it is impractical or uneconomical to provide excitation systems of sufficient power to maintain voltage. The function of a practical excitation system during major transients is to provide maximum forcing action to damp out generator power and angle swings as early as possible. This calls for a system with high ceiling voltage and high speed of response. Static excitation systems have the most desirable characteristics in this respect.

An excitation system, as well as having the high gain and high ceiling voltage required for maximum effect on transient stability, must also operate satisfactorily during normal steady-state or "small oscillation" conditions on the system. A static exciter in fact, also has desirable characteristics from this point of view, in that it has the ability to maintain essentially constant terminal voltage for small perturbations[5]. Performance equivalent to an effective generator impedance of zero, appears to be possible in the steady-state. However, certain other problems arise under these conditions.

For a synchronous machine equipped with a high gain fast-acting voltage regulator, it has been shown[6] that

negative damping effects can be introduced into the system under certain conditions of loading and generator angle. This is particularly the case when operating close to or within the "dynamic region" which is the region beyond the normal steady-state stability limit for an unregulated machine[7]. The negative damping effect may cancel out the inherent damping of the machine, and under such conditions, continuous oscillations will result, often becoming of such magnitude as to be unacceptable in normal operation or to cause loss of synchronism.

The remainder of this chapter is confined to the investigation of the influence of a generator static excitation system upon its small-perturbation stability for a wide range of loading conditions.

2.5 Power System Model and Assumptions

The analysis of the phenomena of stability of a power system under small perturbation - in this section - is carried out by examining the case of a single machine connected to a large system through external reactance. The circuit in Figure 2.3 is considered the simplification of a multigenerator system from the view point of studying the stability performance of one machine in the system. Thus the external reactance and infinite bus represents the system as seen from the terminals of the machine studied. In other words, the emphasis is on describing the machine behaviour as affected by the

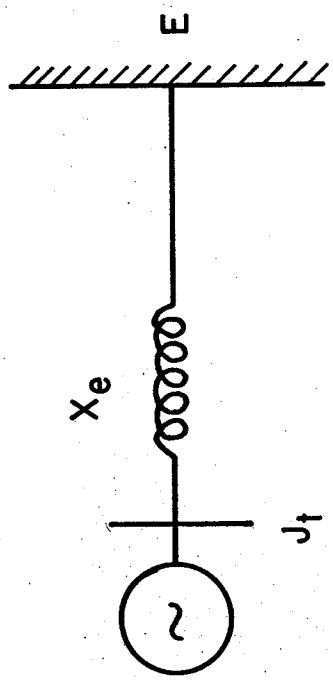

Fig. 2.3 External impedance system configuration for single machine against infinite bus

connected system, rather than attempting a full description of the power system itself.

The following assumptions are also made :

1. Since in general, the reactive power - voltage loop is much faster than the real power - frequency loop, due to the mechanical inertia constants and the larger time constants of the hydraulics in the latter[8], it can be assumed that the transients in the reactive power - voltage loop are essentially over before the real power - frequency loop reacts[9]. Accordingly, the turbine-governor system is not included in the analysis.

2. The local load is zero. This is a "worst case" assumption since local loads have a stabilizing effect[10].

3. The excitation system investigated is one typical of thyristor-type systems. It is characterized by a small time constant (0.05 seconds).

4. The voltages due to the rate of change of direct and quadriture axis flux linkages and to the rate of change of speed are negligible. Damping caused by machine amortisseurs windings is neglected. The armature and tie-line resistances are neglected.

5. The linearized model of the machine given by Heffron and Phillips[7] is adopted in the analysis.

A common method for analyzing the small-signal per-

formance of a single -machine infinite bus system is to write the general equations describing the system. A particular operating point is then assigned. The equations are then rewritten to consider the effect of small changes in different variables about their values at this point. The result is a set of linear differential equations.

The linear differential equations describing the steady state operation of a synchronous machine connected to an infinite bus through an external reactance are[6,7]:

$$(Mp^2+Dp)\Delta\delta = \Delta T_m - \Delta T_{e\ell} \tag{2.1}$$

$$\Delta T_{e\ell} = \{\frac{E_o \sin\delta_o}{x'_d+x_e}\}\Delta E'_q + \{\frac{x_q-x'_d}{x'_d+x_e} E_o \sin\delta_o\, i_{qo} + \frac{E_o E_{qo} \cos\delta_o}{x_e+x_q}\}\Delta\delta \tag{2.2}$$

$$\Delta E'_q = \{\frac{x'_d+x_e}{x_d+x_e} \frac{1}{1+pT'_{dz}}\}\Delta E_{fd} - \{\frac{x_d-x'_d}{x_d+x_e} \frac{E_o}{1+pT'_{dz}} \sin\delta_o\}\Delta\delta \tag{2.3}$$

$$\Delta v_t = \{\frac{x_q}{x_e+x_q} \frac{v_{do}}{v_{to}} E_o \cos\delta_o - \frac{x'_d}{x'_d+x_e} \frac{v_{qo}}{v_{to}} E_o \sin\delta_o\}\Delta\delta + \{\frac{x_e}{x_e+x'_d} \frac{v_{qo}}{v_{to}}\}\Delta E_{fd} \tag{2.4}$$

and

$$T'_{dz} = \frac{x'_d+x_e}{x_d+x_e} T'_{do} \tag{2.5}$$

All variables with subscript o are values of the variables evaluated at the pre-disturbance steady state operating point. Prefix Δ indicates deviations of the variables from their values at the steady state operating point.

Eqn. 2.2 to eqn. 2.5 may be rewritten in the form:

$$\Delta v_t = K_5 \Delta\delta + K_6 \Delta E'_{fd} \tag{2.6}$$

$$\Delta E'_q = \frac{K_3}{1+pT'_{dz}} \Delta E_{fd} - \frac{K_3 K_4}{1+pT'_{dz}} \Delta\delta \tag{2.7}$$

$$\Delta T_{e\ell} = K_1 \Delta\delta + K_2 \Delta E'_q \tag{2.8}$$

$$T'_{dz} = K_3 T'_{do} \tag{2.9}$$

where
$$K_1 = \frac{x_q - x'_d}{x'_d + x_e} E_o \, i_{qo} \sin\delta_o + \frac{E_o E_{qo}}{x_e + x_q} \cos\delta_o \tag{2.10}$$

$$K_2 = \frac{E_o}{x'_d + x_e} \sin\delta_o \tag{2.11}$$

$$K_3 = \frac{x'_d + x_e}{x_d + x_e} \tag{2.12}$$

$$K_4 = \frac{x_d - x'_d}{x_e + x'_d} E_o \sin\delta_o \tag{2.13}$$

$$K_5 = \frac{x_q}{x_e + x_q} \frac{v_{do}}{v_{to}} E_o \cos\delta_o - \frac{x'_d}{x_e + x'_d} \frac{v_{qo}}{v_{to}} E_o \sin\delta_o \tag{2.14}$$

and
$$K_6 = \frac{x_e}{x_e + x'_d} \frac{v_{qo}}{v_{to}} \tag{2.15}$$

The constants $K_1, K_2 \ldots K_6$ represent the interaction between the load and voltage control loops of the synchronous generator. These constants, with the exception of K_3 which is only a function of the ratio of the reactances, change with the actual real and reactive power loading as well as the excitation levels in the machine, making the dynamic behaviour of the machine quite different at different operating points.

The steady state operating values of the variables required to calculate the values of the constants $K_1, K_2, \ldots K_6$ are evaluated from known values of v_{to}, P_o and Q_o as given by the following equations:

$$i_{qo} = P_o\, v_{to}\, \{P_o^2\, x_q^2 + (v_{to}^2 + Q_o x_q)^2\}^{-\frac{1}{2}} \tag{2.16}$$

$$v_{do} = i_{qo} x_q \tag{2.17}$$

$$v_{qo} = (v_{to}^2 - v_{do}^2)^{\frac{1}{2}} \tag{2.18}$$

$$i_{do} = \frac{(Q_o + x_q i_{qo}^2)}{v_{qo}} \tag{2.19}$$

$$E_o = \{(v_{do} + x_e\, i_{qo})^2 + (v_{qo} - x_e\, i_{do})^2\}^{\frac{1}{2}} \tag{2.20}$$

$$\delta_o = \tan^{-1} \left(\frac{v_{do} + x_e\, i_{qo}}{v_{qo} - x_e\, i_{do}}\right) \tag{2.21}$$

The above equations were derived from the standard machine vector diagram.

Figure 2.4 represents the block diagram for the single-machine infinite bus system. The additional relation:

$$\Delta E_{fd} = -\frac{K_e}{1 + pT_e}\, \Delta e_t \tag{2.22}$$

represents the effects of the voltage regulator excitation system. The load loop, the excitation loop and the interaction coefficients are indicated. Although the excitation loop itself will not go unstable for high values of exciter gain K_e (assuming no changes in rotor angles), the negative damping effect in the load loop is important at high gain.

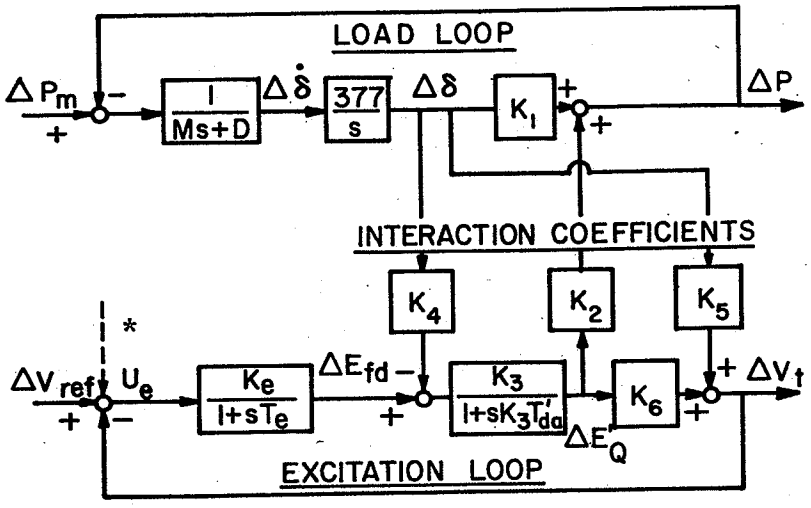

Fig. 2.4 Block diagram of the single machine infinite bus system including the effects of voltage regulator excitation system (*stabilizing input to be introduced later)

2.6 Eigen-Value Analysis of the Effect of Static Exciter on Machine Dynamic Stability

The effects of a thyristor-type excitation system on the stability of a single machine connected to an infinite bus have been investigated[6]. In this section, a small-perturbation stability analysis is performed using eigen-value techniques, for a wide range of system real and reactive power loading.

In a recent paper[10], the effect of changing environment on the commonly named Heffron-Phillips parameters $K_1, K_2, \ldots K_6$ is recognized with the assumption that changing real and reactive power levels are the most significant environmental changes. It is shown here that the concept of changing P and Q environment as well as its direct effect on the small-signal stability of the system can be usefully displayed in the complex-frequency plane.

The block diagram relations shown in Figure 2.4 may be expressed as a set of differential equations:

$$\frac{d}{dt}(\Delta\delta) = \omega_o \Delta p\delta \tag{2.23}$$

$$\frac{d}{dt}(\Delta p\delta) = \frac{\Delta T_m}{M} - \frac{K_1}{M}\Delta\delta - \frac{D}{M} p\delta - \frac{K_2}{M}\Delta E'_q \tag{2.24}$$

$$\frac{d}{dt}(\Delta E'_q) = -\frac{K_4}{T'_{do}}\Delta\delta - \frac{1}{T'_{do}K_3}\Delta E'_q - \frac{1}{T'_{do}}\Delta E_{fd} \tag{2.25}$$

$$\frac{d}{dt}(\Delta E_{fd}) = \frac{K_5 K_e}{T_e}\Delta\delta + \frac{K_6 K_e}{T_e}\Delta E'_q - \frac{1}{T_e}\Delta E_{fd} + \frac{K_e}{T_e}\Delta v_{ref} \qquad (2.26)$$

For the set of state variables

$$\underline{X}' = [\Delta\delta,\ \Delta p\delta,\ \Delta E'_q,\ \Delta E_{fd}] \qquad (2.27)$$

and disturbance vector

$$\underline{U}' = [\Delta T_m,\ \Delta v_{ref}] \qquad (2.28)$$

The linearized small-perturbation equations can be written in the state equations format:

$$\dot{\underline{X}} = A\,\underline{X} + \Gamma\,\underline{u} \qquad (2.29)$$

The system matrix A and the disturbance distribution matrix Γ defined as follows:

$$A = \begin{bmatrix} 0 & \omega_o & 0 & 0 \\ -\frac{K_1}{M} & -\frac{D}{M} & -\frac{K_2}{M} & 0 \\ -\frac{K_4}{T'_{do}} & 0 & -\frac{1}{K_3 T'_{do}} & -\frac{1}{T'_{do}} \\ \frac{K_5 K_e}{T_e} & 0 & \frac{K_6 K_e}{T_e} & -\frac{1}{T_e} \end{bmatrix} ; \Gamma = \begin{bmatrix} 0 & 0 \\ \frac{1}{M} & 0 \\ 0 & 0 \\ 0 & \frac{K_e}{T_e} \end{bmatrix} \qquad (2.30)$$

The four eigen-values of the system matrix A, determine the character of the time response and hence the stability of the system. It is clear that the eigen-values of the system are functions of the constants $K_1, K_2, \ldots K_6$, and therefore depend on the system real and reactive power loading. In the analysis to come after, the following numerical data for the single machine infinite bus system will be used[6]:

Synchronous Machine	$x_d = 1.6$	$x'_d = 0.32$
	$x_q = 1.55$	$T_{do} = 6.0$ sec
	$v_{to} = 1.0$	$\omega_o = 377$ rad/sec
	$D = 0.0$	$M = 10.0$
Tie Line	$x_e = 0.4$	$r_e = 0.0$
Exciter	$K_e = 50.0$	$T_e = 0.05$
Loading	$P = (0.1, 0.2, \ldots 1.0)$	
	$Q = (-0.3, -0.2, -0.1, \ldots 1.0)$	

By varying the real power and/or the reactive power loading, to cover a large number of operating points, it is possible to calculate the values of the constants K_1, K_2, .. K_6 (as given by eqns. 2.10 - 2.15), then for every real power-reactive power combination, to determine the eigen-values of the system matrix A. The locations[5] of the eigen-values in the complex-frequency domain determine the stability of the system.

The values of the Heffron-Phillips constants, for the entire loading range considered, are plotted in Figure 2.5a through e, for K_1, K_2, K_4, K_5 and K_6 respectively. K_3 is excluded because it does not depend on the system loading. One can observe from these figures that all Heffron-Phillips constants, with the exception of K_5 which becomes negative for high loading and/or leading power factor, do not change signs as the real power and/or the reactive power increase.

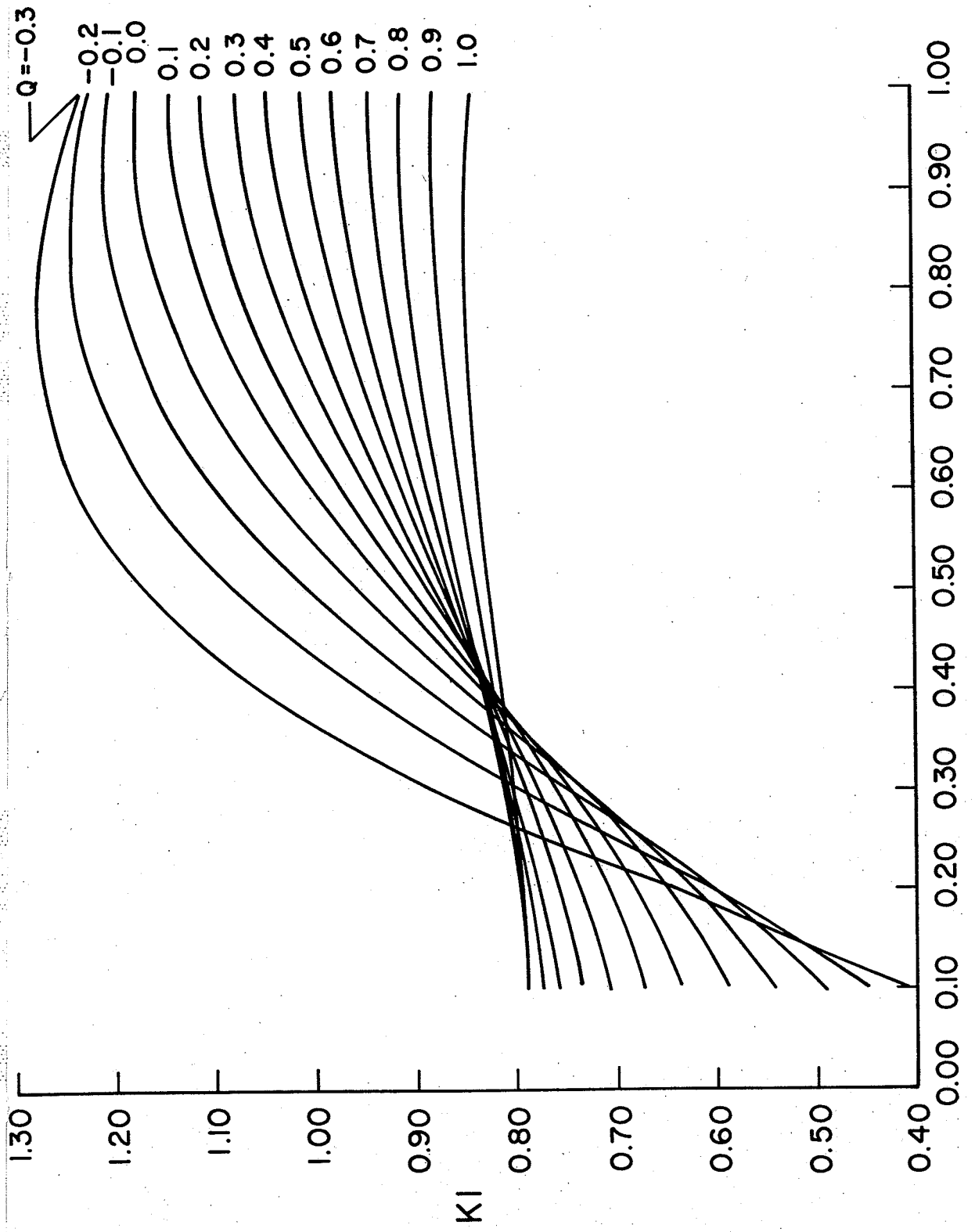

Fig. 2.5a Variation of K_1 with real and reactive loading

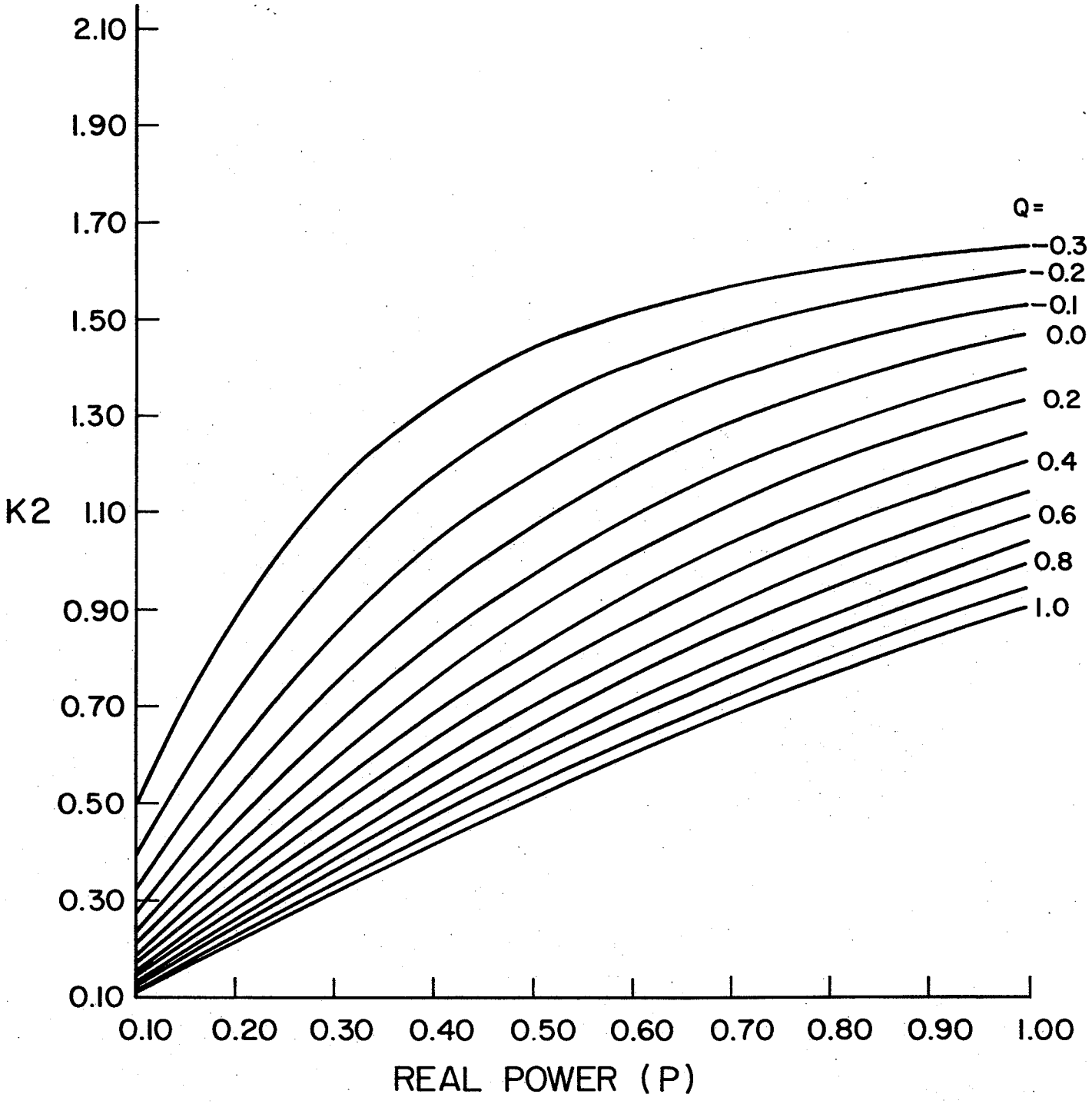

Fig. 2.5b Variation of K_2 with real and reactive loading

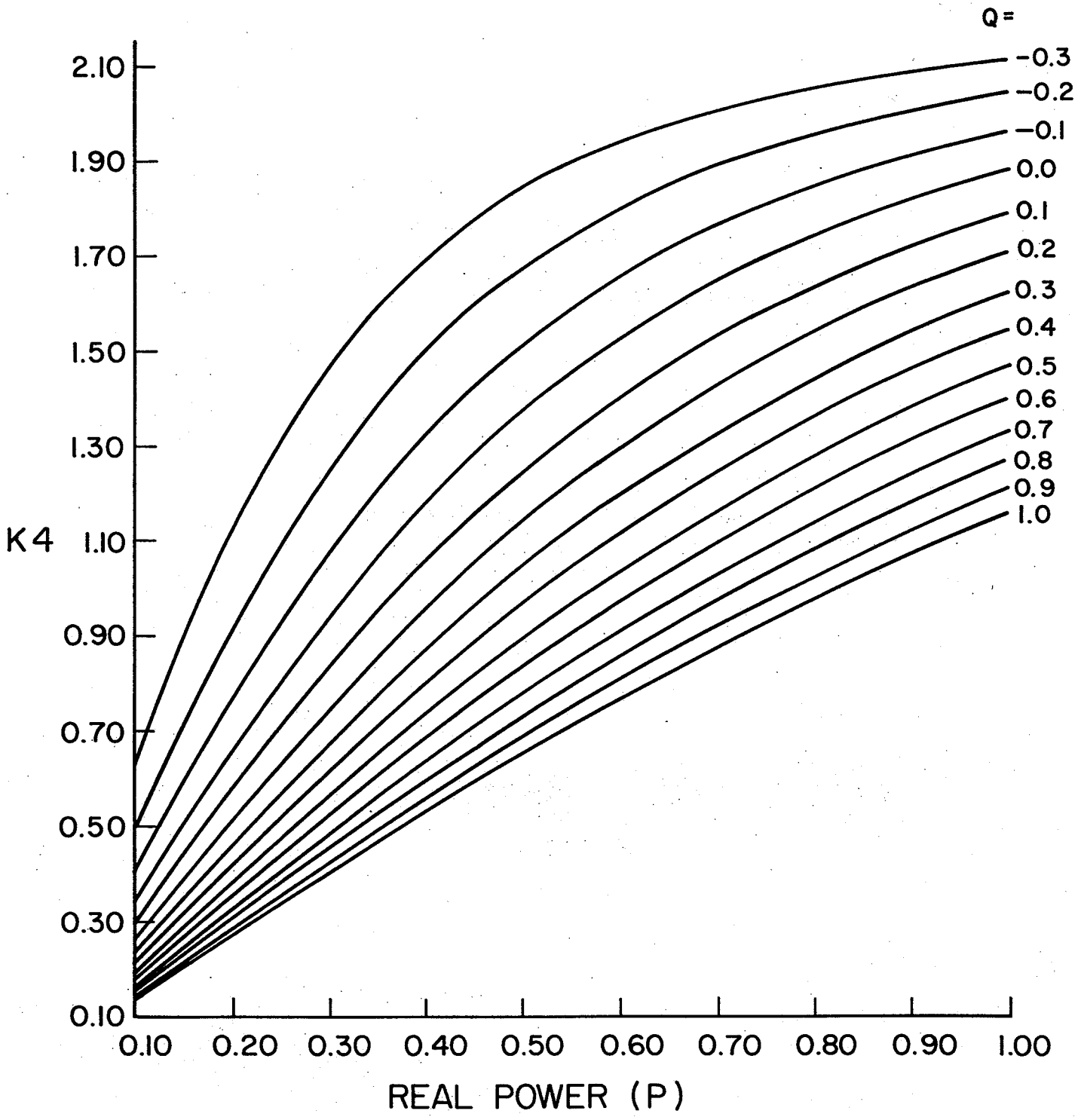

Fig. 2.5c Variation of K_4 with real and reactive loading

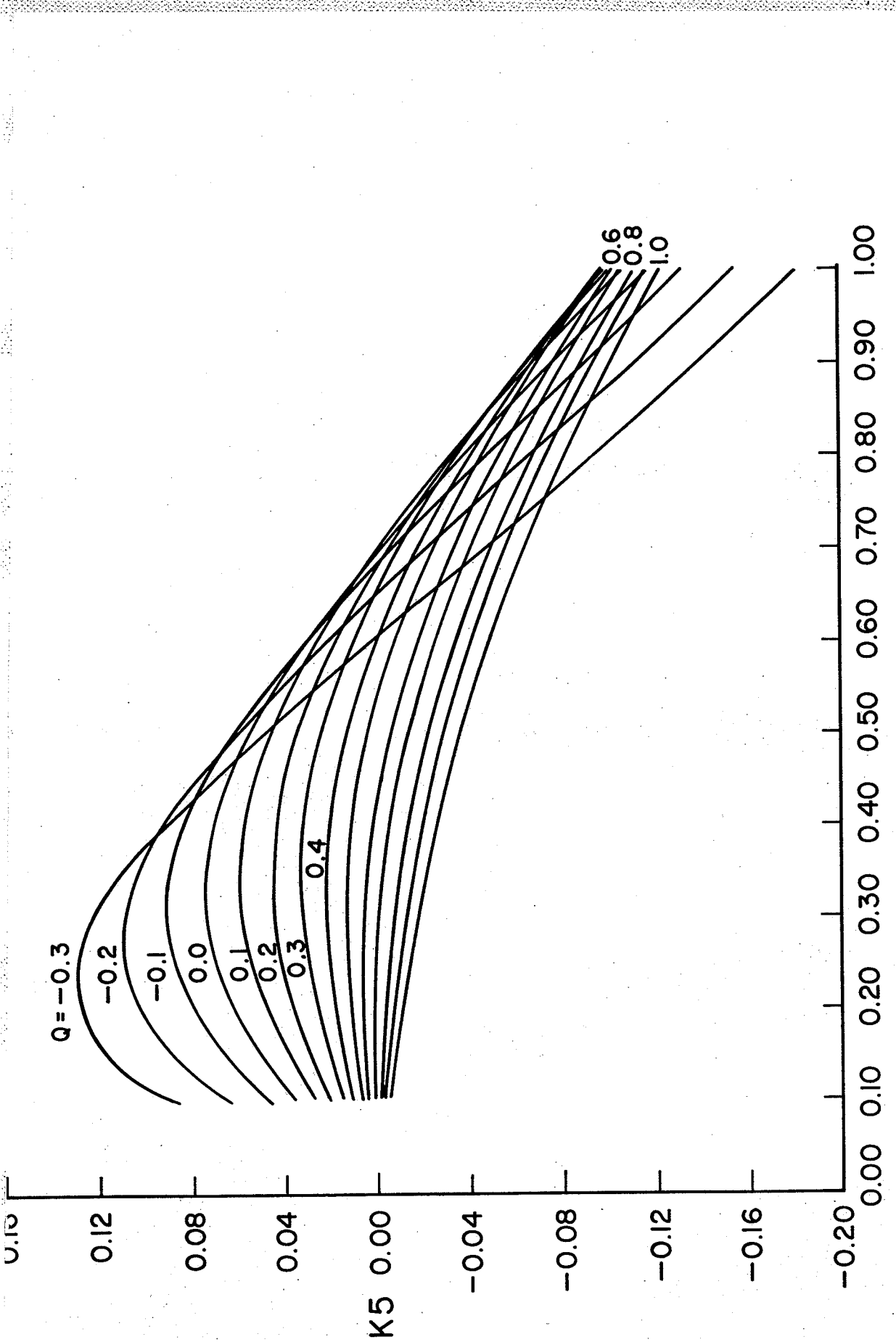

Fig. 2.5d Variation of K_5 with real and reactive loading

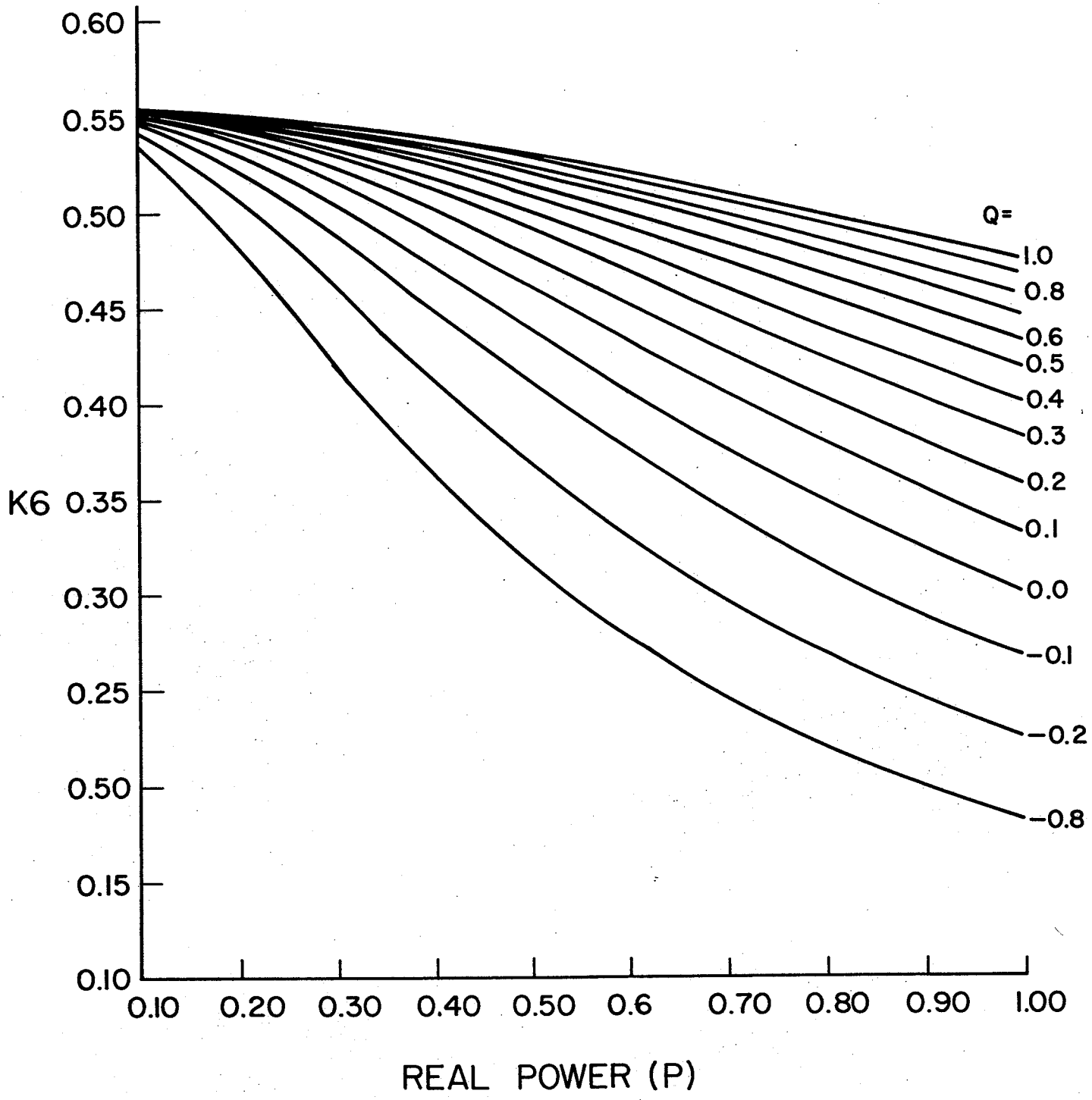

Fig. 2.5e Variation of K_6 with real and reactive loading

Results

A computer program was written to compute the eigen-values of the system matrix A as the loading changes. It was found that two of the four eigen-values of the system were negative real and were located in the complex frequency plane, to the left of a line $s = -3.0$ for the loading range examined, and therefore have a minor effect on the system dynamics. The two remaining eigen-values are complex conjugate and located on both sides of the imaginary axis and close to it, and hence are considered the dominant eigen-values of the system. Figure 2.6 shows the location of the dominant eigen-value (with positive imaginary part) in the complex frequency domain for all combinations of $P = 0.1$ to $P = 1.0$, and $Q = -0.3$ to $Q = 1.0$, as determined by computer solution for steps in P and Q of 0.1; in other words 140 combinations. Constant real power lines and constant reactive power lines are also shown, giving a more complete plant portrait.

Such curves display the dynamic stability characteristics for the system without the need of repeatedly perturbing the system with step-like disturbances in the mechanical torque and/or the voltage reference. Instability of the system is easily perceived for moderate and high loading. This result is in agreement with the qualitative results obtained previously[6].

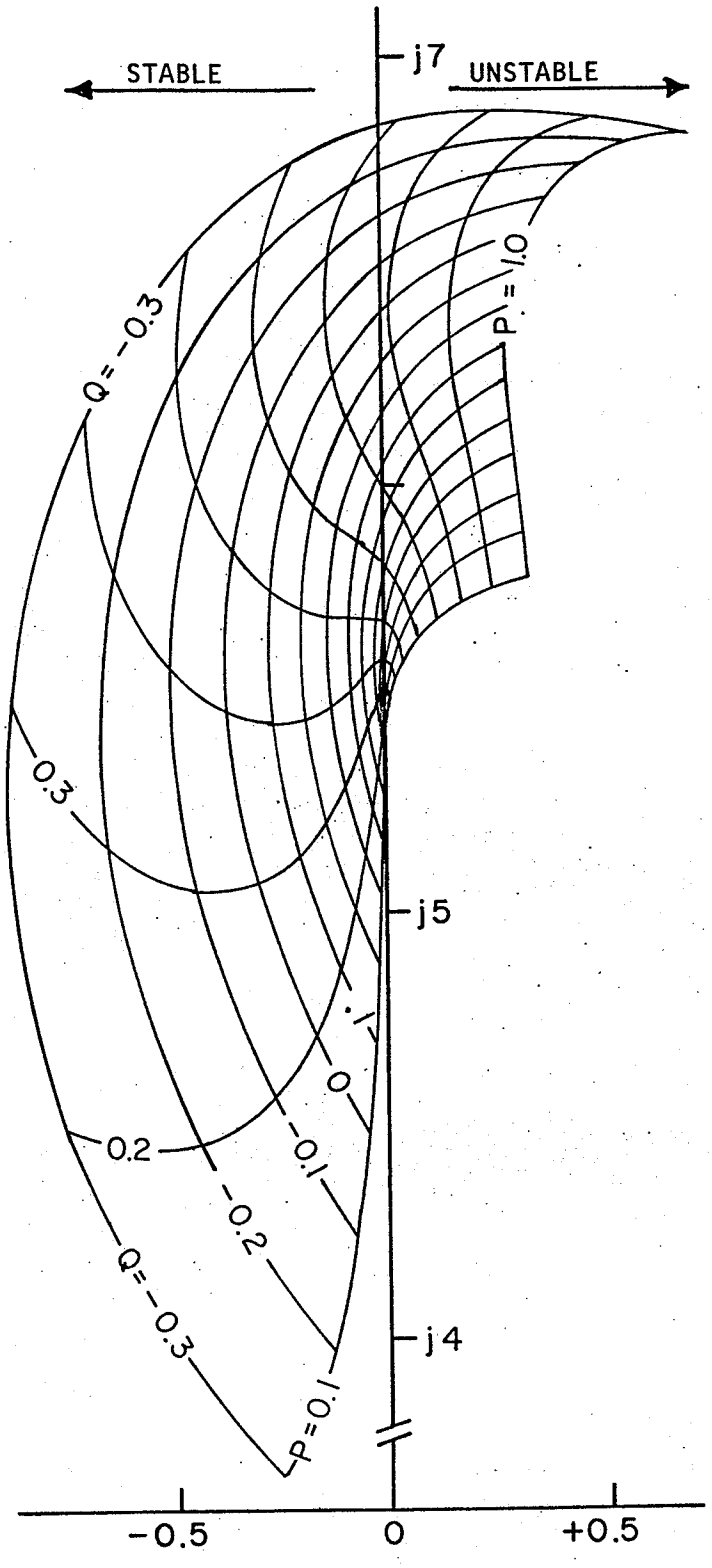

Fig. 2.6 Constant real-power lines and constant reactive-power lines in the complex frequency plane (T_e = 0.05 secs)

As a matter of interest, the effect of a slower exciter (T_e = 2.0 sec) on the location of the dominant eigen-values in the complex-frequency plane is shown in Figure 2.7. Only the boundary lines of constant real-power and reactive power are shown. The dominant eigen-values are located in a narrower area compared to the fast exciter case (T_e = .05 sec). The system is stable although highly oscillatory.

The method of eigen-value analysis - besides developing insight into effects of static excitation system - helps to establish an understanding of the stabilizing requirements for such systems. The method can easily be extended to excitation systems with different dynamic characteristics.

2.7 Correlation Between the Eigen-Value Technique and the Synchronizing-Damping Torques Technique

The concept of synchronizing and damping torques[6] is used in this section. The results obtained are shown to agree with the results obtained through eigen-value analysis.

At any given oscillation frequency, braking torques are developed in phase with machine rotor angle δ (synchronizing torques) and in phase with machine rotor speed $p\delta$ (damping torques). The torque developed by any means can be broken down into these components for stability determination. Sufficient and necessary conditions for the system to be

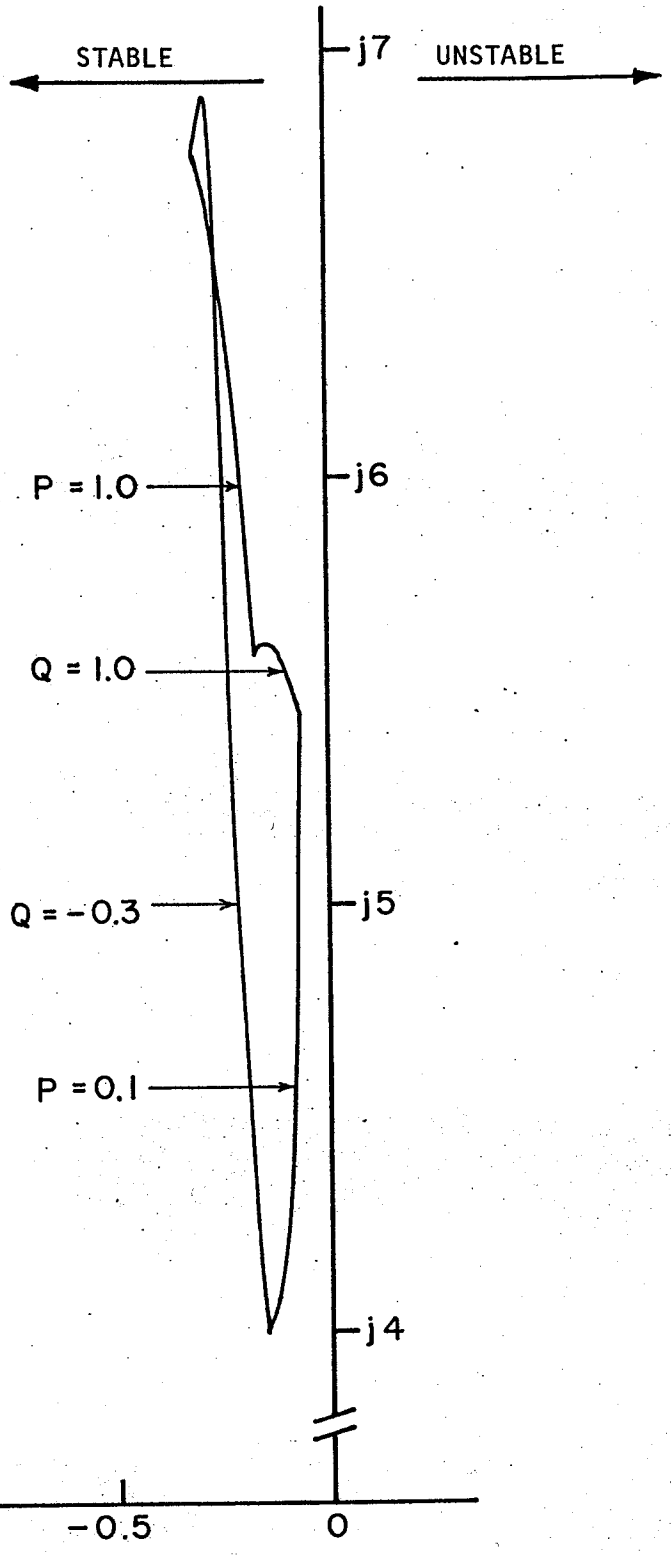

Fig. 2.7 Boundary constant real-power lines and constant reactive-power lines in the complex frequency plane (T_e = 2.0 secs)

stable are that both synchronizing torque and damping torque coefficients be greater than zero.

The system block diagram given in Figure 2.4 may be reduced to the form shown in Figure 2.8 where

$$\Delta T_{e\ell} = H(s)\ \Delta\delta \tag{2.31}$$

and

$$H(s) = K_1 - \frac{K_2 K_5 K_e + K_2 K_4 (1+sT_e)}{s^2 T'_{do} T_e + s\left(\frac{T_e}{K_3} + T'_{do}\right) + K_6 K_e + \frac{1}{K_3}} \tag{2.32}$$

It is possible to rewrite eqn. (2.31) in the form:

$$\Delta T_{e\ell} = \Delta T_s\ \Delta\delta + \Delta T_d\ \Delta p\delta \tag{2.33}$$

where ΔT_s and ΔT_d are the synchronizing and damping torque coefficients. They are obtained by replacing the laplace operator s in the transfer function $H(s)$ with the frequency of oscillation $j\omega_{osc}$. This substitution reduces $H(s)$ into a complex quantity. Interpreting imaginary coefficient of $\Delta\delta$ as real coefficient of $p\delta$, it is possible to write down expressions for ΔT_s and ΔT_d. Eqn. 2.31 may be rewritten as:

$$\Delta T_{e\ell} = \{R_e[H(j\omega_{osc})] + j\ \frac{\omega_{osc}}{\omega_o} \cdot \frac{\omega_o}{\omega_{osc}}\ IM[H(j\omega_{osc})]\}\Delta\delta \tag{2.34}$$

Taking into consideration that:

$$\Delta\delta = \Delta p\delta \cdot \frac{\omega_o}{j\omega_{osc}} \tag{2.35}$$

Eqn. 2.34 becomes:

$$\Delta T_{e\ell} = R_e[H(j\omega_{osc})]\ \Delta\delta + \frac{\omega_o}{\omega_{osc}}\ IM[H(j\omega_{osc})]\ \Delta p\delta \tag{2.36}$$

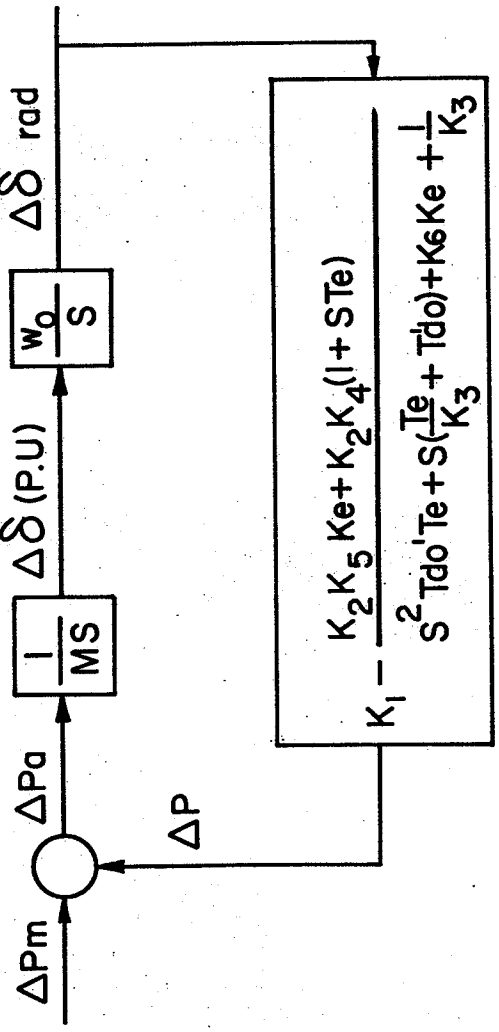

Fig. 2.8 Reduction of linearized small perturbation model for the single machine infinite bus system

From eqns. 2.32 and 2.36, it follows that:

$$\Delta T_s = K_1 - \frac{(K_2K_5K_e+K_2K_4)(K_6K_e+\frac{1}{K_3}-\omega_{osc}^2 T'_{do}T_e)+\omega_{osc}^2 K_2K_4T_e(T'_{do}+\frac{T_e}{K_3})}{(\frac{1}{K_3}+K_6K_e-\omega_{osc}^2 T'_{do}T_e)^2+\omega_{osc}^2(\frac{T_e}{K_3}+T'_{do})^2} \tag{2.37}$$

$$\Delta T_d = \omega_o \left[\frac{(K_2K_5K_e+K_2K_4)(T'_{do}+\frac{T_e}{K_3})-K_2K_4T_e(K_6K_e+\frac{1}{K_3}-\omega_{osc}^2 T'_{do}T_e)}{(\frac{1}{K_3}+K_6K_e-\omega_{osc}^2 T'_{do}T_e)^2+\omega_{osc}^2(\frac{T_e}{K_3}+T'_{do})^2} \right] \tag{2.38}$$

The torque-angle loop defining the synchronizing and damping torque coefficients is shown in Figure 2.9.

One important point remains to be clarified. It must be noted that the oscillation frequency ω_{osc}, which is needed as an input parameter to obtain values of ΔT_d and ΔT_s, is in fact an unknown quantity. However, ω_{osc} could be obtained directly from Figure 2.6 for the entire loading range considered. This is possible because the dynamics of the system are dominated by the two complex conjugate eigenvalues. Under the circumstances, ω_{osc} is equal to the imaginary part of any one of the two dominant complex eigenvalues.

Figure 2.10 and Figure 2.11 give the synchronizing and damping torque coefficients for the wide range of system loading examined. It is clear that ΔT_s remains always

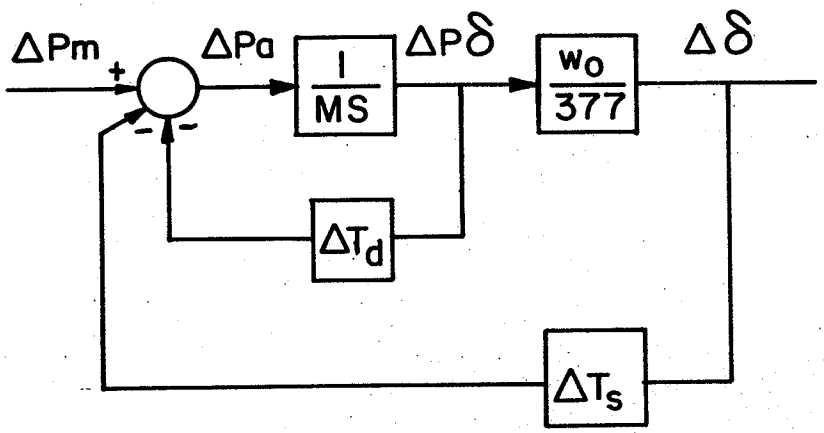

Fig. 2.9 The load-loop showing synchronizing and damping torque

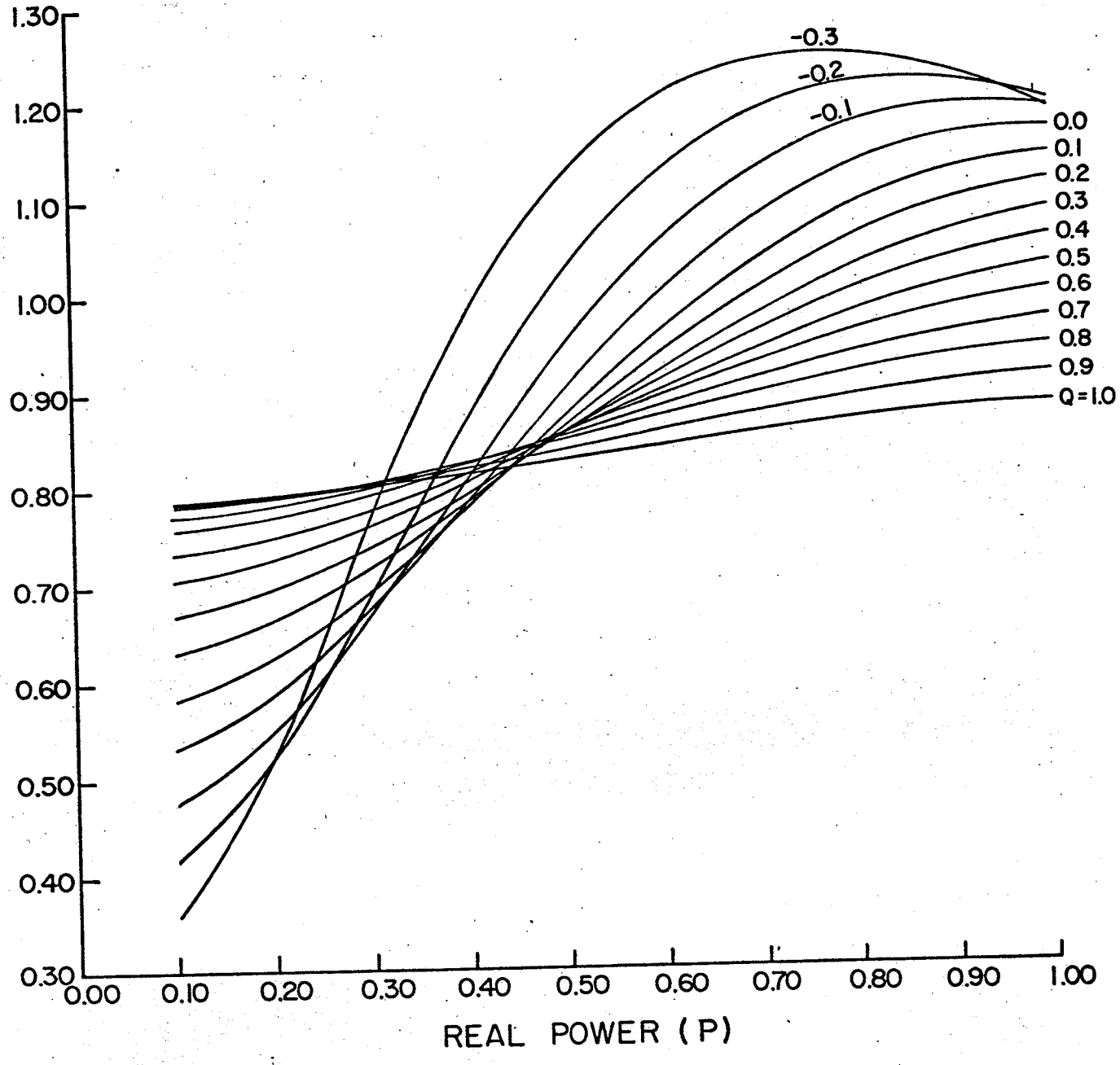

Fig. 2.10 Variations of synchronizing torque coefficient with real and reactive loading

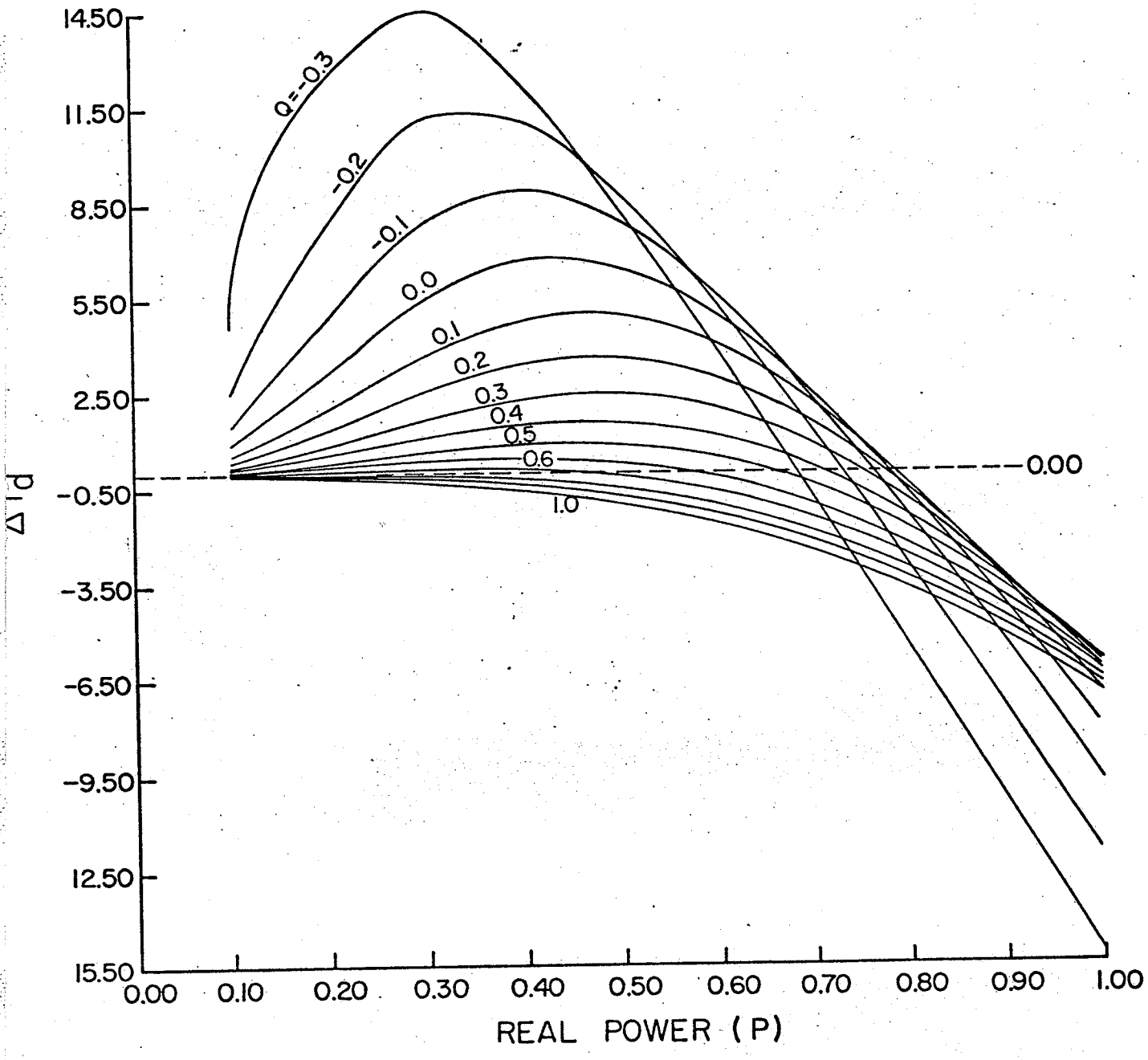

Fig. 2.11 Variation of damping torque coefficient with real and reactive loading

positive, while ΔT_d becomes negative, indicating instability for higher loading and/or lower power factors. The results obtained by this method are in full agreement with that of the eigen-value analysis.

chapter three

VARIABLE-STRUCTURE POWER STABILIZER TO SUPPLEMENT STATIC EXCITATION SYSTEM

3.1 Review of Stabilizing Signals

In Chapter 2, it has been shown with the aid of eigen value analysis, how a static excitation system can destroy the damping component of the electrical torque under certain conditions of loading and generator angle. It can be easily concluded that, to gain any real advantage from static exciters, it is necessary to introduce special control signals to increase the system dynamic stability and to damp out machine swings.

Significant advances have been made which increase stability through the use of stabilizing signals derived from speed, frequency, real power and/or reactive power, rate of change of terminal voltage, acceleration and mechanical power. A number of published reports document both studies and field tests.

Watson[5] and Dandeno et al[11] have reported that analog computer studies showed that the most effective damping of generator swings could be obtained by introducing an additional signal to the excitation control, proportional to the rate of change of generator angle ($\frac{d}{dt}\delta$). Consideration was given to various methods of obtaining a signal proportional to changes in generator speed, including the derivation of the

signal from the measurement of electrical quantities at the generator terminals. However as a result of certain limitations, development work was subsequently concentrated on a method of direct measurement from the generator rotor. Studies have shown that the speed signal should be derived directly from the generator shaft itself. Stability tests made on a special radial system arrangement showed an increase in both steady-state stability limits (up to 97 per cent of that theoretically possible with generators of zero internal impedance) and transient stability limits.

The possibility of obtaining generator speed signals by measurement of various electrical quantities on the machine and applying appropriate transfer functions, as alternatives to direct measurement of the mechanical quantities, was investigated by Ontario Hydro[12]. An angle transducer was developed to provide a d.c. signal approximately proportional to phase angle between generator internal voltage and remote system voltage. (These voltages were obtained from simulating networks.) This signal was then differentiated to provide the required damping signal ($p\delta$). Unavoidable time lags in the measurement, and the instability of the device when actual system impedance was much lower than the preset value utilized in the similarity network, were the main reasons behind abandoning this method. A signal based upon the integral of accelerating power was then utilized. Under the assumption of constant mechanical power input, variation in machine speed was expressed as:

$$\Delta(p\delta) = \frac{-1}{M} \int \Delta P_e \, dt \qquad (3.1)$$

Such an arrangement was found to function satisfactorily except when it was required to change the loading on the machine by changing the gate position (for a hydraulic unit). The stabilizing signal had to be disconnected to prevent excessive excursions of field current and reactive power during real power changes on the generator, which led to the immediate loss of the stability of the machine. Consequently, this method was also abandoned in favour of direct measurement of shaft speed.

Ellis et al[13] have reported the results of an investigation made to find a suitable signal for stabilizing machine swings. Different stabilizing signals were considered including the rate of change of terminal voltage, speed error, acceleration, rate of change of field current, subtransient direct axis field current, subtransient quadrature axis field current and rate of change of armature current. The signals were evaluated using a simplified system representation on an electronic differential analyzer, with the excitation fully represented and fixed input shaft power. Several of the signals considered showed a stabilizing influence and the most promising of these were the rate of change of field current and the speed error. The latter gave particularly good results, indicating that it could produce any degree of damping desired. The rate of change of field current signal exhibited signs of instability because of a closed positive feedback loop in the

excitation system, so the signal was abandoned.

The use of a signal proportional to the rate of change of voltage to supplement the control of excitation has been shown[14] to produce either positive or negative damping, depending upon the relative gains and time constants. The maximum positive damping it can yield is much less than that obtainable from a frequency deviation function. It was further shown that a control signal offering the most promise for improving the stability is a complex function of frequency amounting to frequency deviations for slow rates of swing and rate-of-change of frequency for high rates of swings. It was pointed out that the second derivative of frequency may also be needed to achieve efficient damping at very high swing frequencies.

Excitation voltage control by reactive power stabilizing signals, excitation current signals, speed signals and integral of the acceleration power have been considered for stabilizing the Hydro Québec system[8]. Computer tests and field tests have clearly shown that any relation between generator speed and reactive power is subject to too many contingencies for this control signal to be effective and reliable. It was even shown, that, in some cases, a signal proportional to the rate of change of reactive power could cause a further reduction of the damping coefficient.

Shier et al[15] described a purely electrical approach

to obtain a speed signal. The approach was based on the fact that the speed of the machine could also be considered stored rotational energy. For transient performance, the input power variations could be ignored and the change in output energy could be a reasonably close measurement of change in rotor energy. A watt transducer was used to measure output power, which was then converted to the final speed signal using operational amplifiers.

The effectiveness of a damping signal proportional to electrical power has also been investigated [16,17]. The stabilizing signal, which is derived from a single-phase Hall-watt transducer, amplified, filtered, and applied to a derivative-type circuit, was shown to be very effective in damping machine swings.

Gerhart et al [18] presented a valuable contribution toward shedding some light on the procedure for installation and adjustment of power system stabilizers.

A different type of series compensation for the improvement of dynamic stability of an excitation control has been developed and tested [19,20]. The device incorporates complex zeros to compensate for the adverse effects of the under-damped complex poles, which mathematically, characterize the dynamic behaviour of a synchronous machine operating at high loading and high torque angle. Investigations to determine the sensitivity of the technique to misplacement of the zero's

which compensate the complex dynamic poles remain to be carried out.

3.2 Problem Description and Approach

From the review given in the previous section, it is evident that a variety of supplementary signals that attempt to improve the small-signal dynamic performance of synchronous machine is currently available. Most of these supplementary signals act on the voltage regulator through various combinations of fixed-structure lead-lag networks (commonly referred to as compensators or stabilizers). The design of such compensators is usually carried out for one set of machine parameters corresponding to one operating point.

Since machine parameters change, in a rather complex manner, with loading, making the dynamic behaviour of the machine quite different at different operating points, it is difficult to reach general conclusions, as to stabilizer structure based on only one operating point. As a result, the characteristics of the stabilizer have to be adjusted properly to give the desired performance over the expected range of system loading. In other words, it is essential to incorporate variable-structure stabilizers that are altered to compensate for variations in system dynamics caused by load changes, if optimum dynamic performance is to be maintained as operating conditions change.

The purpose of this study is to investigate the possibility of designing such variable-structure self-adjusting stabilizers.

The supplementary stabilizing signal considered in this study is one proportional to electrical power. A derivative type power stabilizer with two poles is considered.

An open-loop adaptive technique that is based on measurements of the operating environment that are directly related to the values of the plant parameters (i.e. real and reactive power) is used. Figure 3.1 represents a block diagram for the basic scheme of the suggested adaptive technique. The idea is to determine the optimum values of the stabilizer adjustable parameters in conjunction with the minimum of a performance criterion. The procedure is performed off-line for a selected set of grid points in the real power-reactive power domain. (The mesh size in the grid, of course, depends on the quantum of change in load.) The optimum settings thus obtained are to be stored in a Micro-processor memory. The values of the real power and the reactive power are to be continuously measured using available Watt and Var transducers. A control signal is then sent to the stabilizer to update its parameters in step with changes in the system loading in the ensuing steady-state. Thus the stabilizers will always be prepared to cope with disturbances.

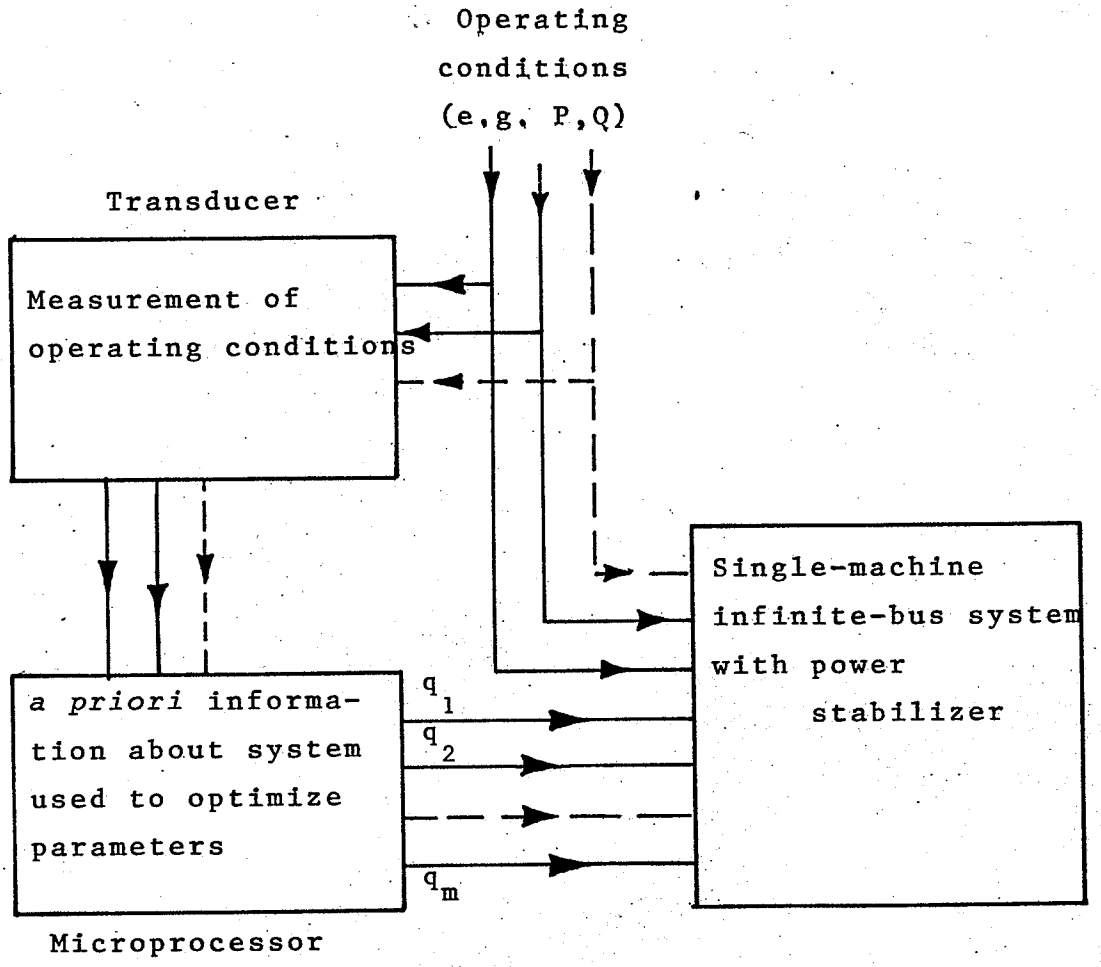

Fig. 3.1 Block diagram of the open-loop adaptive technique (q_1, q_2, ... q_m represent the adjustable parameters)

3.3 Performance Criterion and Parameter Optimization

Scalar integral performance criteria have proved to be the most meaningful and convenient measures of dynamic performance[9]. The performance criterion chosen for this study is the so-called integral-of-the-squared-error (ISE) to a step input. ISE is used here for two reasons:

i) Its validity has been demonstrated as a performance index[21]

ii) ISE may be conveniently evaluated with a digital computer on the basis of Parseval's theorem or using Lyapunov's second method.

Consider an initially displaced system:

$$\dot{\underline{X}}(t) = A\,\underline{X}(t) \quad ; \quad \underline{X}(o) = \underline{X}_o \tag{3.2}$$

where $A = A(q)$ is given and is assumed asymptotically stable for all q. Vector q includes all parameters that are to be specified by the automated design procedure. Assume, in addition, that the performance criterion

$$j = \int_o^\infty \{\underline{X}'(t)\ W\ \underline{X}(t)\}\ dt \tag{3.3}$$

is assigned to the transient response of the system given by eqn. 3.2, where the weighting matrix W is assumed to be positive semi-definite real symmetric, for all q of interest. It is desired to determine the values of the adjustable parameters, so as to minimize the performance criterion j. The second method of Lyapunov allows the computation of the

performance criterion given by eqn. 3.3 along the dynamic solution of the system represented by eqn. 3.2 without integrating the system equations and evaluating the infinite integral. Use of the state transition equation:

$$\underline{X}(t) = \exp(At)\ \underline{X}_o \tag{3.4}$$

permits rewriting eqn. 3.3 in the more convenient form:

$$j = \underline{X}_o'\ R\ \underline{X}_o \tag{3.5}$$

where,

$$R = \int_o^\infty \{\exp(A't)\ W\ \exp(At)\}\ dt \tag{3.6}$$

An alternate form for R is derived from the integration by parts occurring in:

$$RA = \int_o^\infty \{\exp(A't)\ WA\ \exp(At)\}\ dt \tag{3.7}$$

$$RA = \exp(A't)\ W\ \exp(At)\ \Big|_{t=o}^{t=\infty} - \int_o^\infty \{A'\ \exp(A't)\ W\ \exp(At)\}\ dt \tag{3.8}$$

In particular, matrix R is the unique solution of the well-known relationship

$$A'R + RA = -W \tag{3.9}$$

Once the solution of eqn. 3.9, which is often referred to as the Lyapunov equation, is obtained the parameter optimization problem is accomplished by minimizing j. Since the optimization procedure was to be repeated for numerous grid points in the real power-reactive power domain, it was essential to use an efficient computer solution for the Lyapunov equation.

An algebraic method of solution of the equation, via a similarity transformation of the system matrices to companion form has been used. The method is given in detail in Appendix A and follows Molinari[22].

The optimization technique used to locate the minimum value of the performance criterion is the "Nelder and Mead" simplex method[23] which is the most efficient of all current sequential techniques[24]. In the simplex method, the objective function is evaluated at (k+1) mutually equidistant points in the space of the k independent variables. Such points being said to form the vertices of a regular simplex. The method is initiated by setting up a regular simplex in the space of the k independent variables, and evaluating the objective function at each vertex. The method, which is derivative free, then adapts itself to the local landscape, using reflected, expanded and contracted points to locate the minimum. The general iteration procedure is given in Appendix B.

Since the procedure described to evaluate the performance criterion is only valid if the system matrix A is asymptotically stable, the simplex method had to be modified to take that into consideration. A check on the eigen values locations of A was performed at every iteration prior to the evaluation of the performance criterion.

3.4 Adaptive Stabilizing Signals Design

The transfer function of the power stabilizer is given by:

$$G_c = K \frac{s}{(1+sT_1)(1+sT_2)} \tag{3.10}$$

where K, T_1, and T_2 are the parameters to be varied to compensate for load changes and optimize system performance.

This particular configuration of the stabilizer was chosen as the result of extensive studies of root-locus diagrams for numerous loading conditions. These studies have also shown that the choice $T_1 = T_2$ would give very close results to the case where T_1 is not equal to T_2.

With that in mind and in order to reduce the large computation costs associated with optimization techniques, T_1 was taken equal to T_2. The stabilizer transfer function in this case reduces to:

$$G_c = K \frac{s}{(1+sT)^2} \qquad \text{where} \qquad (T_1 = T_2 = T) .$$

Figure 3.2 represents the block diagram of the small-perturbation model for the single machine infinite bus system with the power stabilizer. The state equations for the complete system are given by:

$$\frac{d}{dt} X_1 = \omega_o X_2 \tag{3.11}$$

$$\frac{d}{dt} (X_2) = \frac{-K_1}{M} X_1 - \frac{K_2}{M} X_3 + \frac{\Delta P_m}{M} \tag{3.12}$$

$$\frac{d}{dt} (X_3) = \frac{X_4}{T'_{do}} - \frac{K_4}{T'_{do}} X_1 - \frac{X_3}{T'_{do} K_3} \tag{3.13}$$

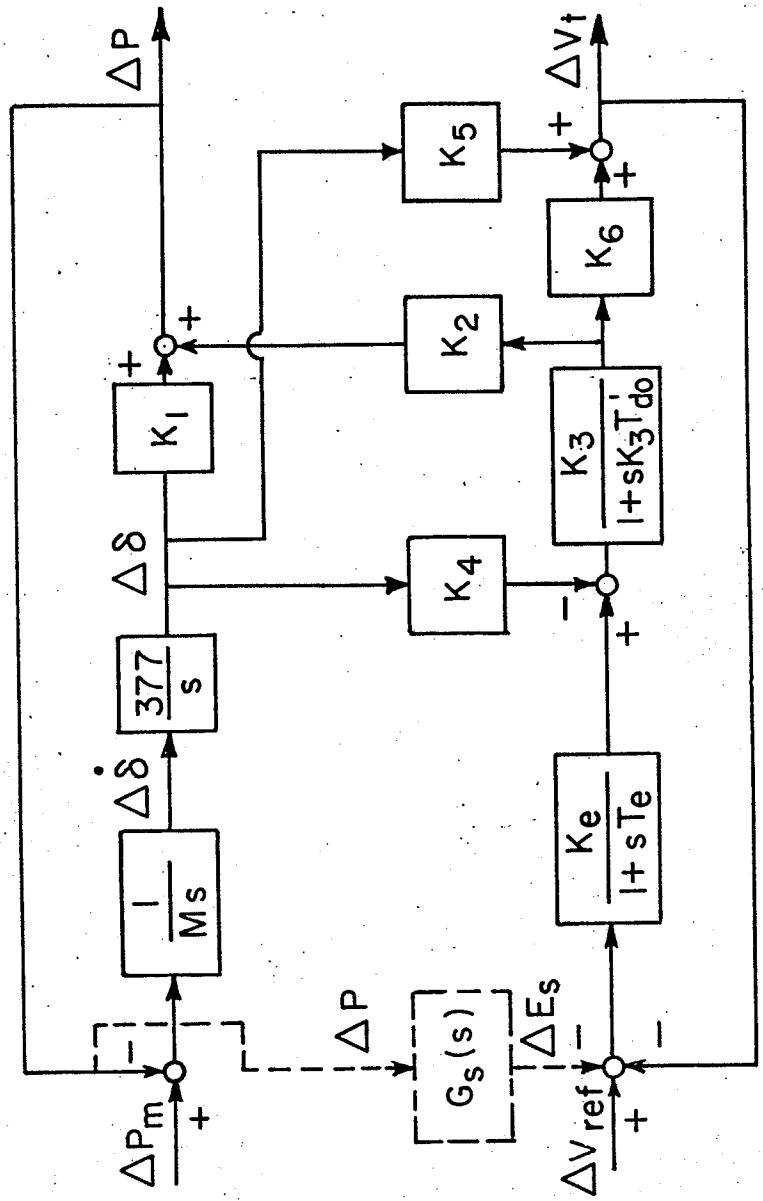

Fig. 3.2 Linearized small-perturbation block diagram of the single machine infinite bus system with the power stabilizer

$$\frac{d}{dt}(X_4) = \frac{-K_e K_5}{T_e} X_1 - \frac{-K_e K_6}{T_e} X_3 - \frac{X_4}{T_e} - \frac{X_6 K_e}{T_e} \qquad (3.14)$$

$$\frac{d}{dt}(X_5) = \frac{KK_1}{T} X_1 + \frac{KK_2}{T} X_3 - \frac{X_5}{T} \qquad (3.15)$$

$$\frac{d}{dt}(X_6) = \frac{KK_1}{T^2} X_1 + \frac{KK_2}{T^2} X_3 - \frac{X_5}{T^2} - \frac{X_6}{T} \qquad (3.16)$$

The system equations can be summarized in the canonical form:

$$\frac{d\underline{X}}{dt} = A\underline{X} + \Gamma\underline{U} \qquad (3.17)$$

where $\underline{X}$ and $\underline{U}$, the state vector and the perturbation vector respectively, are given by:

$$\underline{X} = [\Delta\delta,\ \Delta p\delta,\ \Delta E'_q,\ \Delta E_{fd},\ d_1,\ d_2] \qquad (3.18)$$

$$\underline{U} = [o,\ \Delta p_m,\ o,\ o,\ o,\ o] \qquad (3.19)$$

The system matrix A and the disturbance distribution matrix are given by:

$$A = \begin{bmatrix} 0 & \omega_o & 0 & 0 & 0 & 0 \\ \frac{-K_1}{M} & 0 & \frac{-K_2}{M} & 0 & 0 & 0 \\ \frac{-K_4}{T'_{do}} & 0 & \frac{-1}{T'_{do}K_3} & \frac{1}{T'_{do}} & 0 & 0 \\ \frac{-K_e K_5}{T_e} & 0 & \frac{-K_e K_6}{T_e} & \frac{-1}{T_e} & 0 & \frac{-K_e}{T_e} \\ \frac{K_1 K}{T} & 0 & \frac{K_2 K}{T} & 0 & \frac{-1}{T} & 0 \\ \frac{K_1 K}{T^2} & 0 & \frac{K_2 K}{T^2} & 0 & \frac{-1}{T^2} & \frac{-1}{T} \end{bmatrix} \qquad (3.20)$$

(for the case $T_1 = T_2 = T$)

$$\Gamma = \begin{bmatrix} 0 & \frac{1}{M} & 0 & 0 & 0 & 0 \end{bmatrix} \tag{3.21}$$

The system represented by eqn. 3.17 can be reduced to the form of eqn. 3.2 as follows:

The states are redefined in terms of their steady-state values, i.e.

$$X_i^1 \triangleq X_i - X_{iss} \qquad i = 1, 2, \ldots n \tag{3.22}$$

hence

$$\frac{d}{dt}(X_i^1) = \frac{d}{dt}(X_i) \tag{3.23}$$

Eqn. 3.17 becomes:

$$\frac{d}{dt}(\underline{X}^1) = A(\underline{X}^1 + \underline{X}_{ss}) + \Gamma\,\underline{U} \tag{3.24}$$

Therefore, the change of variables puts the system in the form:

$$\frac{d}{dt}(\underline{X}^1) = A\,\underline{X}^1 \quad ; \quad \underline{X}^1(o) = -\underline{X}_{ss} \tag{3.25}$$

This means that by redefining the states in terms of their steady-state values, the reference position of the system has been shifted. To prevent unnecessary notation problems, the superscript 1 will be dropped. Note that the matrix A remains unchanged.

For the partial case where U is a step-like perturbation, the steady state value of the state vector is given by:

$$\underline{X}_{ss} = -A^{-1}\,\Gamma \tag{3.26}$$

Numerical results

The system data are the same as given in Chapter 2. All the elements of the matrix W in eqn. 3.6 are assumed to be zero except for the second diagonal element. In other words, only speed excursions are penalized. Any other choice for the elements of matrix W is allowed.

A digital computer program was written that, when given the system equations, the terminal voltage (1.0 P.U.), and the real and reactive power loading of the machine, calculates the Heffron-Phillips constants K_1, K_2, ... K_6, and determines the values of the adjustable stabilizer parameters K and T that minimize the performance criterion. The computational flow graph is given in Figure 3.3. Several starting points were assumed, and a cross-check with CSMP* was performed. The procedure was repeated for the selected set of grid points in the real-power, reactive power domain. All combinations of P = 0 to P = 1.0, and Q = -0.3 to Q = 1.0 for steps of 0.1 were considered.

The optimum values of T and K , thus obtained, could be stored in the memory of the micro-processor. The stabilizer parameters can then be updated in step with the continuously monitored load changes. The result is: optimum performance

---

* Continuous system modelling program

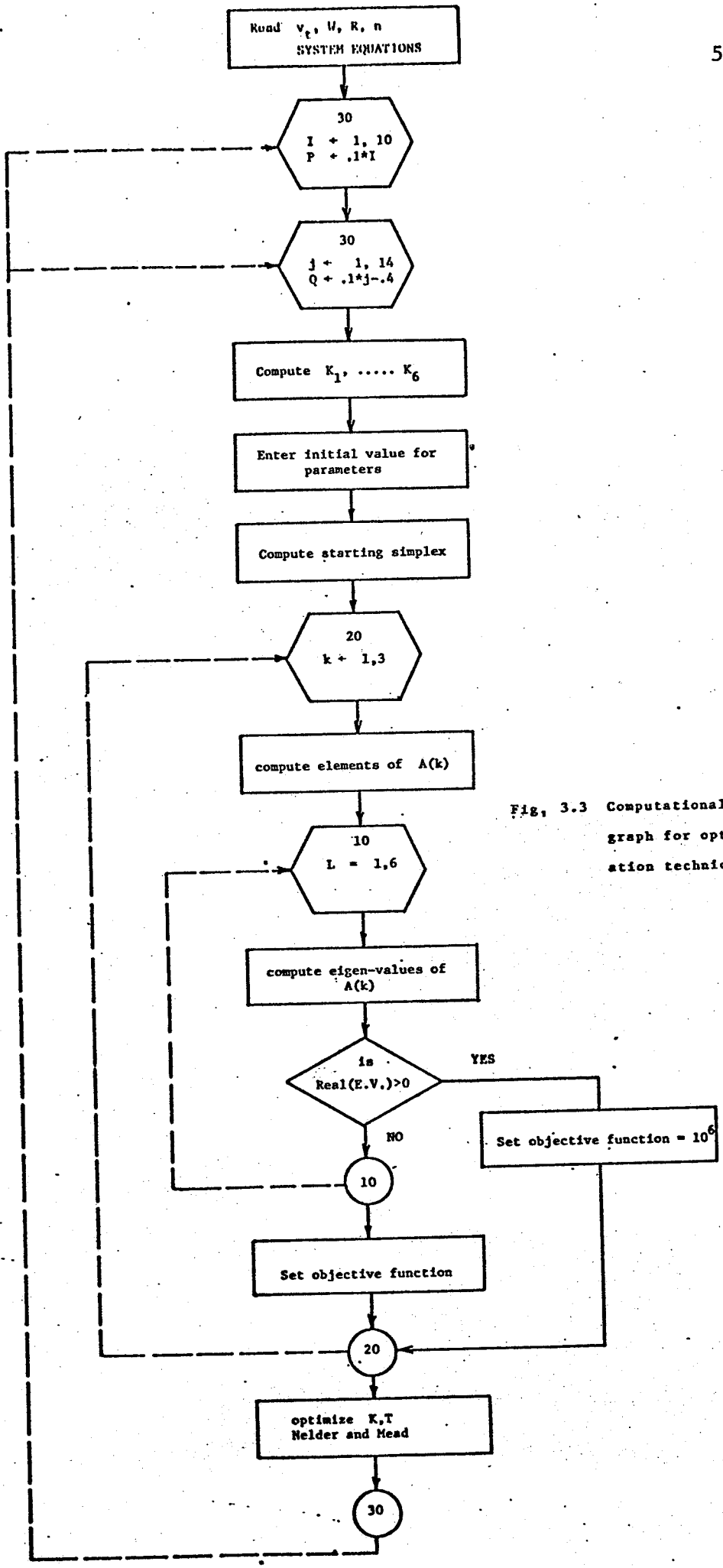

Fig. 3.3 Computational flow graph for optimization technique

for a wide loading range.

Tables I and II show the optimum values of the adjustable stabilizer parameters K and T for 140 different points in the loading range considered. It is evident that - if optimum performance is to be maintained over the entire loading range - the structure of the stabilizer has to be altered.

3.5 Analog Computer Tests and Results

The single machine-infinite bus system with the optimum stabilizer gain and time constants was simulated on a TR-48 analog computer. A step-like disturbance in mechanical torque was used to perturb the system from its operating state. Figure 3.4 - 3.19 are sample results of the analog study illustrating some significant aspects of the system response. The traces shown are deviations in speed. The system responses displayed are for three cases:

i) Excitation system unsupplemented.

ii) Settings of the power stabilizer parameters kept fixed - irrespective of load changes - corresponding to a particular design point (P = 1.0, Q = -.3) originally unstable.

iii) Optimum settings for the power stabilizer parameters altered with loading as given by Tables I and II.

From the results, it is observed that:

1) The power stabilizer considered significantly

TABLE I

Variation of stabilizer gain K with real and reactive loading

	P=0.1	P=0.2	P=0.3	P=0.4	P=0.5	P=0.6	P=0.7	P=0.8	P=0.9	P=1.0
Q = -0.3	4.265	0.757	0.204	0.138	0.134	0.143	0.157	0.173	0.195	0.217
Q = -0.2	5.350	1.469	0.493	0.249	0.190	0.176	0.179	0.190	0.206	0.224
Q = -0.1	5.987	2.053	0.853	0.433	0.284	0.234	0.219	0.218	0.226	0.241
Q = 0.0	5.976	2.499	1.181	0.646	0.415	0.317	0.272	0.258	0.258	0.268
Q = 0.1	6.246	2.822	1.479	0.872	0.562	0.414	0.343	0.313	0.297	0.298
Q = 0.2	6.459	3.115	0.727	1.059	0.721	0.531	0.427	0.376	0.350	0.341
Q = 0.3	6.629	3.319	1.951	1.246	0.869	0.646	0.523	0.447	0.409	0.390
Q = 0.4	6.766	3.488	2.149	1.409	1.013	0.801	0.603	0.531	0.471	0.447
Q = 0.5	8.027	3.698	2.439	1.765	1.265	0.898	0.726	0.602	0.531	0.512
Q = 0.6	8.322	3.674	2.579	1.762	1.308	1.015	0.839	0.691	0.608	0.589
Q = 0.7	9.946	3.688	2.718	1.946	1.515	1.206	0.954	0.814	0.707	0.669
Q = 0.8	10.084	4.533	2.855	2.207	1.685	1.291	1.107	0.926	0.810	0.761
Q = 0.9	10.063	4.570	3.002	2.290	1.854	1.459	1.197	1.047	0.911	0.867
Q = 1.0	10.506	5.168	3.083	2.464	1.938	1.636	1.368	1.182	1.021	0.987

TABLE II

Variation of Stabilizer Time Constant T with Real and Reactive Loading

	P=0.1	P=0.2	P=0.3	P=0.4	P=0.5	P=0.6	P=0.7	P=0.8	P=0.9	P=1.0
Q = -0.3	1.602	1.030	0.525	0.356	0.299	0.276	0.267	0.263	0.264	0.267
Q = -0.2	1.391	1.069	0.703	0.474	0.369	0.320	0.297	0.286	0.281	0.279
Q = -0.1	1.229	1.031	0.784	0.575	0.444	0.374	0.336	0.314	0.302	0.297
Q = 0.0	1.081	0.977	0.804	0.636	0.508	0.427	0.374	0.345	0.327	0.318
Q = 0.1	0.969	0.918	0.795	0.668	0.553	0.469	0.413	0.378	0.353	0.339
Q = 0.2	0.895	0.872	0.779	0.675	0.585	0.507	0.448	0.409	0.381	0.363
Q = 0.3	0.833	0.826	0.759	0.677	0.602	0.531	0.479	0.437	0.407	0.387
Q = 0.4	0.779	0.788	0.742	0.673	0.613	0.567	0.494	0.463	0.430	0.410
Q = 0.5	0.798	0.765	0.744	0.711	0.648	0.572	0.525	0.479	0.449	0.434
Q = 0.6	0.769	0.719	0.725	0.675	0.630	0.584	0.545	0.502	0.471	0.459
Q = 0.7	0.801	0.685	0.703	0.678	0.659	0.621	0.564	0.531	0.497	0.483
Q = 0.8	0.772	0.722	0.698	0.695	0.664	0.613	0.595	0.553	0.522	0.508
Q = 0.9	0.744	0.702	0.689	0.693	0.674	0.639	0.599	0.576	0.545	0.535
Q = 1.0	0.739	0.726	0.680	0.695	0.670	0.655	0.630	0.602	0.569	0.564

increases the dynamic stability of the system.

2) Altering the structure of the stabilizer to cope with changes in real and/or reactive power loadings, maintains optimum performance for a wide range of system operating conditions.

3) The variable structure power stabilizer provides more damping for the machine speed swings than that obtained from a fixed structure power stabilizer. This is particularly noticeable away from the design point.

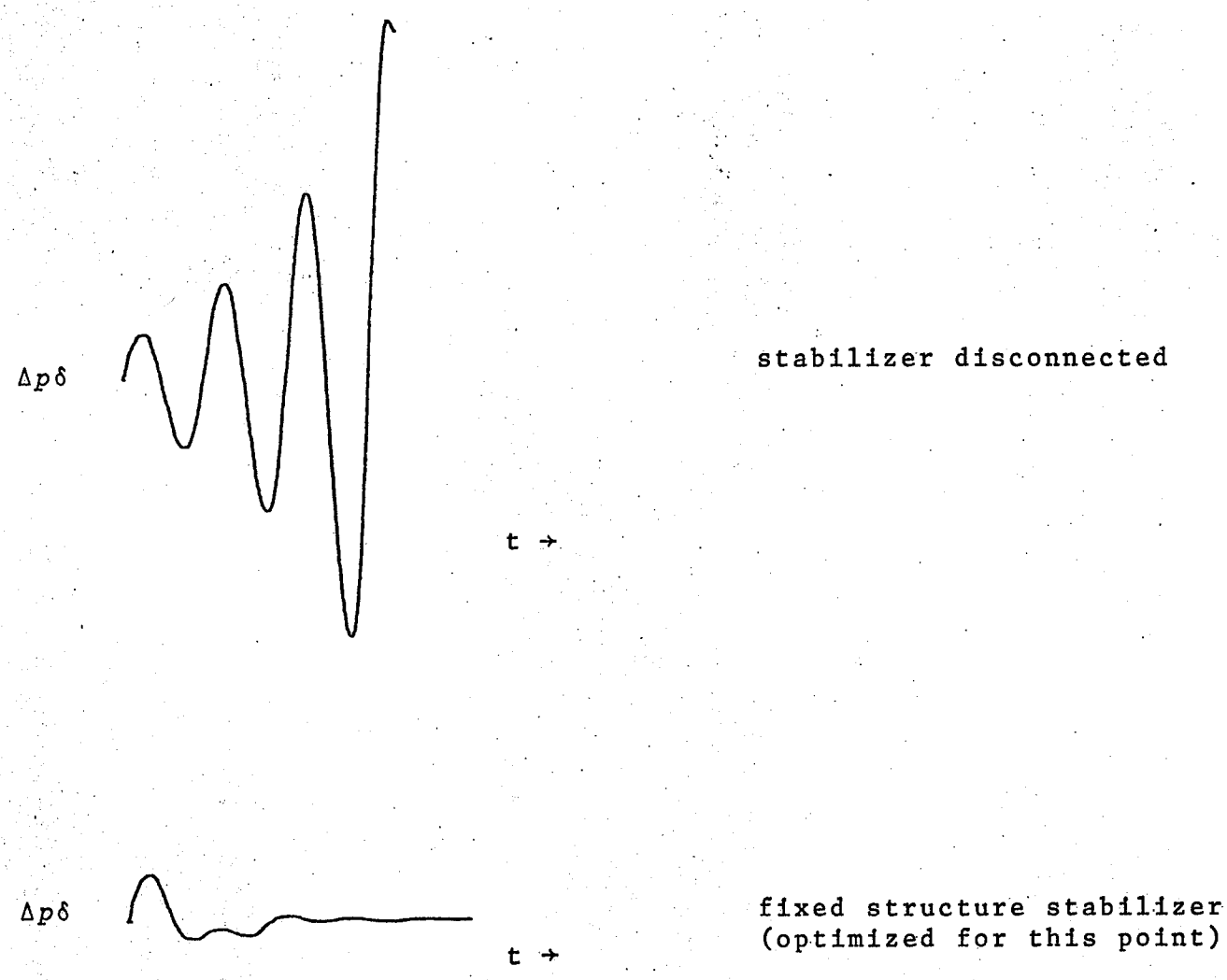

Fig. 3.4 Speed deviation for the fixed structure stabilizer design point: P = 1.0 , Q = -0.3 following a step disturbance in mechanical torque

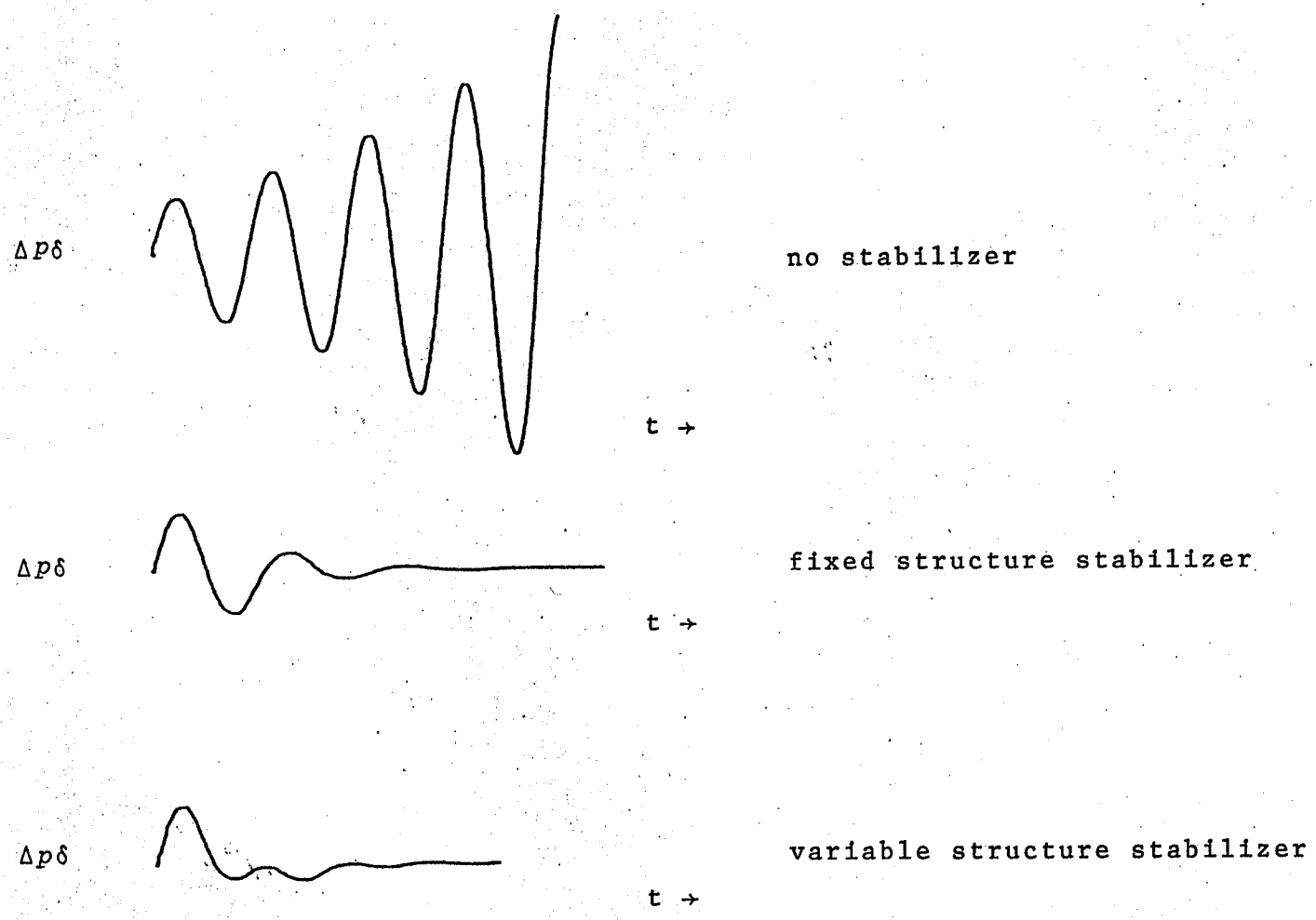

Fig. 3.5 Speed deviation following a small step disturbance in mechanical torque. Loading : P = 1.0 , Q = 1.0

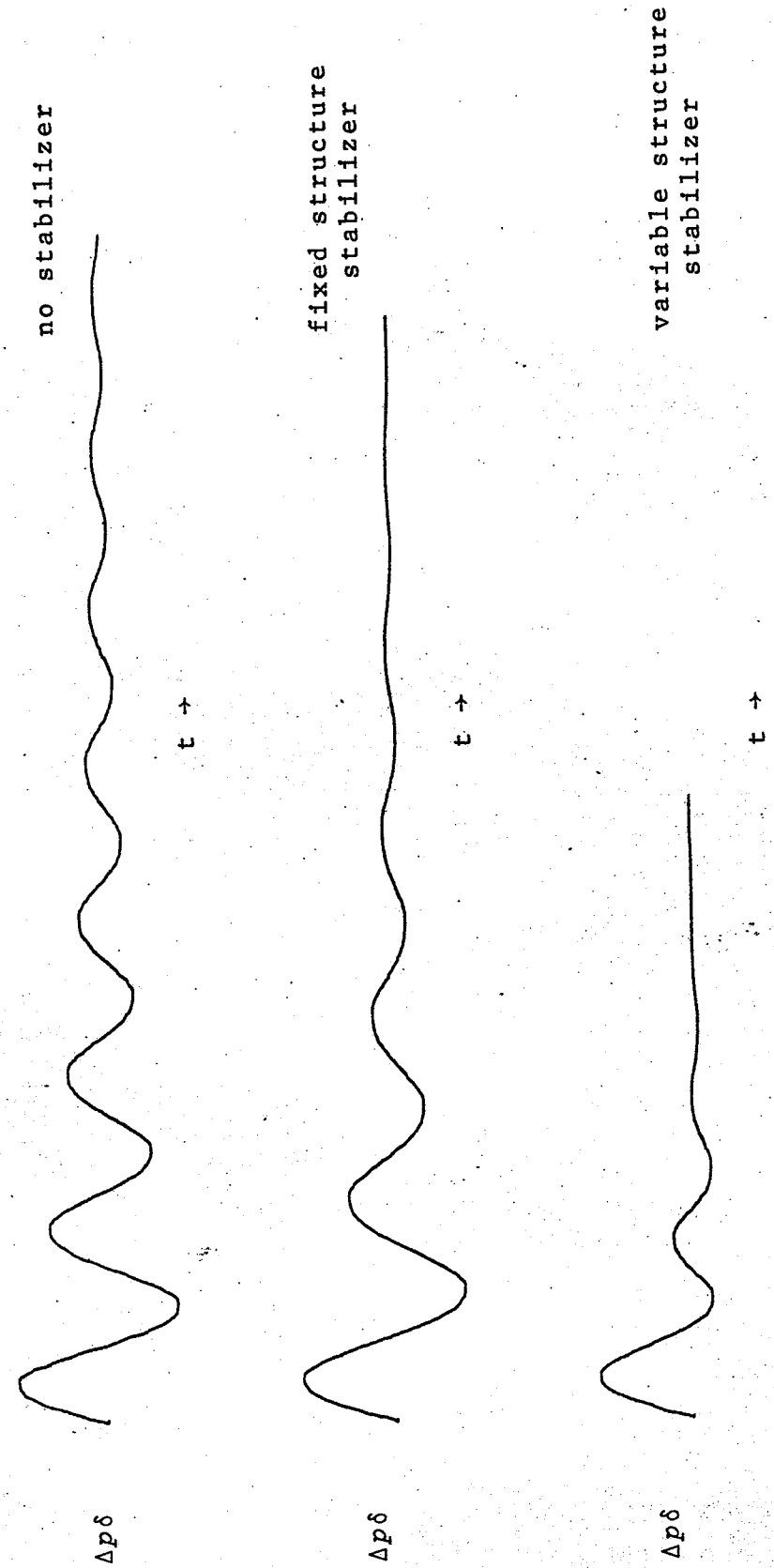

Fig. 3.6 Speed deviation following a small step disturbance in mechanical torque. Loading: P = 0.1 , Q = -0.3

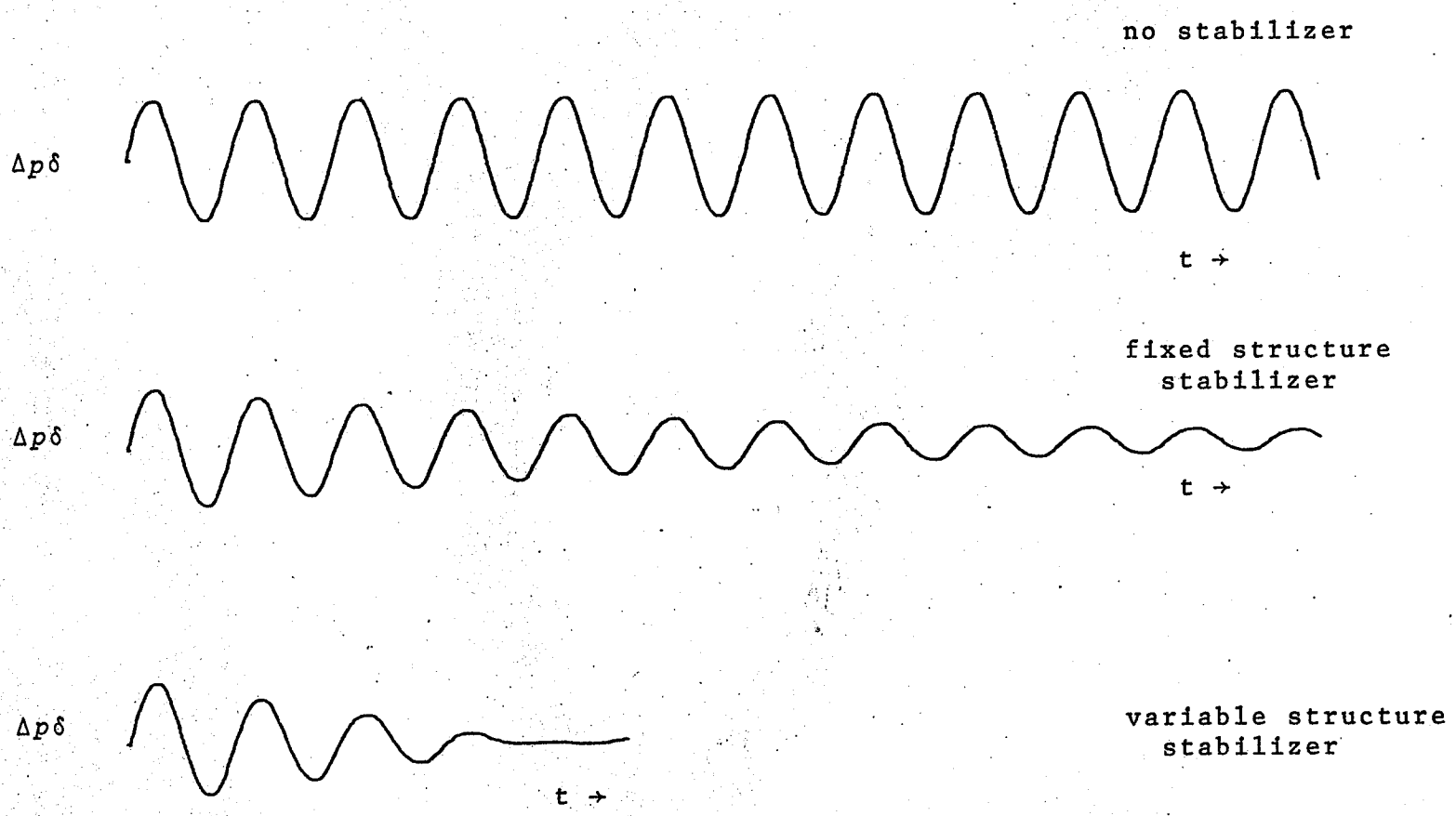

Fig. 3.7 Speed deviation following a small step disturbance in mechanical torque. Loading: P = 0.1 , Q = 1.0

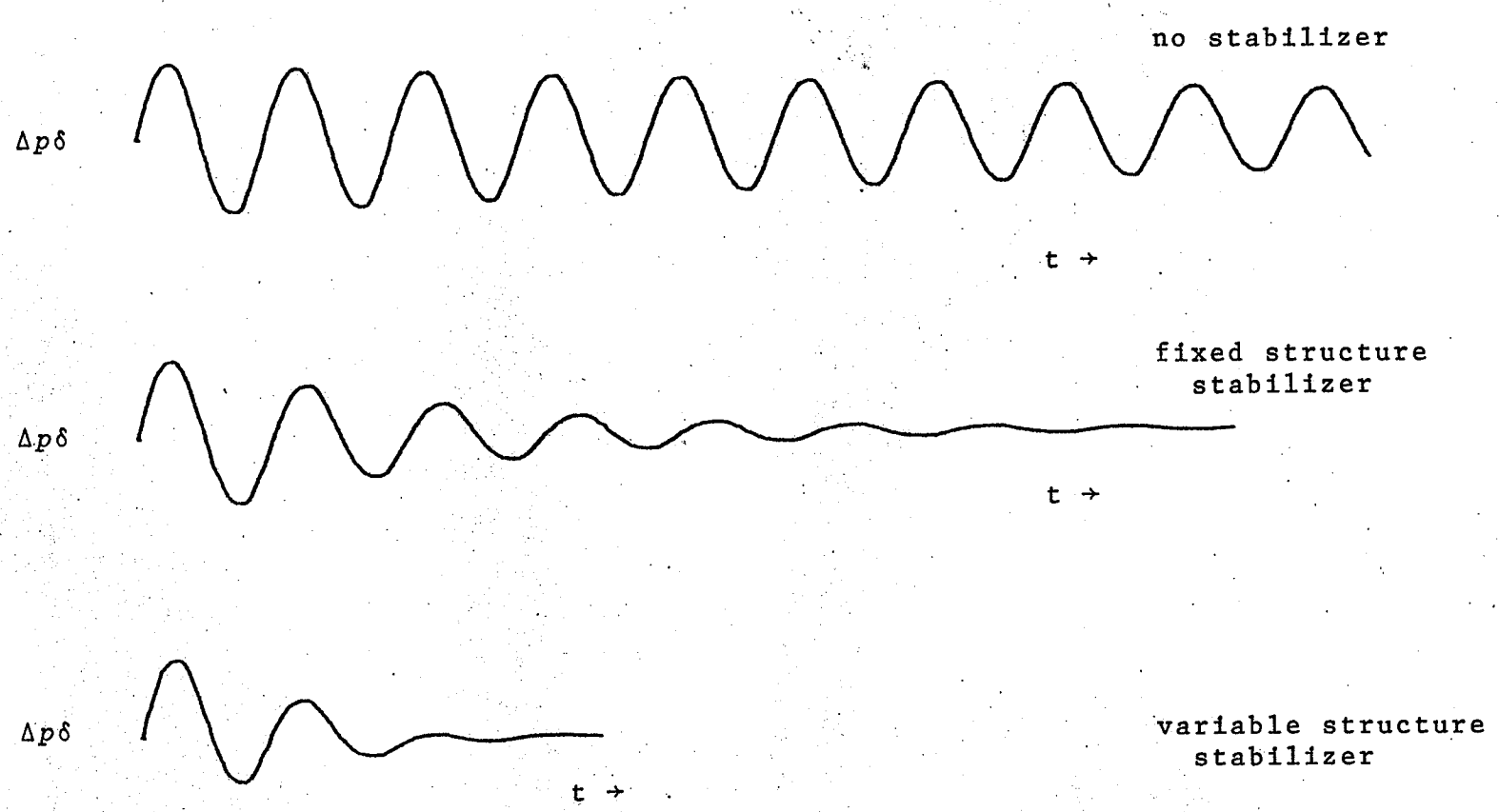

Fig. 3.8 Speed deviation following a small step disturbance in mechanical torque. Loading: P = 0.1 , Q = 0

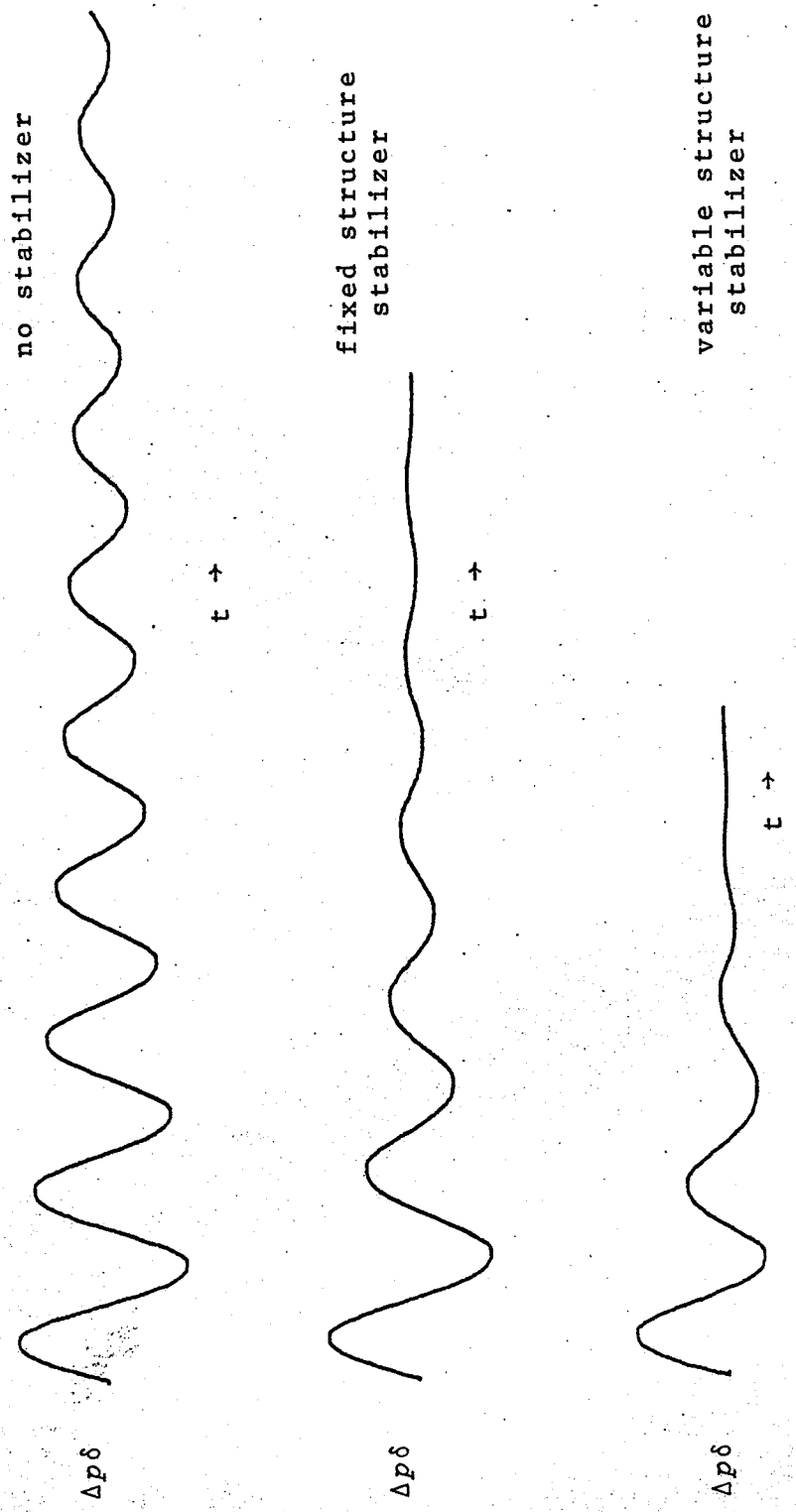

Fig. 3.9 Speed deviation following a small step disturbance in mechanical torque. Loading: P = 0.1 , Q = -0.2

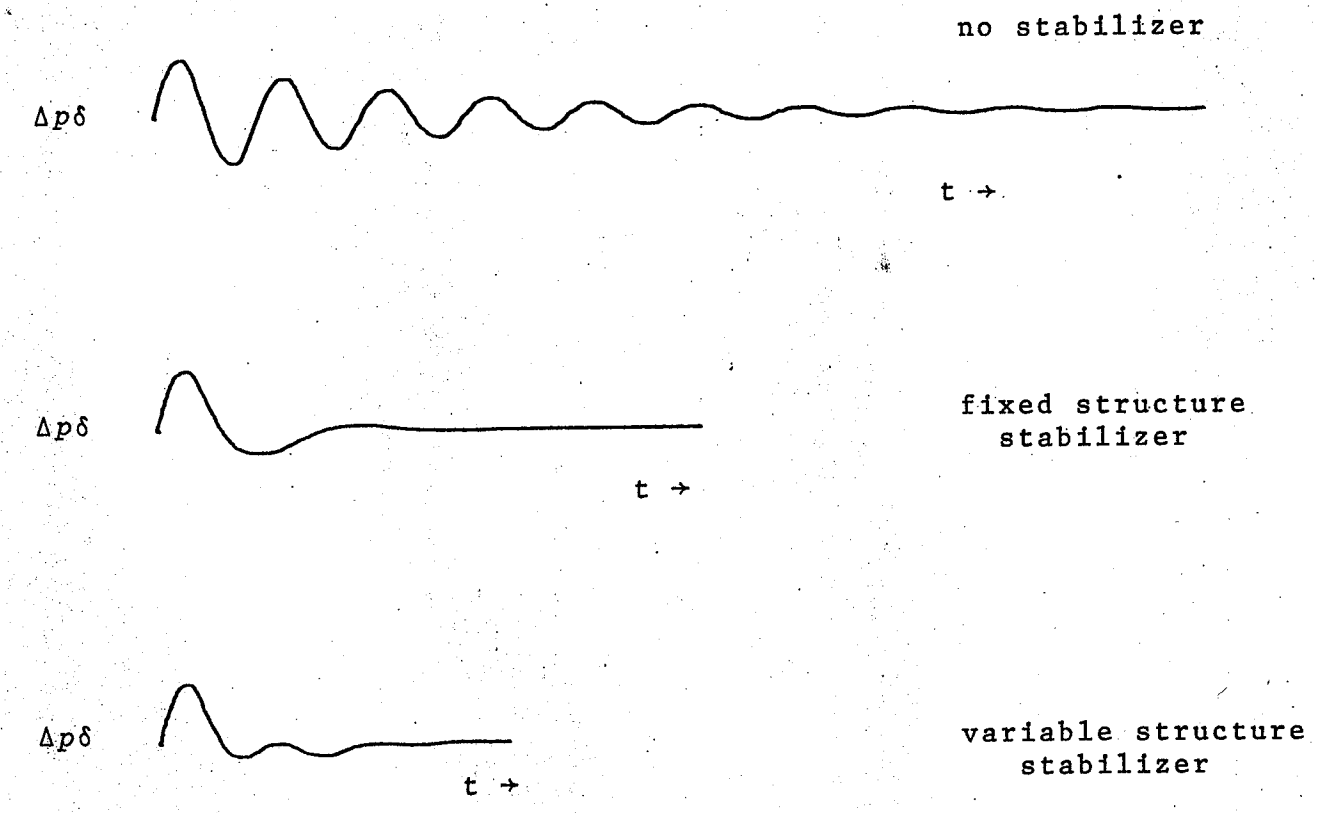

Fig. 3.10 Speed deviation following a small step disturbance in mechanical torque. Loading: P = 0.5 , Q = 0

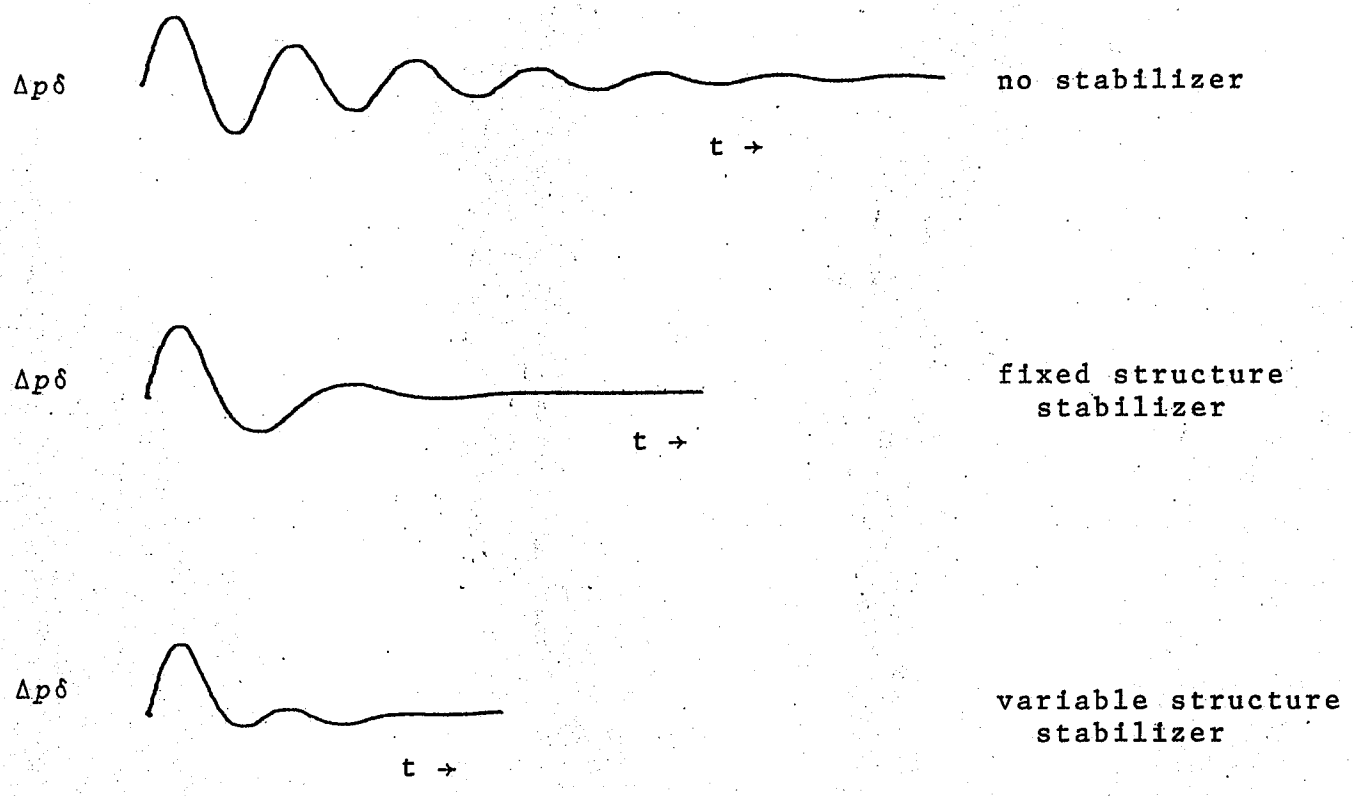

Fig. 3.11 Speed deviation following a small step disturbance in mechanical torque. Loading: P = 0.3 , Q = -0.1

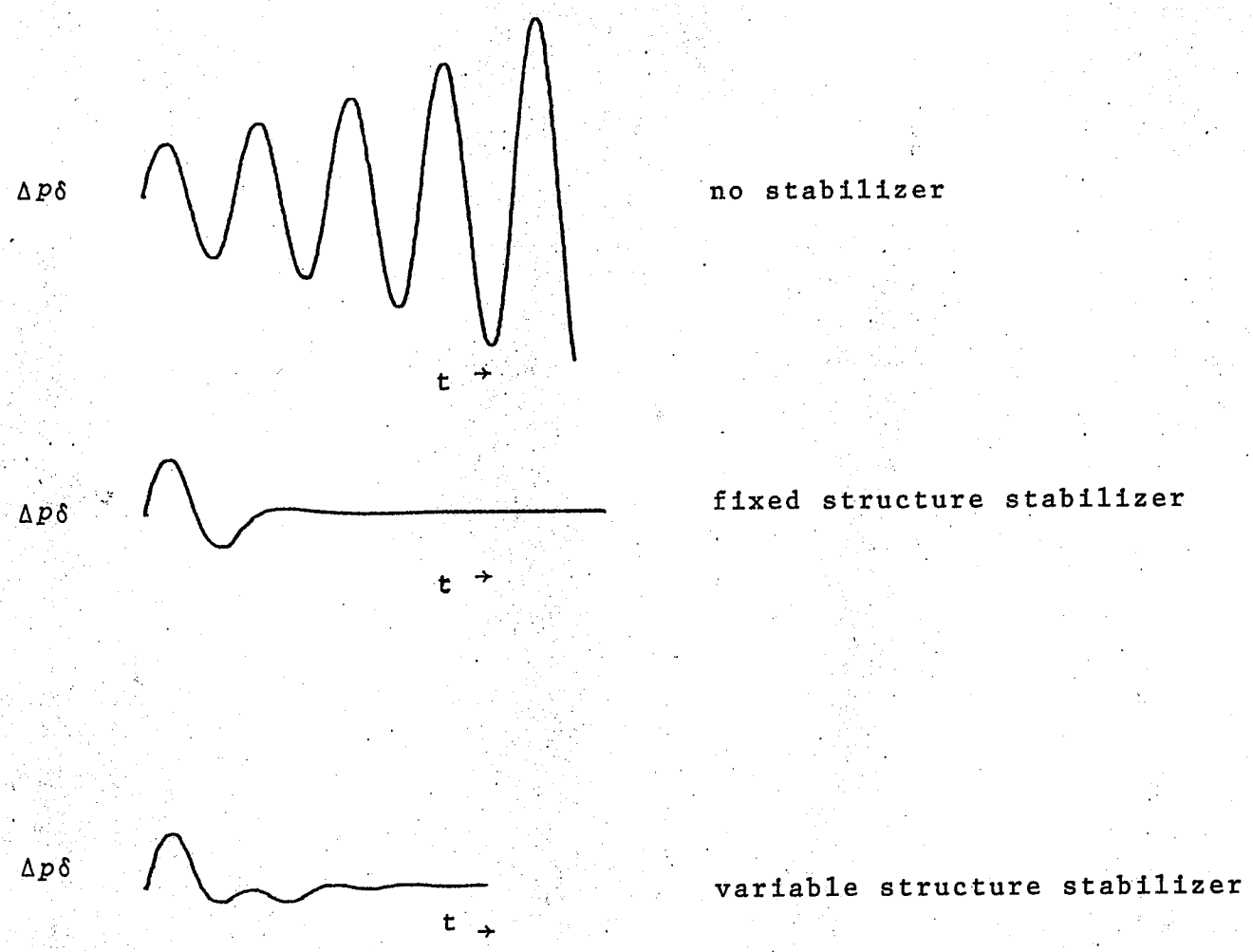

Fig. 3.12 Speed deviation following a small step disturbance in mechanical torque. Loading: P = 1.0 , Q = 0.6

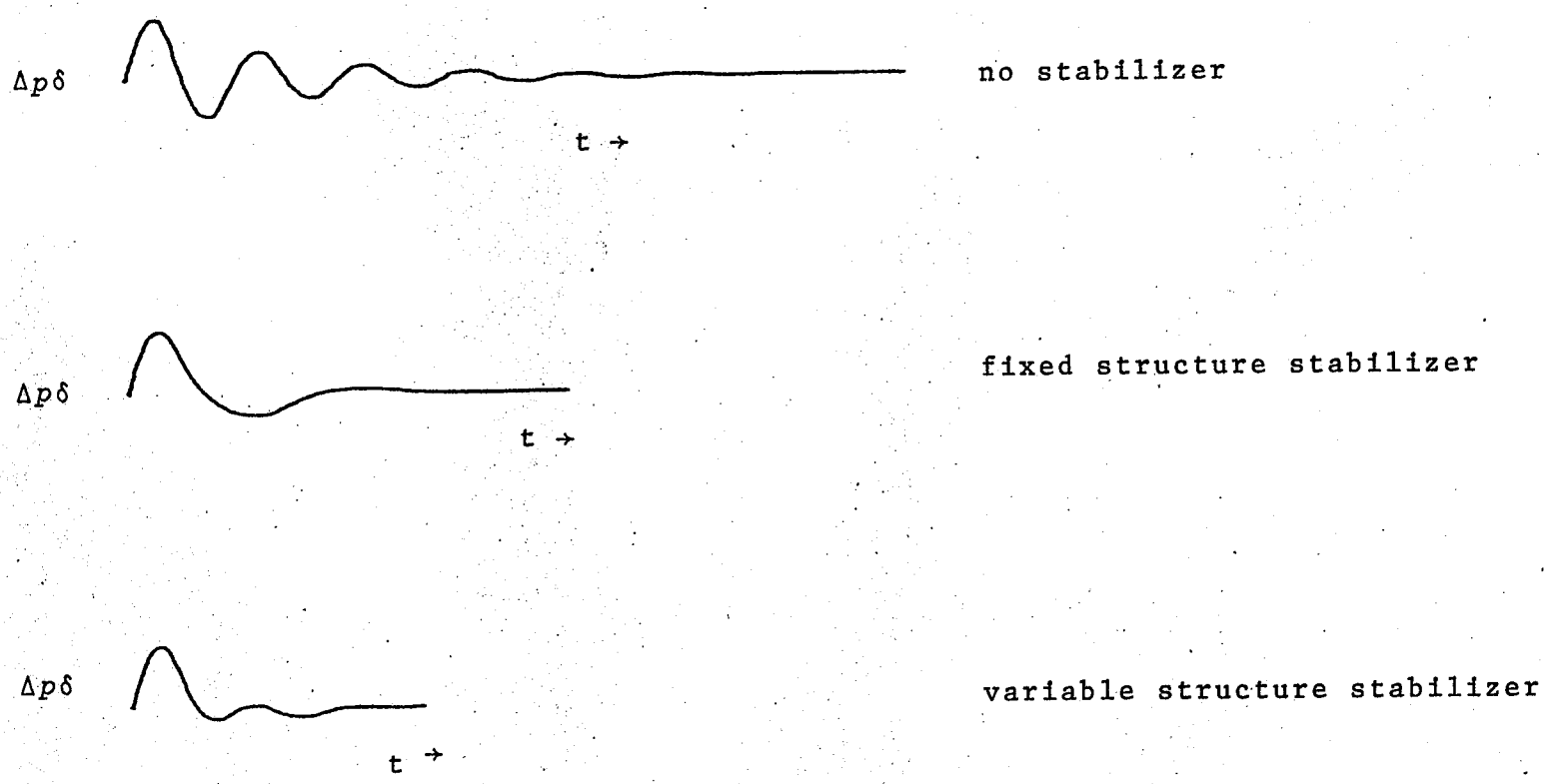

Fig. 3.13 Speed deviation following a small step disturbance in mechanical torque. Loading: P = 0.4 , Q = -0.2

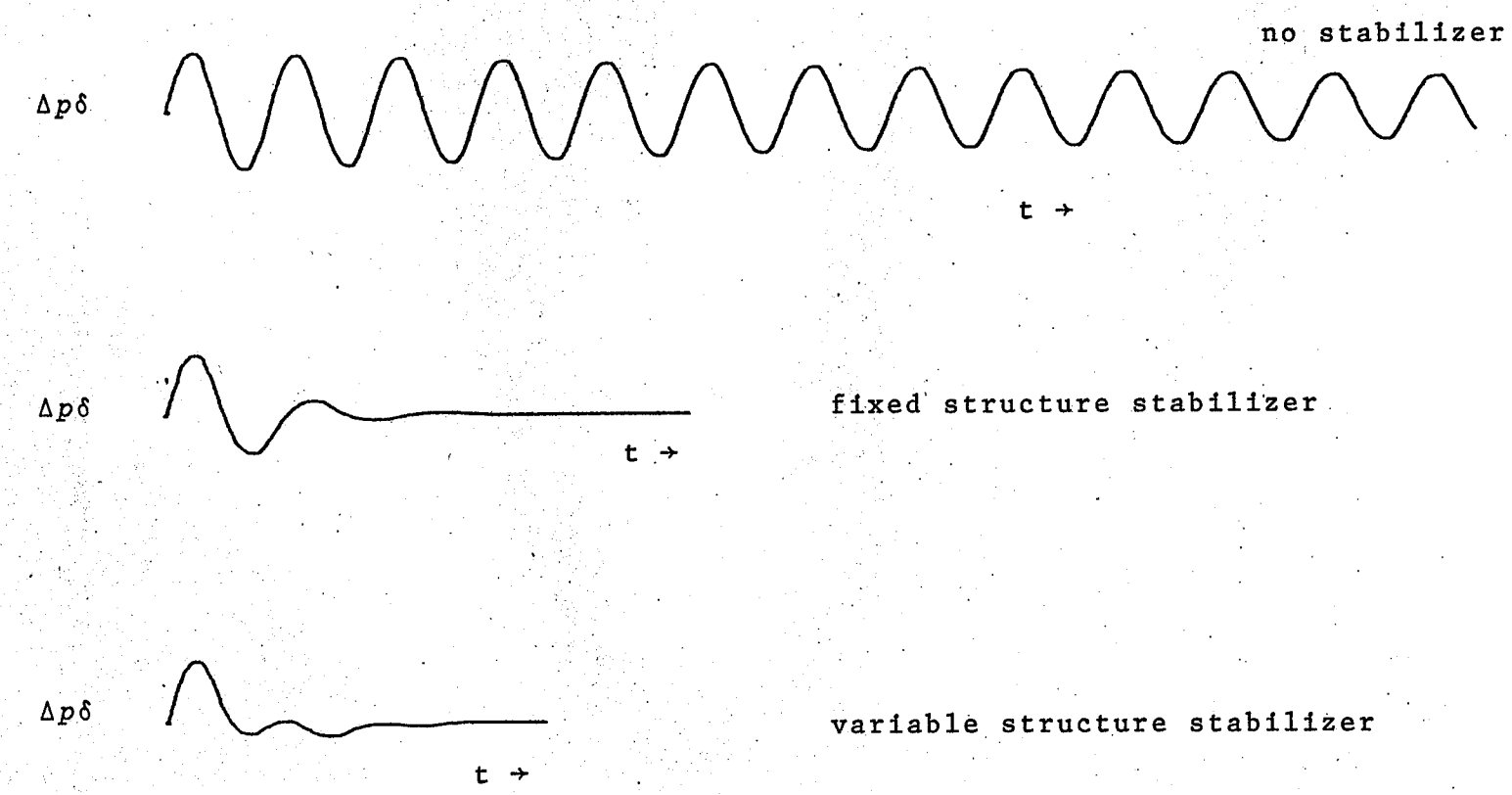

Fig. 3.14 Speed deviation following a small step disturbance in mechanical torque. Loading: P = 0.5 , Q = 0.5

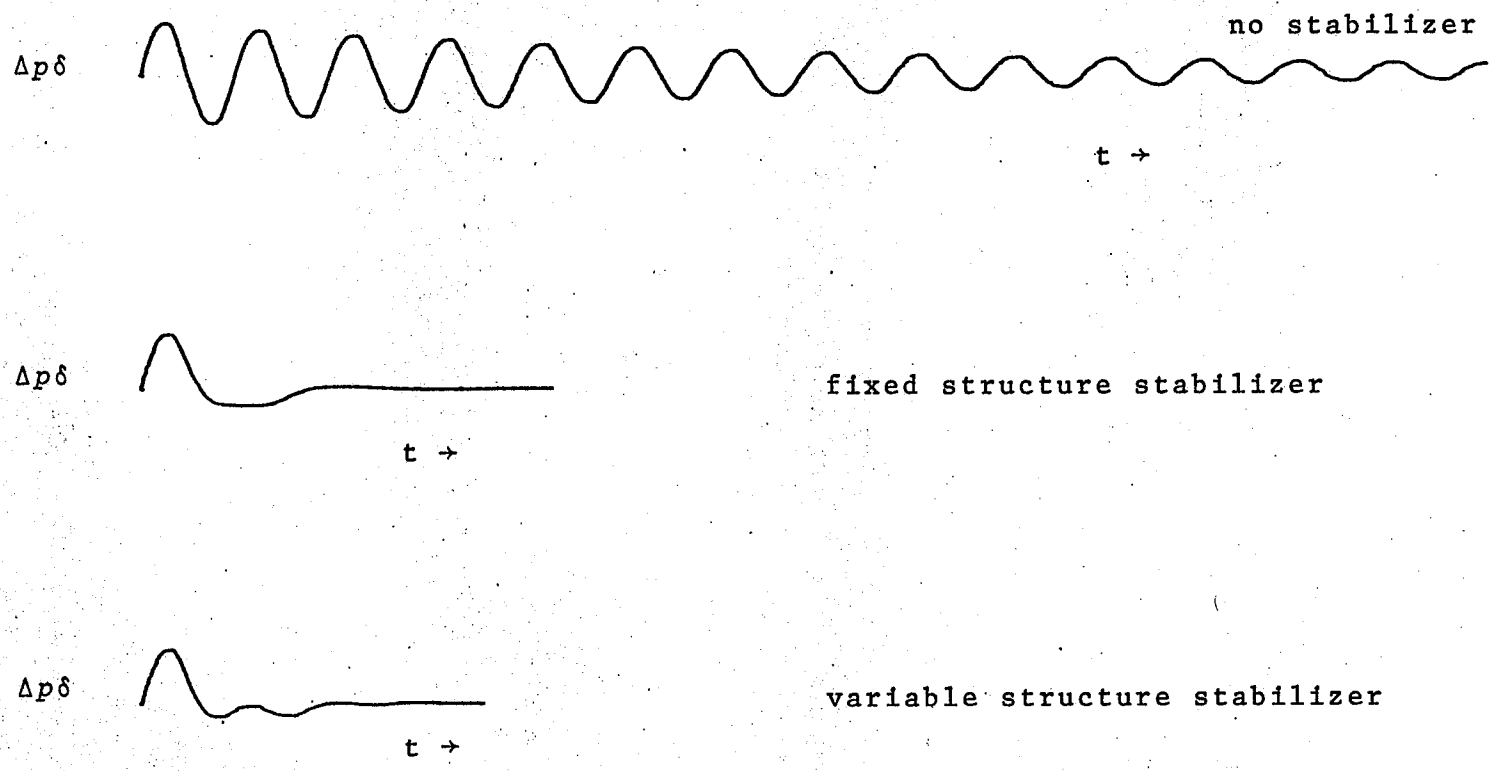

Fig. 3.15 Speed deviation following a small step disturbance in mechanical torque. Loading: P = 0.7 , Q = 0.

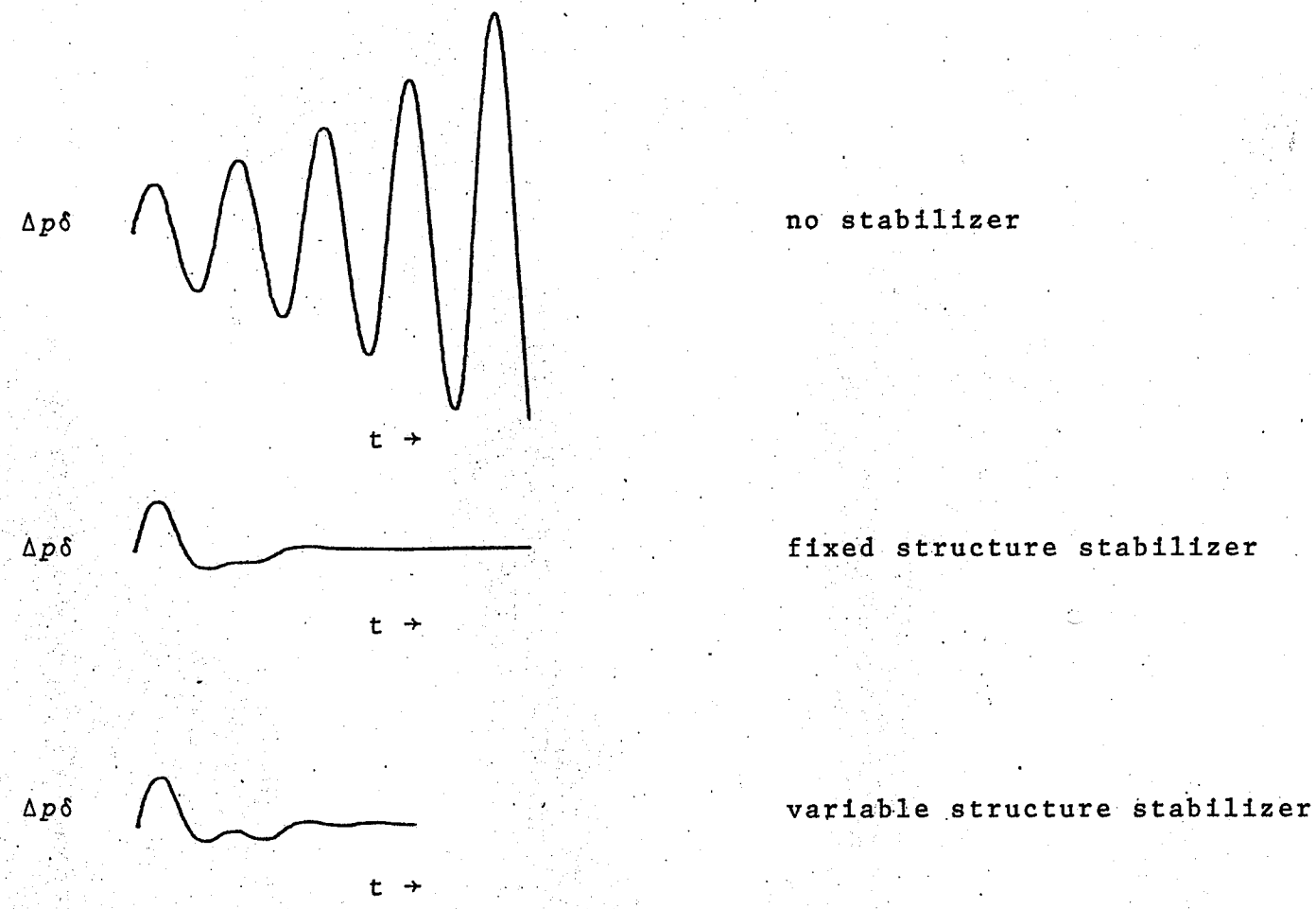

Fig. 3.16 Speed deviation following a small step disturbance in mechanical torque. Loading: P = 1.0 , Q = 0.

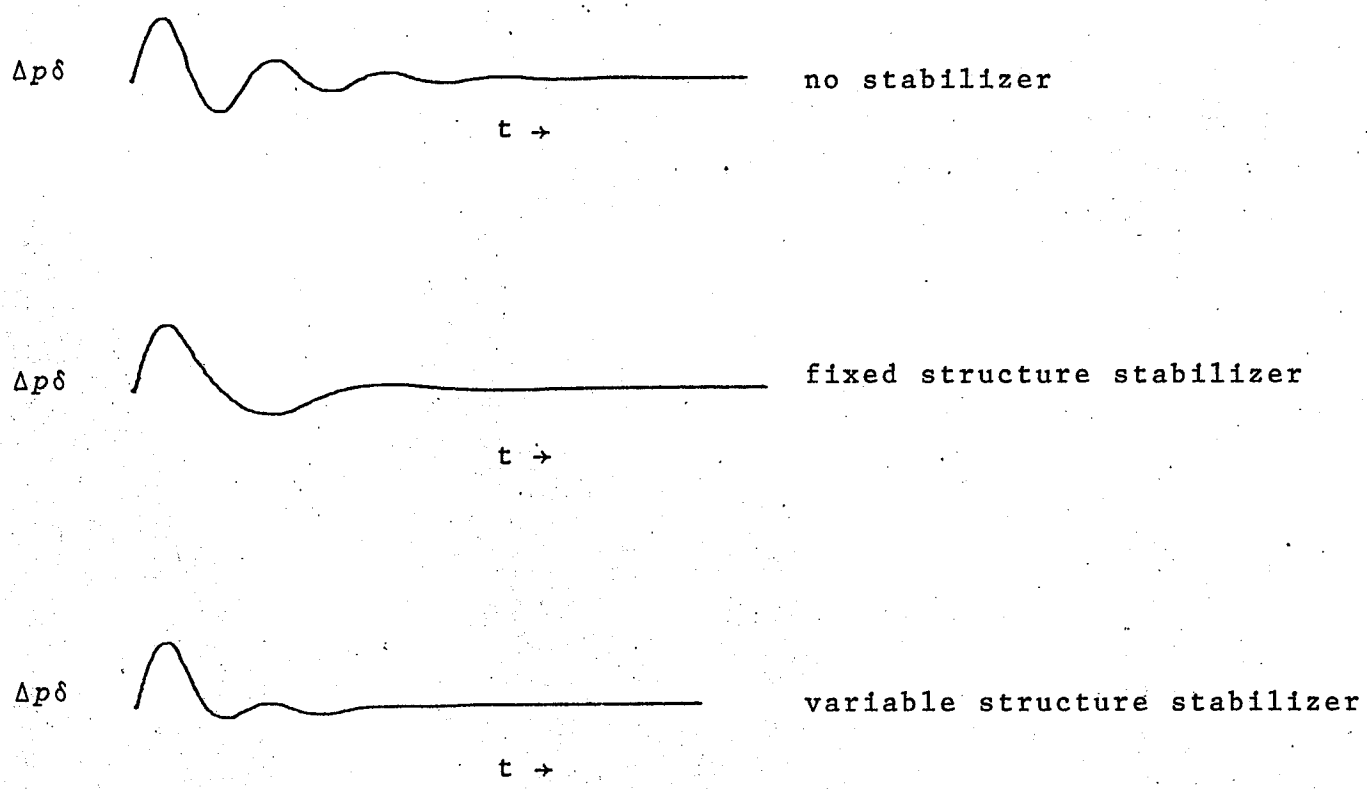

Fig. 3.17 Speed deviation following a small step disturbance in mechanical torque. Loading: P = 0.3 , Q = -0.3

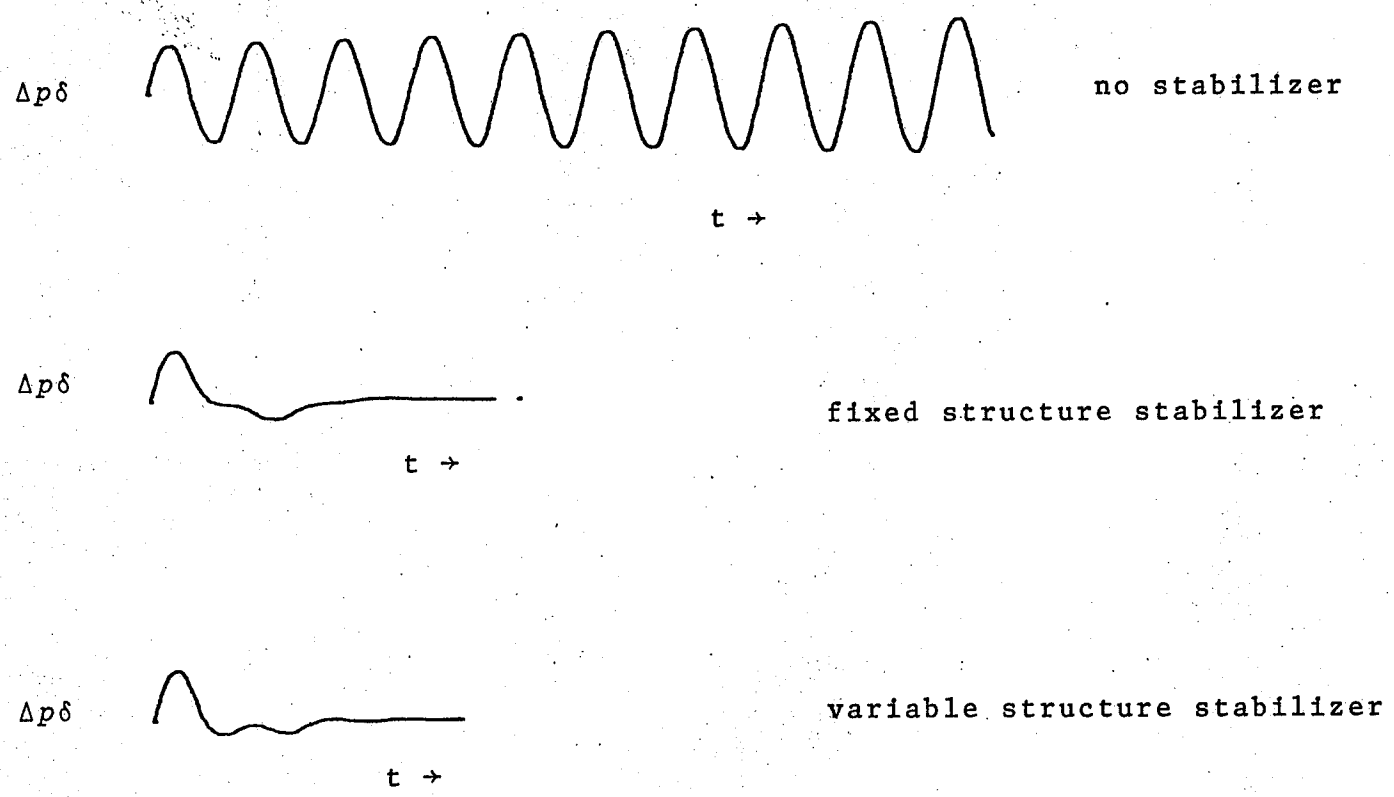

Fig. 3.18 Speed deviation following a small step disturbance in mechanical torque. Loading: P = 0.7 , Q = -0.3

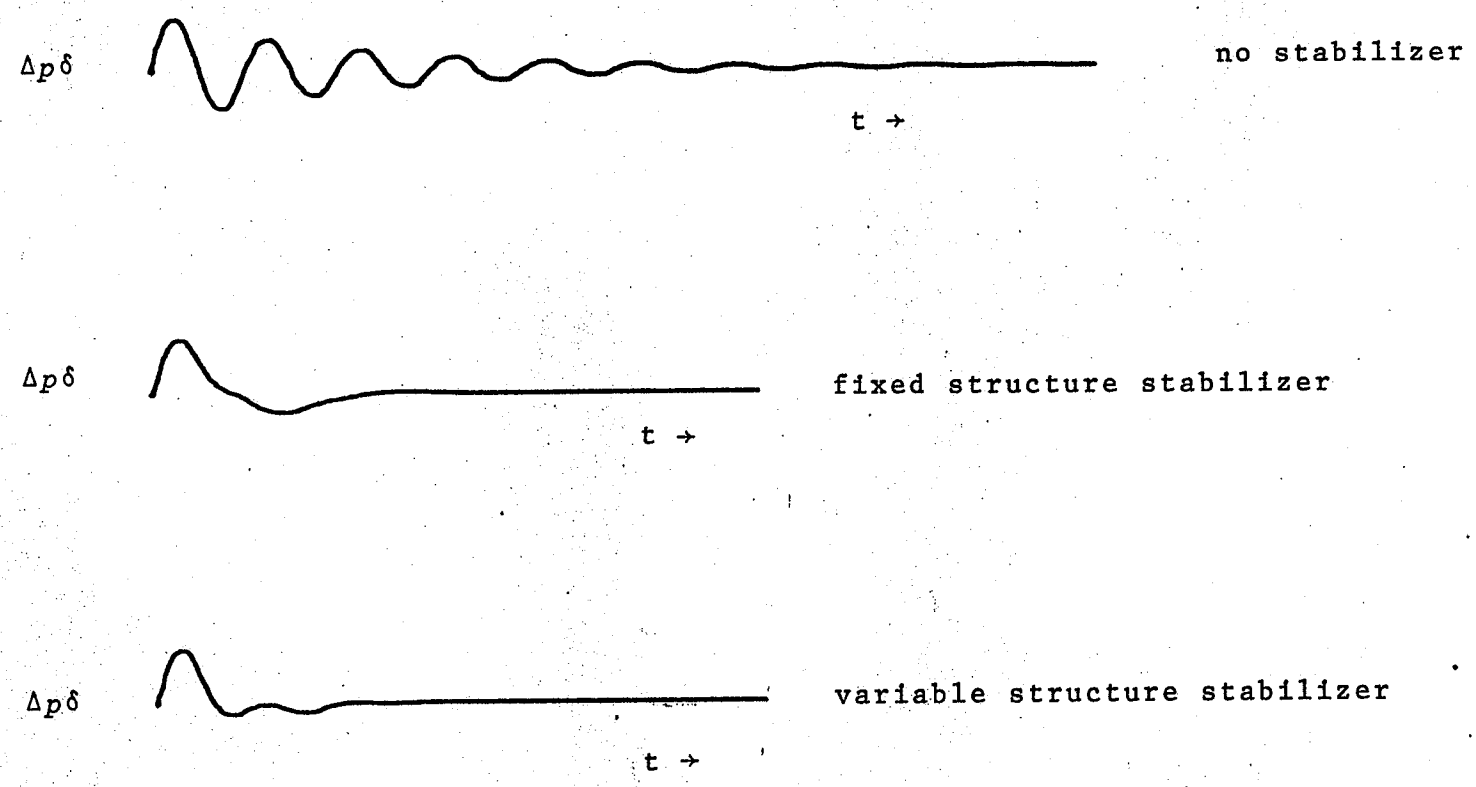

Fig. 3.19 Speed deviation following a small step disturbance in mechanical torque. Loading: P = 0.5 , Q = -0.3

Chapter four

A MODEL REFERENCE ADAPTIVE CONTROLLER TO COMPENSATE FOR VARIATIONS OF THE INCREMENTAL SPEED REGULATION WITH LOAD

4.1 Problem Description

In general, power system disturbances caused by load changes result in the deviation of several parameters from their nominal or design values. In particular, generator-governing characteristics representing steady-state frequency-power output curves are not straight line over the full-range of operation. Instead, a typical characteristic[30,31] has an irregular pattern of piecewise straight line segments as shown in Figure 4.1. The negative of the slope of each segment represents the incremental speed regulation, which depending on the load level may vary widely over the full range of operation[32].

Due to the fact that controller design is conventionally based on constant plant parameter values, it is easily recognizable that any changes in the plant parameters from their nominal values will de-rate the system design performance. One design approach is to use sophisticated control theories to design controllers insensitive to changes in the controlled system. An alternative design approach is to use adaptive control techniques.

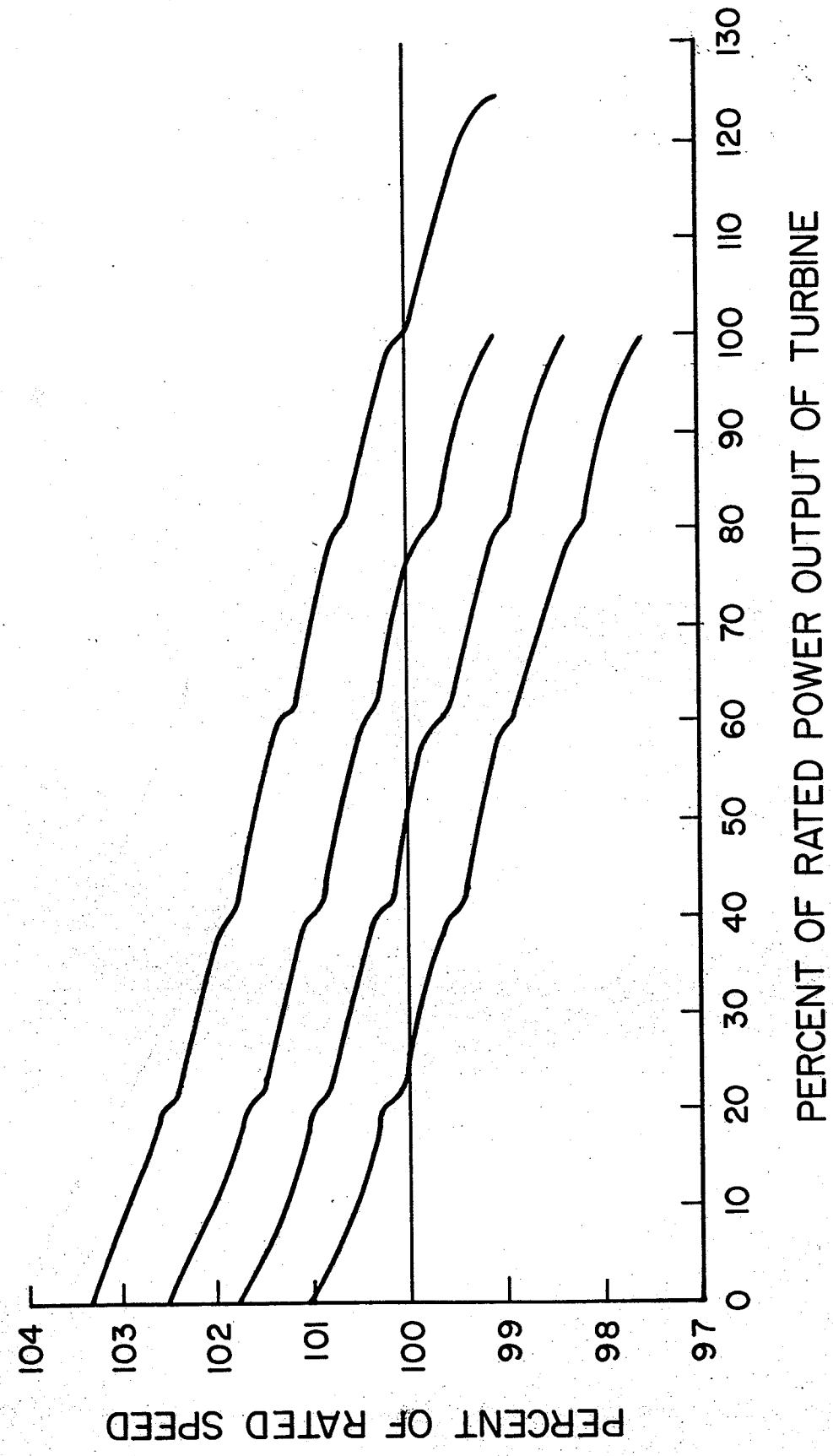

Fig. 4.1 Typical speed-power output curves for different speed changer settings

It is shown in this chapter that the model reference adaptive control concept can be successfully used to compensate for the variations of the incremental speed regulation parameter caused by incremental load changes. The analysis is done by examining the case of a steam turbo-alternator on isolated load. Several model reference adaptive control (MRAC) techniques are considered. A brief review on the MRAC techniques is presented in the next section.

4.2 Model Reference Adaptive Technique

One of the general categories into which the broad scope of adaptive control systems may be subdivided is referred to as the model-reference adaptive control approach. The MRAC has been a popular approach to the control of systems operating in the presence of parameter and environmental variations. In such a scheme, the desirable dynamic characteristics of the plant are specified in a reference model, and the controllable parameters of the plant are adjusted continuously or discretely, so that its response will duplicate that of the model as closely as possible. The identification of the plant dynamics is not necessary and hence a fast adaptation can be achieved.

Generally speaking, there are two approaches to the synthesis of MRAC systems: one is based on the minimization of a performance index and the other on a Lyapunov

function. Each of these approaches has its own merits and limitations. A brief but up-to-date survey on the various MRAC techniques is in order. For a more detailed account of the different design rules, refer to Landau[33].

The MRAC system was first designed by the performance index minimization method proposed by Whitaker[34] of the M.I.T. instrumentation laboratory and has since then been referred to as the M.I.T. design rule. The performance index is the integral squared of the response error. This rule has been very popular due to its simplicity in practical implementation. An improved design rule with respect to the speed of response has then been proposed by Donaldson[35] who used a more general performance index than that of Whitaker, but additional filters and the measurements of the state vectors are required.

The need of the sensitivity filters can be avoided by a gradient method developed later on by Dressler[36]. Price[37] suggested an accelerated gradient method which is easy to implement and is capable of achieving faster adaptations compared with other gradient techniques.

A design rule based on the application of sensitivity analysis but with only one sensitivity filter for the multivariable parameter adjustments, has been developed by Kokotovic et al[38,39]. Winsor[40] has also modified the M.I.T. Rule to reduce the sensitivity of the response to the loop

gain, at the expense of additional instrumentation. In all the design rules mentioned, a good compromise between the stability and the speed of adaptation will have to be decided by simulation studies.

Green[41] extended the work of Dressler by solving the global stability problem. However, the adaptive rule is not attractive because the first derivatives of the state vectors are often required for its implementation.

In the Lyapunov synthesis approach, the adaptive rule is obtained by selecting the design equations to satisfy conditions derived from Lyapunov's second method, so that the system stability is guaranteed for all inputs. Butchart and Shakcloth[42] first suggested the use of a quadratic Lyapunov function, which was employed later on by Parks[43] to redesign systems formerly designed by the M.I.T. rule. The use of different Lyapunov functions by Phillipson[44] and Gilbert et al[45] has resulted in the introduction of feed forward loops that would improve the damping of the adaptive response. The main disadvantage of the Lyapunov synthesis approach is that the entire state vector must be available for measurement, which is not often possible. Recent efforts by Monopoli[46] have permitted one to eliminate or reduce the number of differentiators required for implementing the design rule. Currie and Stear[47] have suggested the use of a Kalman filter to avoid the use of derivative networks. Another disadvantage

of the Lyapunov method is that the Lyapunov design rule may not be applicable to cases where the plant parameters cannot be adjusted.

Three of the methods described, namely the M.I.T. design rule, Dressler method and the Lyapunov design approach were applied to the power system considered. The theoretical basis and the adaptation equations for these methods are explained in the next section.

4.3 Theory of Adaptation Mechanisms

4.3.1 M.I.T. Design Rule

The index of performance that has been chosen is the integral squared response error, and the criterion for successful adaptation is that the integral squared error be the minimum value obtainable with the parameter variation provided. The response error is the difference between the system and the model outputs. The performance index is given by eqn. 4.1

$$\int e^2 \, dt = \int (C_s - C_m)^2 dt = \text{minimum} \qquad (4.1)$$

where C_s and C_m are the outputs of the system and the model respectively. According to the selected performance index, the desired operating state for the system is one at which the parameter value corresponds to the minimum value of the error function. At this point, we have:

$$\frac{\partial}{\partial \alpha} \{ \int e^2 \, dt \} = 0 \tag{4.2}$$

where α is the adaptive parameter.

If the limits of integration are independent of α and if the integral of the derivative of the function exists, hence:

$$\frac{\partial}{\partial \alpha} \{ \int e^2 \, dt \} = 2 \int \frac{\partial e}{\partial \alpha} \cdot e \cdot dt \tag{4.3}$$

The performance index then requires that this error quantity be zero. Under these conditions, the net change in the parameter over some interval of time is proportional to the integral error function, that is

$$\frac{\partial \alpha}{\partial t} = \mu \, e \, \frac{\partial e}{\partial \alpha} \tag{4.4}$$

or equivalently

$$\frac{\partial \alpha}{\partial t} = \mu \, e \, \frac{\partial C_s}{\partial \alpha} \tag{4.5}$$

where μ is the adaptive gain.

Eqn. 4.5 yields the rate at which α is to be adjusted and is the basic equation upon which the adjusting mechanism works.

The determination of the quantity $\frac{\partial C_s}{\partial \alpha}$ can be accomplished in two ways. In one of these, a straight-forward partial differentiation of the differential equation for C_s as a function of the input quantities can be made. An alternative method is to represent the controllable parameter as a variable sensitivity, S_α, in some signal path of the

system. The effect of the change, ∂S_α, can be considered as a disturbance entering the system at a point following S_α or following the summation point for signal paths that parallel S_α in the forward loop. For a variable S_α in a feed back loop, the disturbance can be considered as entering at the feed back summation point[48]. As a result, $\frac{\partial C_s}{\partial \alpha}$, can be generated by taking the signal that occurs at the input to the variable parameter and feeding it through a suitable filter.

4.3.2 Dressler Design Rule

The adaptive control system (plant plus adaptive controller) is described by the following linear differential equations with time-varying coefficients:

$$\dot{\underline{X}}(t) = A_s(t)\ \underline{X}(t) + B_s(t)\ \underline{U}(t) \qquad (4.6)$$

$$C_s(t) = F\ \underline{X}(t) \qquad (4.7)$$

where $A_s[nxn]$, $B_s[nx\ell]$ and $F[1xn]$ are the system matrix, the input distribution matrix and the output matrix respectively, and $\underline{X}(t)\ [nx1]$, $\underline{U}(t)[\ell x1]$ and $C_s(t)$ are the state vector of the system, the input vector and the scalar output respectively.

The plant to be controlled contains an arbitrary number of physical parameters that vary in an unknown manner; these are contained in matrices A_s and B_s. To achieve the

desired performance, it is necessary to provide the plant with an appropriate adaptive controller. Hence, any elements of A_s and B_s which contain time varying plant parameters will also contain adaptive parameters providing the required compensation. The model which is an implicit characterization of the performance criterion is described by the following linear differential equations with constant coefficients:

$$\dot{\underline{Y}}(t) = A_m \underline{Y}(t) + B_m \underline{U}(t) \tag{4.8}$$

$$C_m(t) = F \underline{Y}(t) \tag{4.9}$$

where $A_m[nxn]$, $B_m[nx\ell]$ and $F[1xn]$ are the system matrix, the input distribution matrix and the output matrix; and $\underline{Y}(t)[nx1]$, $\underline{U}(t)[\ell x1]$ and $C_m(t)$ are the state vector of the system model, the input vector and the model scalar output.

The design objective is to adjust the adaptive parameters so that C_s approximates C_m despite variations in the plant parameters. The matrices $A_s(t)$ and $B_s(t)$ may be decomposed as follows:

$$A_s(t) = A_m + \delta A(t) \tag{4.10}$$

$$B_s(t) = B_m + \delta B(t) \tag{4.11}$$

where $\delta A(t)$ and $\delta B(t)$ contain the adaptive parameters and the time varying portion of the plant parameters. The error criterion:

$$e(t)\ \Delta e(t) \leq 0 \tag{4.12}$$

where $\Delta e(t) \triangleq e(t + \Delta t) - e(t)$ (4.13)

leads to the following adaptation equations[36]:

$$\dot{\alpha}_{ij}(t) = -\mu_{ij}\, Y_j(t)\, e(t) \tag{4.14}$$

$$\dot{\beta}_{m\ell}(t) = -\mu^*_{m\ell}\, U_\ell(t)\, e(t) \tag{4.15}$$

where $\dot{\alpha}_{ij}$ and $\dot{\beta}_{m\ell}$ are elements of the $\delta A(t)$ and $\delta B(t)$

μ_{ij} and $\mu^*_{m\ell}$ are the adaptive loop gains.

The adaptation equations show that the adaptive parameters are adjusted continuously at a rate proportional to the product of the instantaneous values of $e(t)$ and the appropriate model state variable $Y_j(t)$ or input variable $U_\ell(t)$. The various $Y_j(t)$ are readily available from the actual mechanization of the model. The $U_\ell(t)$ are also available since they are the inputs to the system. The adaptive loop gains $(\mu_{ij}, \mu^*_{m\ell})$ are free to be chosen to satisfy the particular requirements of each problem.

4.3.3 Lyapunov Design rule[42,43,49]

In the Lyapunov synthesis approach, the adaptive rule is obtained by selecting the design equations to satisfy conditions derived from Lyapunov's second method[28]. The theory is developed for linear plants and follows Porter and Tatnall[49].

Let the system behaviour be described by the n^{th} order state equation:

$$\dot{\underline{X}}(t) = A_s(t)\ \underline{X}(t) + B_s(t)\ \underline{U}(t) \tag{4.15}$$

where $A_s(nxn)$, $B_s(nxr)$ are matrices with time varying elements; $\underline{X}$ is the n^{th} order plant vector and $\underline{U}$ is the r^{th} order input vector.

Let the model state equations be:

$$\dot{\underline{Y}}(t) = A_m\ \underline{Y}(t) + B_m\ \underline{U}(t) \tag{4.17}$$

where $A_m(nxn)$ and $B_m(nxr)$ are matrices with fixed elements; $\underline{Y}$ is the n^{th} order model vector.

An error vector can be formed by writing:

$$\underline{e}(t) = \underline{Y}(t) - \underline{X}(t) \tag{4.18}$$

$$\text{giving } \dot{\underline{e}}(t) = A_m\ \underline{e}(t) + (A_m - A_s)\ \underline{X}(t) + (B_m - B_s)\ \underline{U}(t) \tag{4.19}$$

Writing:

$$(A_m - A_s) = [\alpha_{ij}] \quad ; \quad (B_m - B_s) = [\beta_{ij}] \tag{4.20}$$

and regarding the α_{ij} and β_{ij} as state variables, a Lyapunov function is chosen as:

$$V = \underline{e}'P\underline{e} + \sum_{i,j}^{n,n} \mu_{ij}\ \alpha_{ij}^2 + \sum_{i,j}^{n,r} \nu_{ij}\ \beta_{ij}^2 \tag{4.21}$$

where P nxn is a positive definite symmetric matrix, μ_{ij} and ν_{ij} are positive constants. It can be shown that:

$$\dot{V} = \underline{e}'\ (A_m'P + PA_m)\ \underline{e} + 2 \sum_{i,j}^{n,n} (\mu_{ij}\dot{\alpha}_{ij} + X_j\underline{p}_i'\underline{e})\ \alpha_{ij}$$
$$+ 2 \sum_{i,j}^{n,r} (\nu_{ij}\dot{\beta}_{ij} + U_j\underline{p}_i'\underline{e})\ \beta_{ij} \tag{4.22}$$

where $\underline{p}_i$ is the i^{th} column of P.

If P is chosen to satisfy

$$A_m'P + PA_m = -I \tag{4.23}$$

and $$\dot{\alpha}_{ij} = -X_j \, \underline{p}_i' \, \underline{e}/\mu_{ij} \quad ; \quad \dot{\beta}_{ij} = -U_j \, \underline{p}_i' \, \underline{e}/\nu_{ij} \tag{4.24}$$

It follows that:

$$\dot{V} = -\underline{e}'\underline{e} \tag{4.25}$$

which is negative semi definite of the state variables e_i , α_{ij} and β_{ij}. Writing matrices A_s and B_s as:

$$A_s = A + \Gamma \quad ; \quad B_s = B + \Delta \tag{4.26}$$

where Γ and Δ are matrices whose elements are generated by the adaptive loops with the object of making the behaviour of the system indistinguishable from that of the model. It follows from eqn. 4.20 that

$$[\alpha_{ij}] = A_m - A - \Gamma \quad ; \quad [\beta_{ij}] = B_m - B - \Delta \tag{4.27}$$

and

$$[\dot{\alpha}_{ij}] = -\dot{\Gamma} = -[\dot{\gamma}_{ij}] \quad ; \quad [\dot{\beta}_{ij}] = -\dot{\Delta} = -[\dot{\delta}_{ij}] \tag{4.28}$$

Therefore the adaptive equations are given by:

$$\dot{\gamma}_{ij} = X_j \, \underline{p}_i' \, \underline{e}/\mu_{ij} \tag{4.29}$$

$$\dot{\delta}_{ij} = U_j \, \underline{p}_i' \, \underline{e}/\nu_{ij} \tag{4.30}$$

It is clear that the practical implementation of the control laws requires access to the states of both model and system and also the ability to change the values of the system parameters.

4.4 Power System Model

The adaptive design equations given in section 4.3 were applied to compensate for variations in the incremental speed regulation with load changes. A classical one area system is used in this study. Figure 4.2 illustrates the block diagram of a steam-turbo alternator on an isolated static load. The inertial generator model is assumed. This is adequate for most governor studies since they are inherently slow in operation so that electrical transients in the machine do not play a significant part in determining the response[1,9]. The area is represented by a single governor-turbine-generator group involving two time constants (governor and turbine). The system equations are linearized and the variables are expressed as differences with respect to the nominal values. The following equations are obtained in Laplace transform calculus:

$$\Delta P_G(s) = (\Delta P_c(s) - \frac{\Delta F(s)}{R_s}) \left[\frac{1}{(1+sT_T)(1+sT_G)}\right] \qquad (4.31)$$

$$\Delta P_G(s) - \Delta P_d(s) = Ms\ \Delta F(s) + D\ \Delta F(s) \qquad (4.32)$$

where Δ denotes the difference between the actual value of a variable and its nominal value, and

F is the frequency of the area

R_s is the system incremental speed regulation that deviates from nominal value with loading

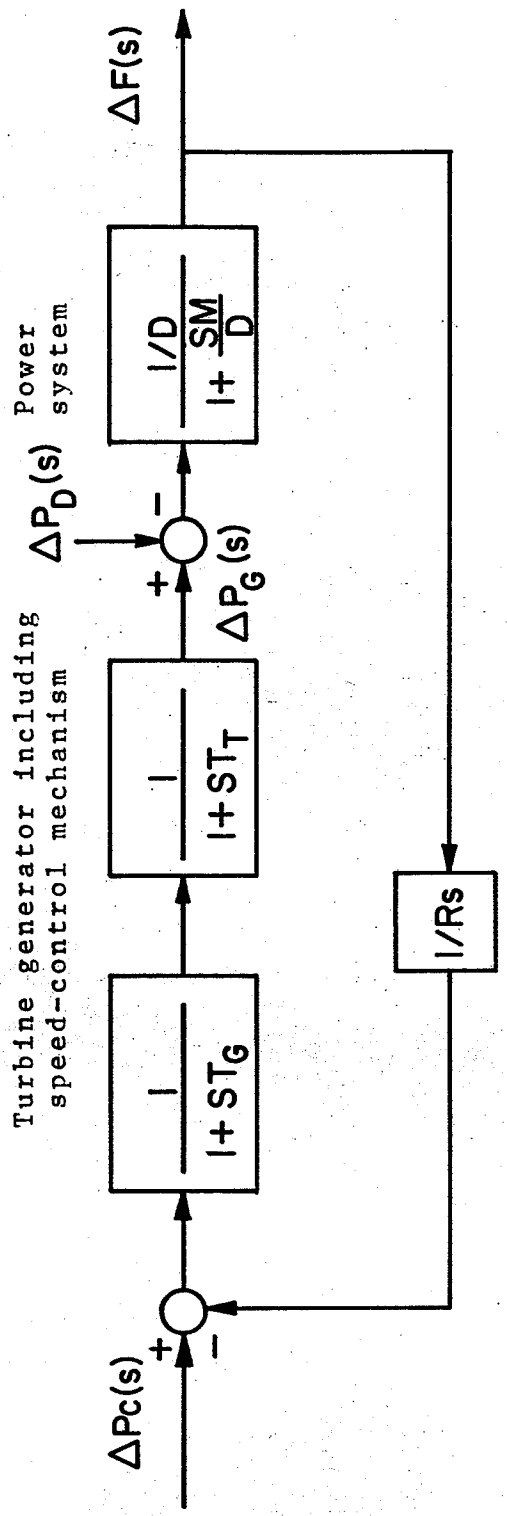

Fig. 4.2 Block diagram representation of a single isolated area with transfer functions for steam turbine and governor

T_T turbine time constant

T_G governor time constant

P_G power generated

P_c speed changer position

P_d operating load of the area

M inertia constant of the area

D Damping coefficient $(\frac{\partial P_{do}}{\partial f})$

In what follows, the speed changer position will be assumed fixed, so that the emphasis will be only on the performance of the adaptive loop. The system equations can be summarized in the canonical form:

$$\dot{\underline{X}}(t) = A_s(t)\underline{X}(t) + B_s\underline{U}(t) \tag{4.33}$$

The state vector $\underline{X}(t)$ and the input vector $\underline{U}(t)$ are given by:

$$\underline{X}'(t) = [\Delta F\ ,\ \Delta P_G,\ z] \quad ;\quad U = \Delta P_d \tag{4.34}$$

where z is an auxiliary variable.

It follows that A_s and B_s are given by:

$$A_s = \begin{bmatrix} -\frac{D}{M} & \frac{1}{M} & 0 \\ 0 & -\frac{1}{T_T} & \frac{1}{T_T} \\ \frac{-1}{R_s T_G} & 0 & \frac{1}{-T_G} \end{bmatrix} \quad ; \quad B_s = \begin{bmatrix} -\frac{1}{M} \\ 0 \\ 0 \end{bmatrix} \tag{4.35}$$

The numerical values for the system, the filters and

the model are[9]:

$M = 1./6$ pu Mw s/Hz

$D = 8.33 \times 10^{-3}$ pu Mw/Hz

$T_T = 0.3$ s

$T_G = 0.08$ s

The design (nominal) value of the incremental speed regulation is assumed to be $R_m = 2.4$ Hz/pu Mw. It is also assumed that with the system operating at a certain loading condition, a step disturbance in the load - large enough to cause the incremental speed regulation to increase to double its nominal value - is suddenly applied. It is then required from the adaptive loop to compensate for this change in the incremental speed regulation.

4.5 Computer Simulation and Results

The results obtained from simulating the system on a TR-48 EAI analog computer and on CSMP are presented in this section. The purpose of these simulations is to demonstrate the performance characteristic of the three adaptation techniques given in section 4.3. These simulations are not intended to be complicated, but rather to give some indication as to the possibility of applying model-reference-adaptive control techniques to power systems.

4.5.1 Adaptive Laws Based on M.I.T. Rule

This case is best illustrated by the block

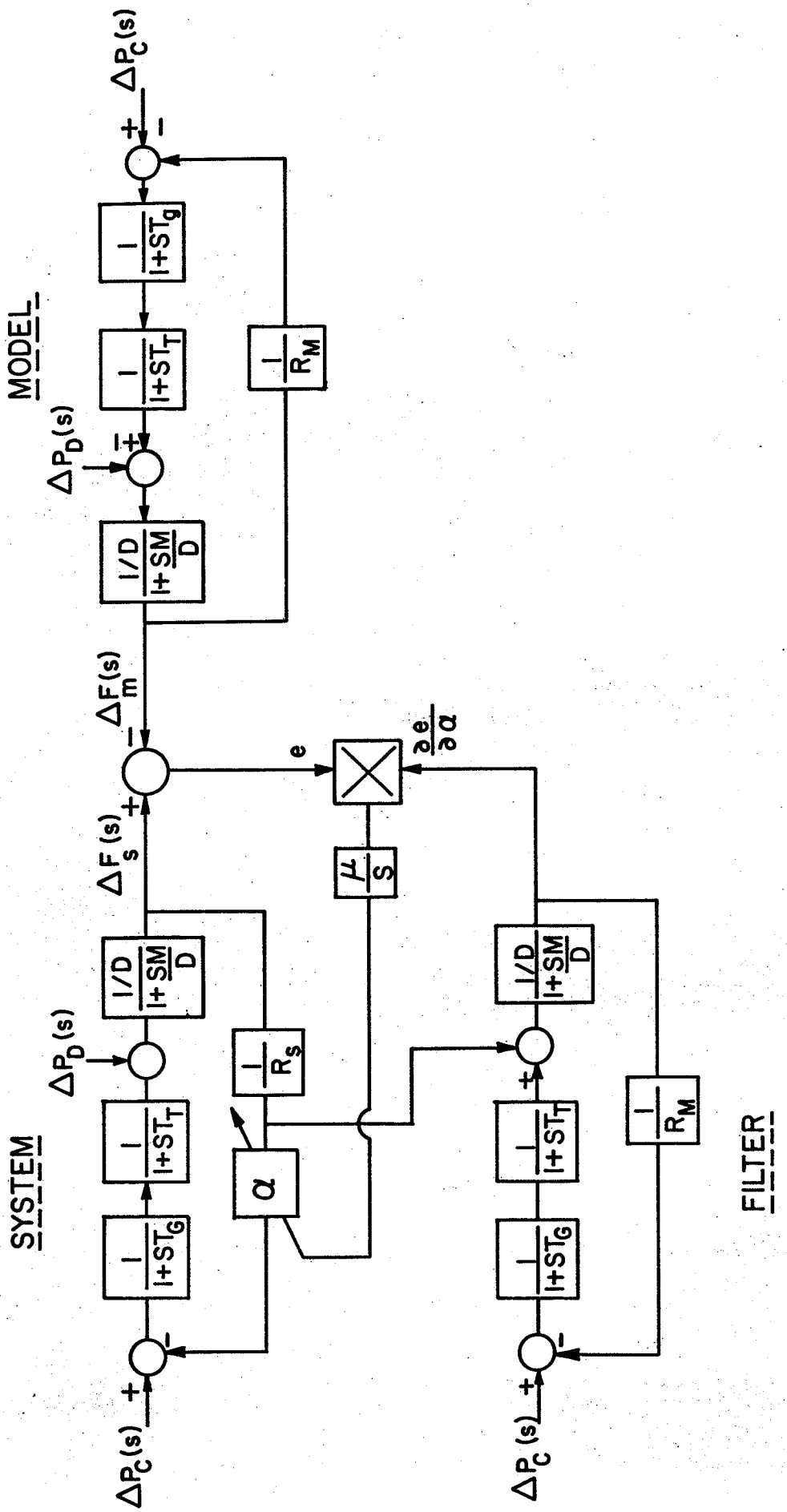

Fig. 4.3 Block diagram representation of the adaptation mechanism based on the M.I.T. design

diagram of Figure 4.3. The filter necessary to obtain $\frac{\partial e}{\partial \alpha}$ was found to have a transfer function similar to that of the model. The responses of the model, the unadapted system and the adapted system to the step disturbance are shown in Figure 4.4a. The action of the adaptive controller to bring the adaptive response error to zero is evident from Figure 4.4b. The adaptive parameter attempt to compensate for the assumed variation in the incremental speed regulation is illustrated in Figure 4.4c. The computer runs shown in Figure 4.4a to Figure 4.4c are for an adaptive loop gain of 0.162.

4.5.2 Adaptive Laws Based on Dressler's Method

Referring to eqn. 4.6, the (system plus adaptive controller) matrices $A_s(t)$ and $B_s(t)$ are given by:

$$A_s(t) = \begin{bmatrix} -\frac{D}{M} & \frac{1}{M} & 0 \\ 0 & \frac{-1}{T_T} & \frac{1}{T_T} \\ (\frac{-1}{R_s T_g} - \alpha_{31}) & 0 & -\frac{1}{T_g} \end{bmatrix} \quad ; \quad B_s(t) = \begin{bmatrix} -\frac{1}{M} \\ 0 \\ 0 \end{bmatrix} \qquad (4.36)$$

where α_{31} is the adaptive parameter that will compensate for deviations in the system incremental speed regulation R_s.

Referring to eqn. 4.8, the model matrices A_m and B_m are:

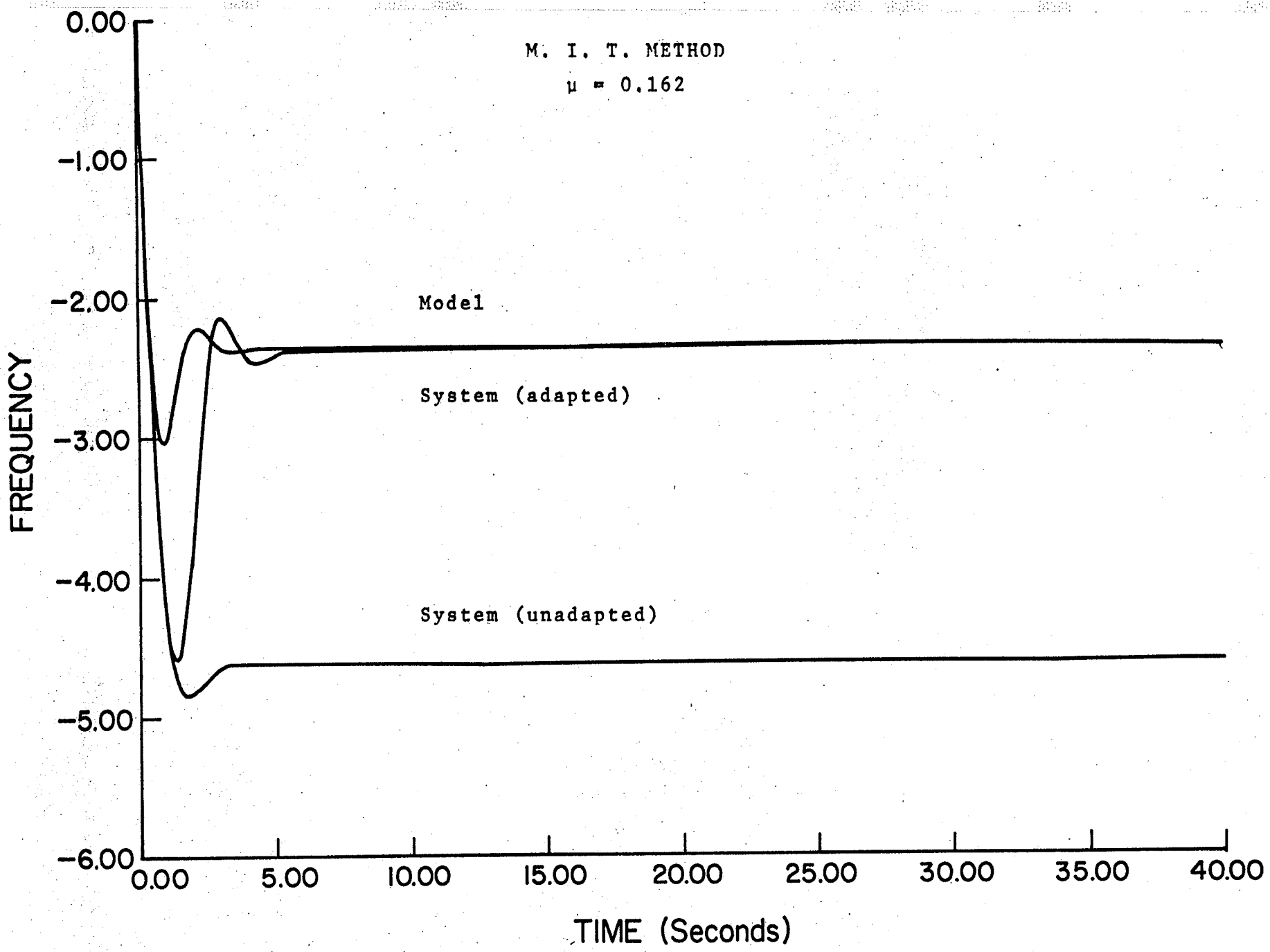

Fig. 4.4a Output deviations following a step-change in load for a) the model b) the system with no adaption 3) the system with adaptation. (M.M.T. design; μ = 0.162)

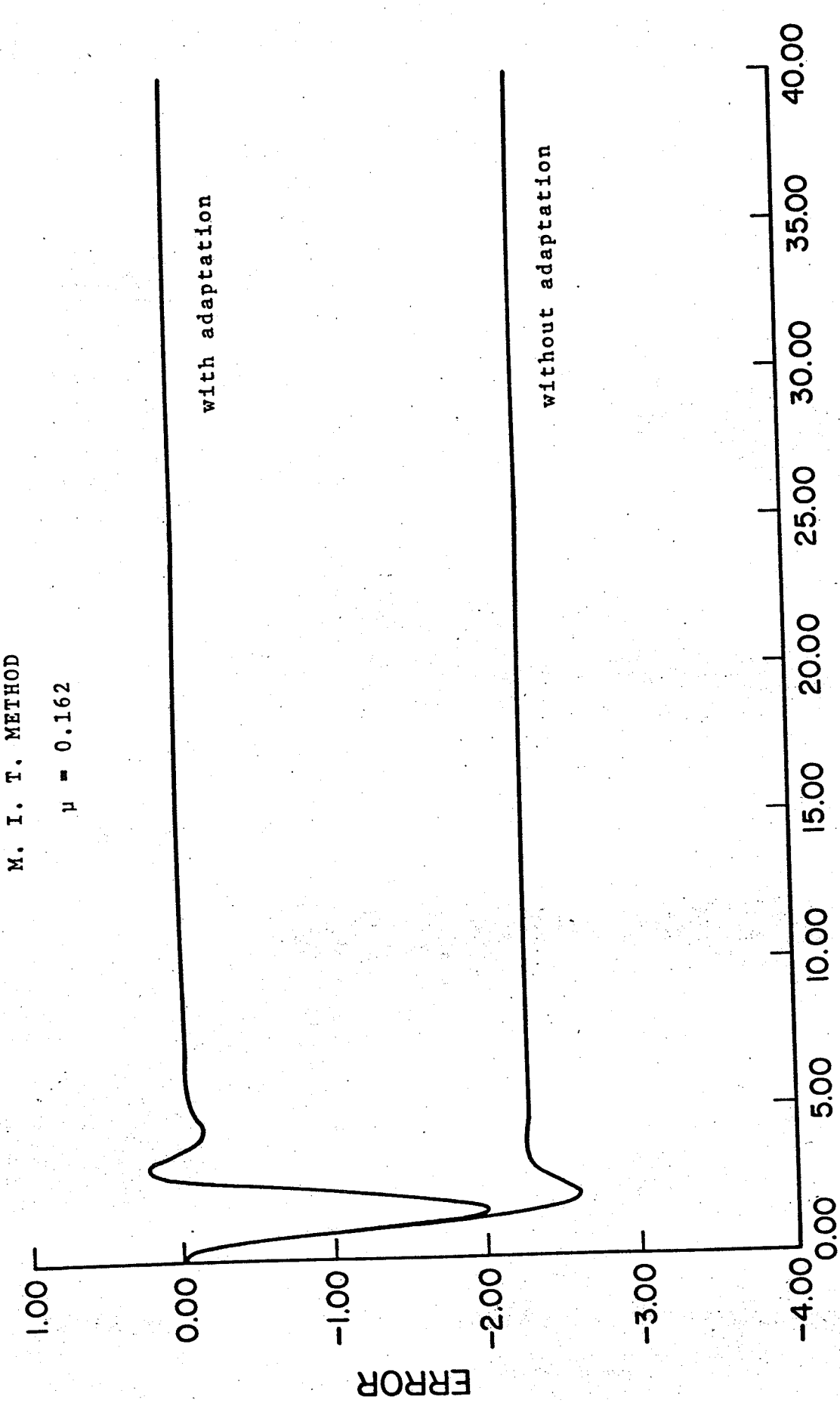

Fig. 4.4b Adaptive error with and without adaptation (M.I.T. design ; μ = 0.162)

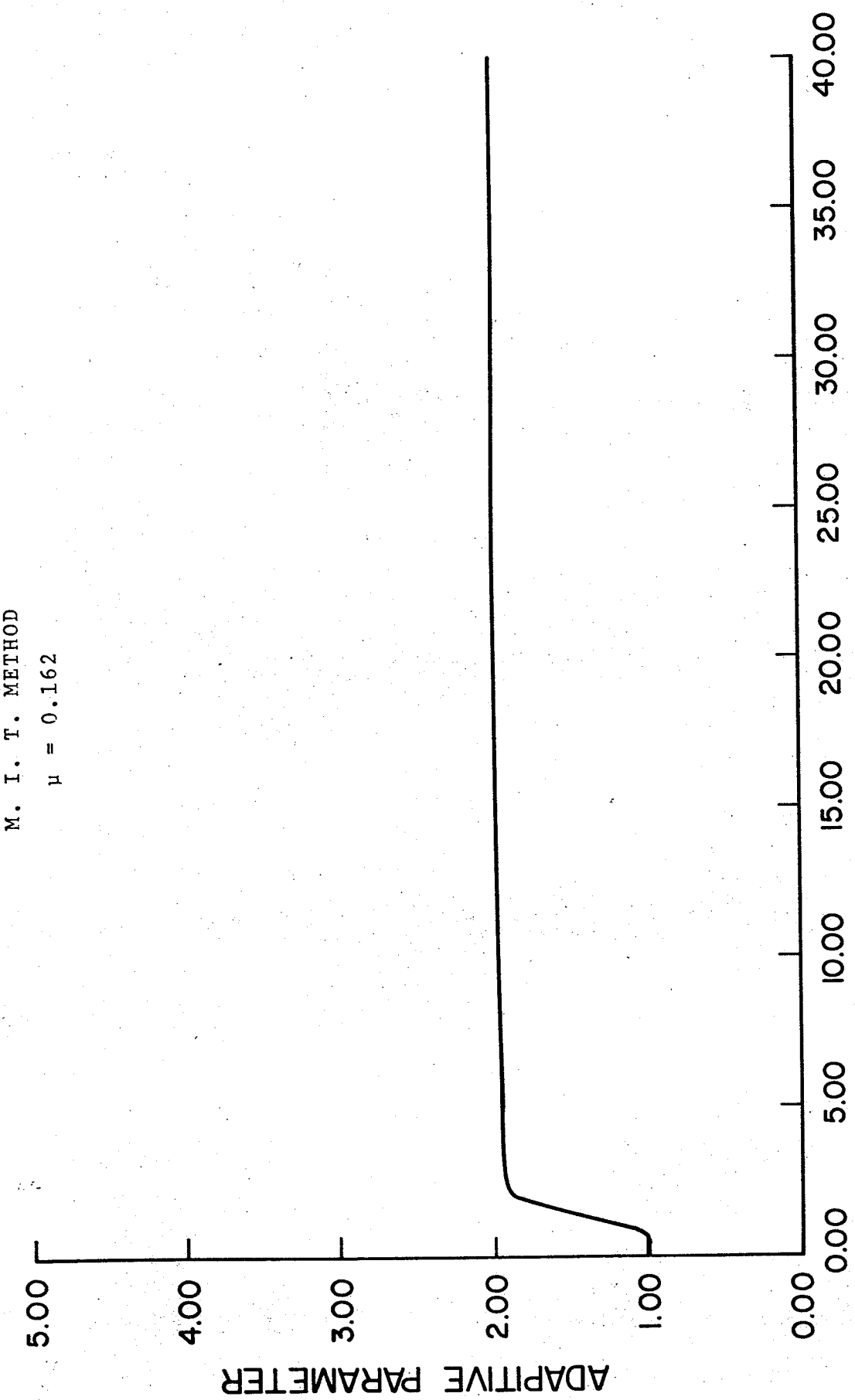

Fig. 4.4c Adaptive parameter variation (M.I.T. design ; μ = 0.162)

$$A_m = \begin{bmatrix} -\frac{D}{M} & \frac{1}{M} & 0 \\ 0 & -\frac{1}{T_T} & \frac{1}{T_T} \\ \frac{-1}{R_m T_g} & 0 & -\frac{1}{T_g} \end{bmatrix} \quad ; \quad B_m = \begin{bmatrix} -\frac{1}{M} \\ 0 \\ 0 \end{bmatrix} \qquad (4.37)$$

The output matrix F is given by $F' = [1\ 0\ 0]$.

The differential equation that governs the operation of the adaptive system, as obtained from eqn. 4.14, is given by:

$$\dot{\alpha}_{31}(t) = \mu_{31}\, Y_1(t)\, e(t) \qquad (4.38)$$

Figure 4.5 shows the block diagram for the "system plus adaptive controller" and the model. Computer runs with the adaptive loop gain $\mu_{31} = 0.39$ showing the behaviour of the unadapted system, the model, the adapted system, adaptive error with and without adaptive controller and the adaptive parameter are presented in Figure 4.6a through 4.6c respectively.

4.5.3 Adaptive Laws Based on Lyapunov's Method

The (system plus adaptive controller) matrices $A_s(t)$ and $B_s(t)$ are the same as given by eqn. 4.36 (except that the adaptive parameter is denoted by γ_{31} instead of α_{31}). The model matrices are also the same as given by eqn. 4.37.

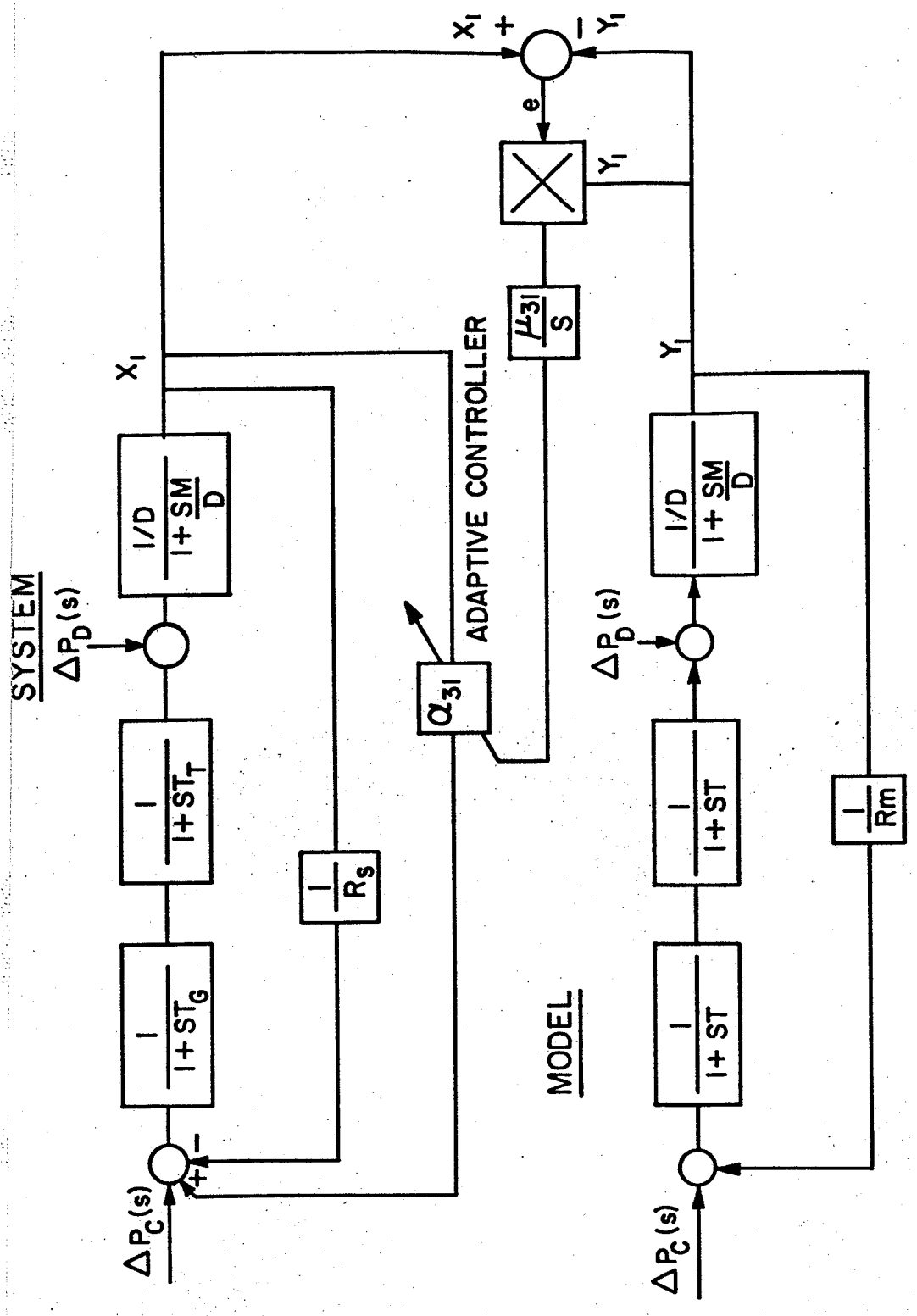

Fig. 4.5 Block diagram representation of the adaptation mechanisms based on Dressler method

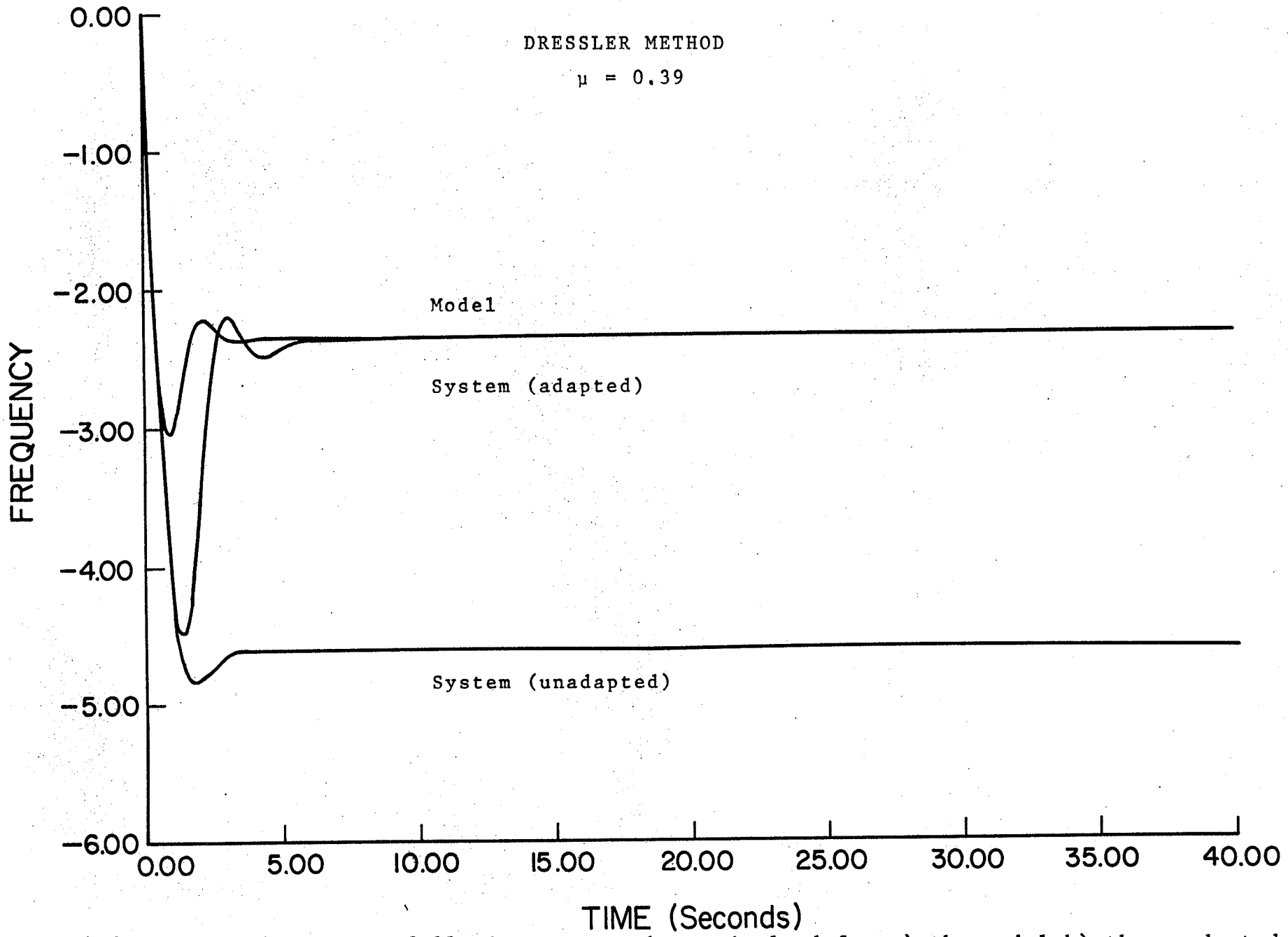

Fig. 4.6a Output deviations following a step change in load for a) the model b) the unadapted system c) the adapted system. (Dressler design ; μ = 0.39)

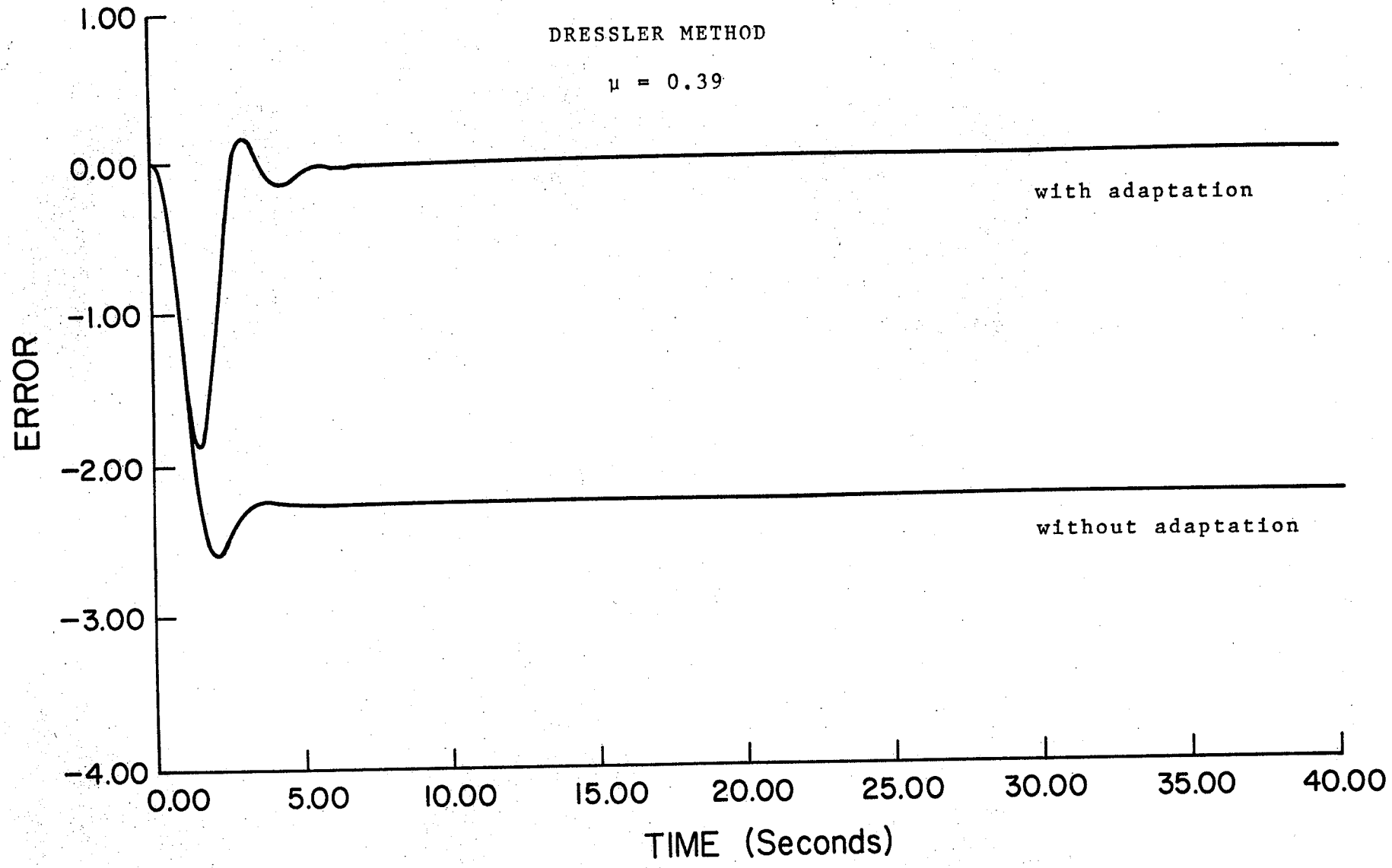

Fig. 4.6b Adaptive error with and without adaptation (Dressler design ; μ = 0.39)

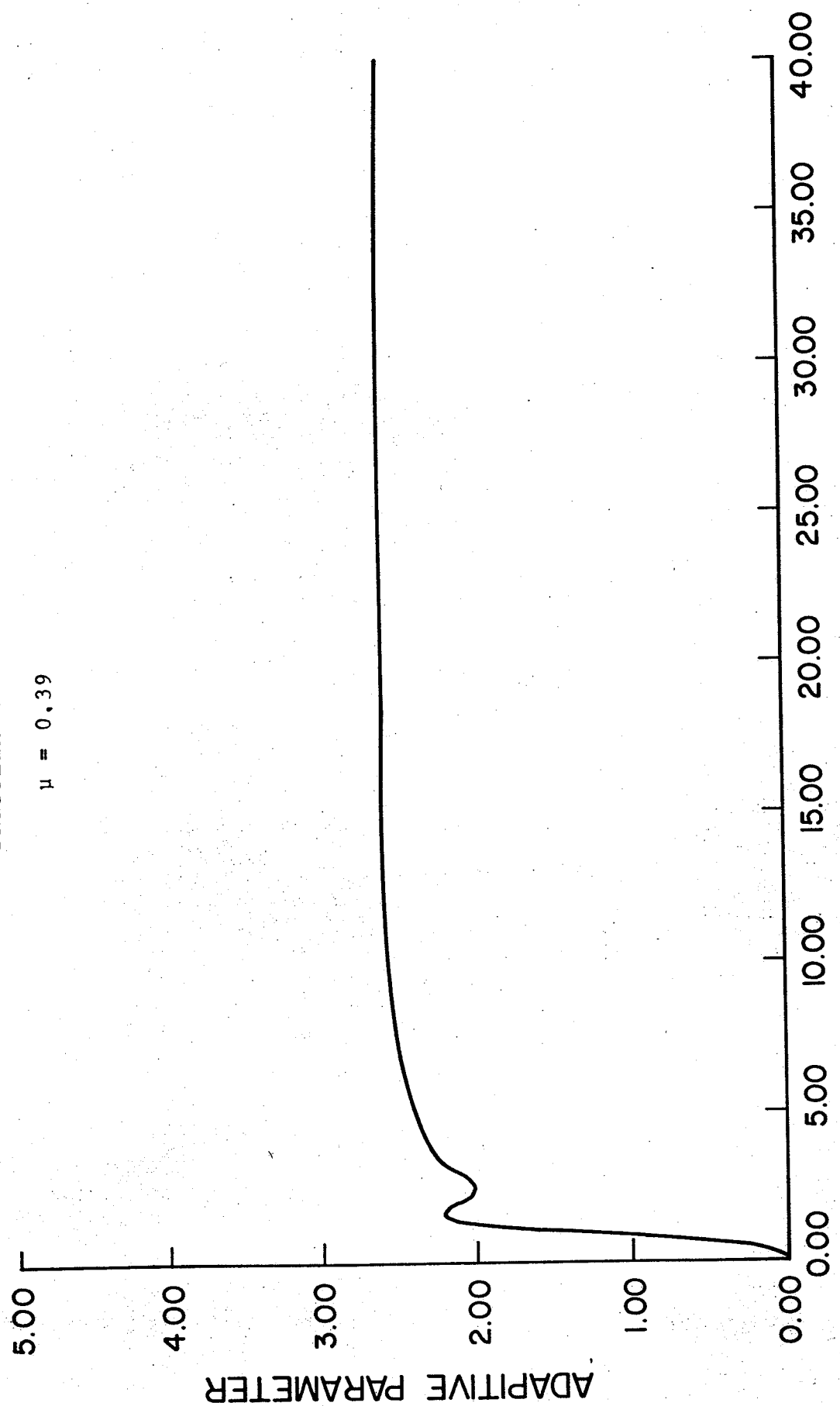

Fig. 4.6c Adaptive parameter variation (Dressler method ; μ = 0.69)

The operation of the adaptive system is governed by the differential equations of eqn. 4.29 ; for this particular case, we have:

$$\dot{\gamma}_{31}(t) = \frac{1}{\mu_{31}} (X_1 \; e' \; \underline{p}_3) \tag{4.39}$$

The adaptive control law of eqn. 4.39 involves the third column $\underline{p}_3$ of the matrix P , hence it is first necessary to evaluate the matrix P . This was done by solving eqn. 4.23, namely:

$$PA_m + A_m'P = - I$$

where I is the unit matrix.

Using the Kronecker product method to solve the above Lyapunov equation, it was found that:

$$P = \begin{bmatrix} 0.516 & 0.514 & 0.091 \\ 0.514 & 1.075 & 0.261 \\ 0.091 & 0.261 & 0.109 \end{bmatrix} \tag{4.40}$$

The adaptive equation becomes:

$$\dot{\gamma}_{31}(t) = \frac{1}{\mu_{31}} X_1 (0.091 \; e_1 + 0.261 \; e_2 + 0.109 \; e_3) \tag{4.41}$$

The complete block diagram showing the system, the model and the adaptive controller is presented in Figure 4.7. A set of curves illustrating the response of the system with and without the adaptive controller, the adaptive error and the adaptive parameters are given in Figure 4.8a through 4.8c respectively.

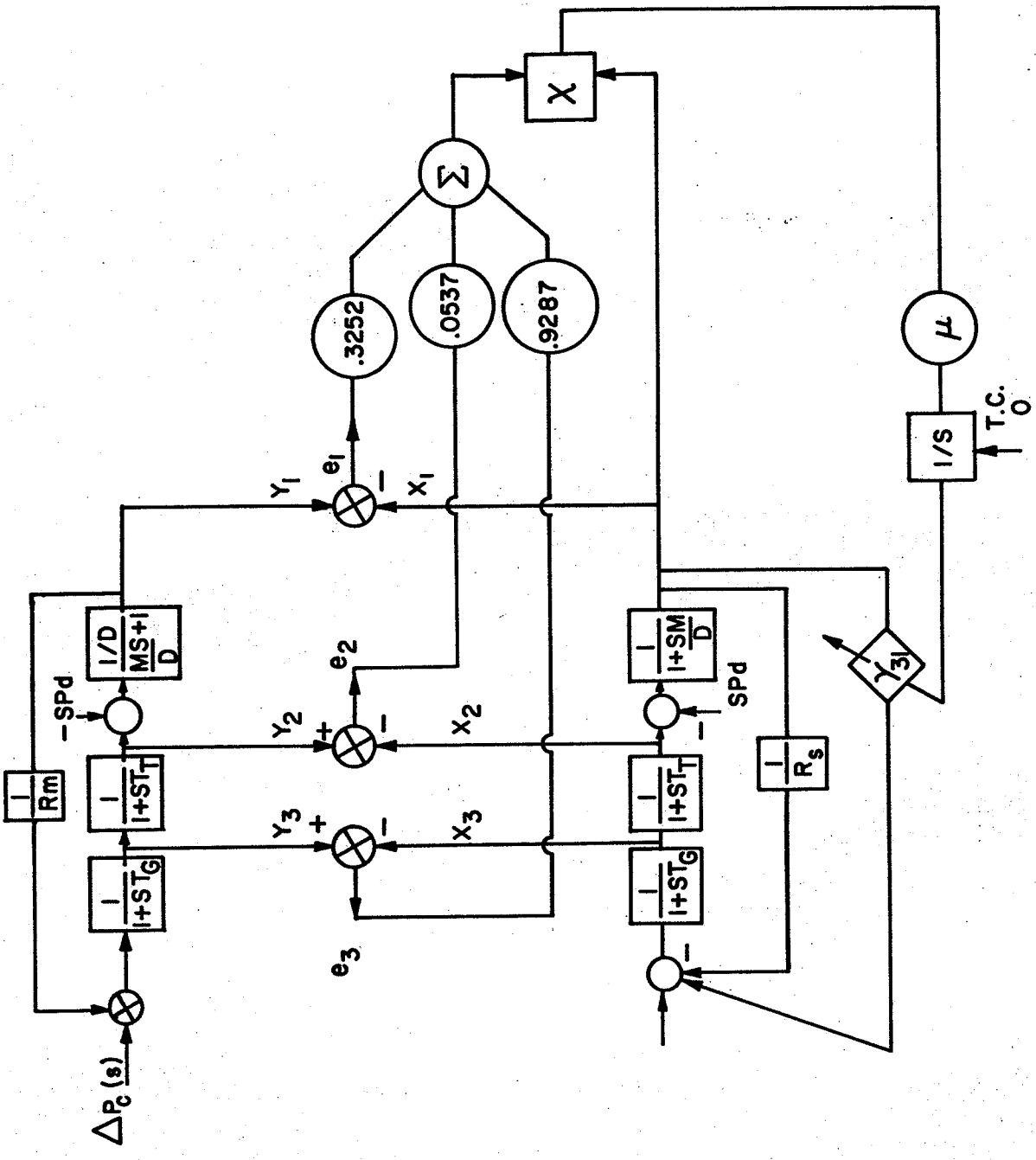

Fig. 4.7 Block diagram representation showing the adaption mechanism based on Lyapunov design

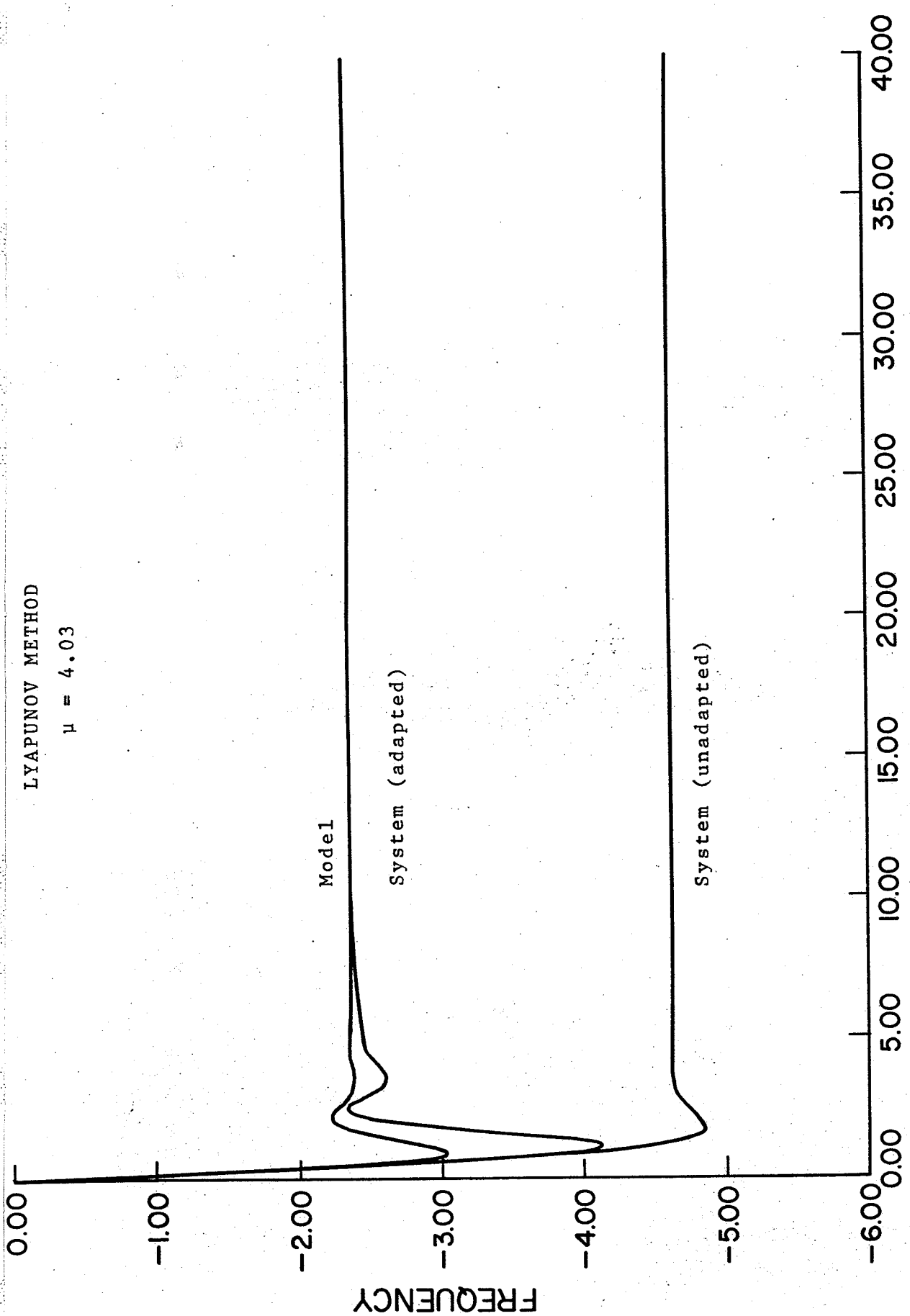

Fig. 4.8a Output deviations following a step change in load for a) the model b) the unadapted system c) the adapted system (Lyapunov design ; μ = 4.03)

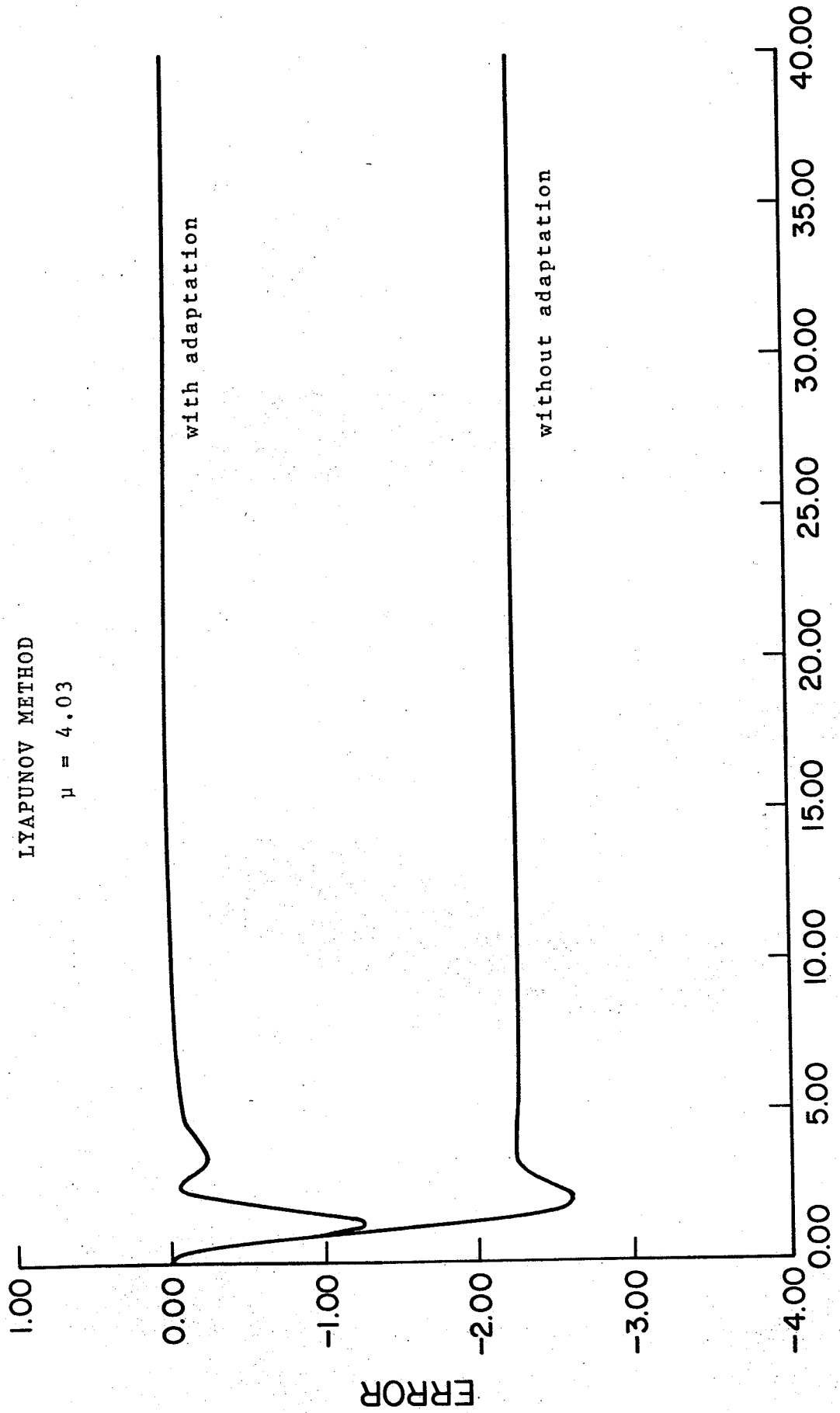

Fig. 4.8b Adaptive error with and without adaptation
(Lyapunov design : μ = 4.03)

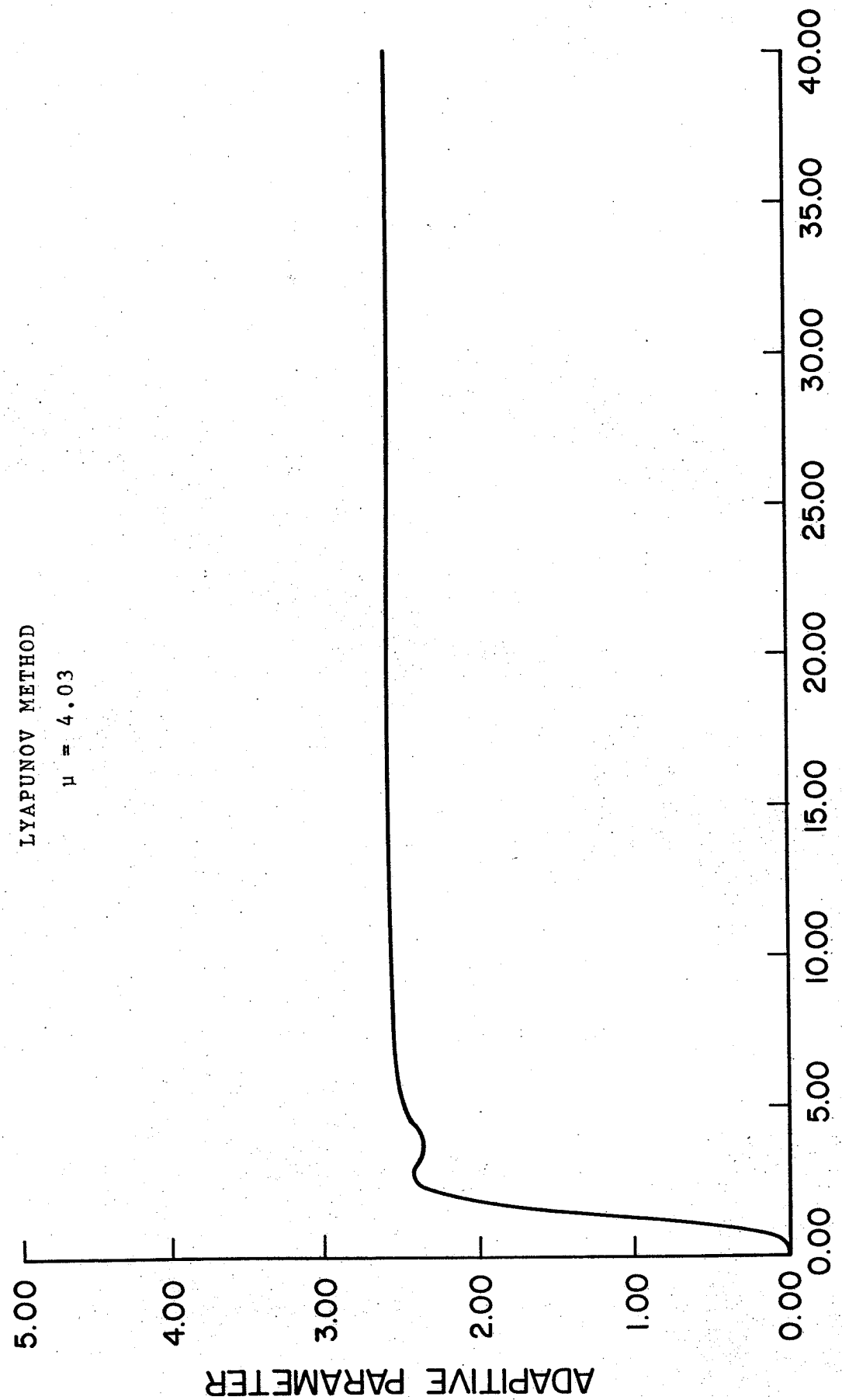

Fig. 4.8c Adaptive parameter variation (Lyapunov design ; μ = 0.69)

chapter five

SUMMARY AND CONCLUSION

The purpose of this research has been to investigate the possible application of various adaptive techniques in the power system area. Two different problems were considered, and in each case a different adaptive technique has been suggested. The first problem deals with the design of a stabilizer to supplement generator static excitation systems. A single machine infinite bus model was assumed and the machine was represented by the so called "Heffron-Phillips" constants. The analysis began with a study of the phenomenon of stability of the system under small perturbation, for a wide range of real and reactive system loading, using eigen-value techniques. The subject of the study was to develop insights into effects of excitation systems and to establish some basis for the stabilizing requirement for such systems. The approach taken to design the stabilizer employs an open-loop adaptive technique. Based on the description of the system, the adaptive controller was synthesized in such a way as to make the overall system optimum with respect to a prescribed criterion, namely the integral of the error squared. A computational algorithm was set to determine the stabilizing parameters settings that provide the optimum system performance for all the operating points considered. Adaptation is then based on measurements of the operating environment (i.e. real and

reactive power) and altering the stabilizer structure.

As a result of study and tests on the system analog computer model, the following conclusions have been reached:

1) The small perturbation dynamic stability of a single machine equipped with thyristor type excitation system and connected to an infinite bus through external impedance can be determined for an extremely wide range of operating conditions using eigen-values analysis.
2) The concept of changing real power and reactive power environment and its direct effect on the small perturbation stability of the system can be usefully displayed (plotted) in the complex frequency plane.
3) The eigen value analysis not only allows the direct determination of the system dynamic stability but can be successfully used in obtaining accurate values of damping and synchronizing torques.
4) The power stabilizer considered $Ks/(1+sT)^2$ significantly increases the dynamic stability of the system.
5) Altering the power stabilizer structure to cope with real and reactive power loading, maintains optimum performance for an extremely wide range of system operating conditions.
6) The variable structure power stabilizer provides more damping for the system than for a fixed structure stabilizer. In the neighborhood of the design point,

of course, the difference between the system responses in both cases is small.

7) It is essential to realize that the fixed-structure stabilizer used was based on a loading condition of $P = 1.0$ and $Q = -0.3$. This choice, which might not be realistic for the machine, is the worst operating point from the stability point of view for the loading range considered.

It is apparent that another choice of the loading condition for which the fixed structure stabilizer is optimized would produce less noticeable improvement. If this is the case, the merit of an adaptive stabilizer over a fixed-structure stabilizer would be reduced and the use of either one is left to engineering judgement.

The second problem also involves deviations of power system parameters from their nominal values, caused by load changes. In contrast to the first problem, the approach taken employs a closed loop adaptive technique. A classical one area "steam turbo-alternator on isolated load" system was considered and the model reference adaptive control concept was used to design adaptive mechanisms that compensate for the deviations of the incremental speed regulation caused by incremental load changes. Three different techniques were applied to the system considered and computer simulations were carried out. From the results shown, the following conclusions are drawn:

1. The model reference adaptive control approach, which employs performance feedback can be applied in the power system area, for the small-disturbance operating regime.
2. The adaptation mechanism, designed by three different methods

namely, the M.I.T. rule, the Dressler's method and the Lyapunov synthesis approach, has operated satisfactorily in compensating for deviation in incremental speed regulation (a 100% change) with the load changes.

3. The adaptive loop is capable of keeping the system parameters unchanged with environment, therefore preventing the de-rating on controllers which are conventionally-based on constant plant-parameter values.

BIBLIOGRAPHY

1. Fleming, R.J. "Automatic control in electric power systems", Notes. University of Saskatchewan, Saskatoon.

2. Heeley, F.S. "Generator exciter systems, an historical review", CEA Transactions, Vol. 8, Part 1, 1969, Paper 69-A-82.

3. Kimbark, E.W. "Power System Stability", John Wiley & Sons, Inc., New York, 1956.

4. Demello, F.G., Ewart, D.N. and Temoshok, M. "Stability of synchronous machines as affected by excitation systems, machine and systems parameters", Proc. American Power Conference, Vol. XXVII, 1965, pp.1150-1159.

5. Watson, W. "Static exciters and stabilizing signals", CEA Transactions, Vol. 7, Part 3, 1968, Paper 68-SP-1971.

6. Demello, F.P. and Concordia, C. "Concepts of synchronous machine stability as affected by excitation", IEEE Transactions, Vol. PAS-88, No.4, 1969, pp.316-327.

7. Heffron, W.G. and Phillips, R.A. "Effect of modern amplidyne voltage regulators on under-excited operation of large turbine generators", AIEEE Transactions, Vol. PAS-71, 1952, pp.592-697.

8. Dubé, C. "Stability of the hydro-Quebec system as affected by effective synchronous machine controls", CEA Transactions, Vol. 8, Part 3, 1969, Paper 69-SP-162.

9. Elgerd, O.I. "Electric Energy Systems Theory", McGraw-Hill, 1971.

10. El-Sherbini, M.K. and Mehta, D.M. "Dynamic systems stability-investigation of the effect of different loadings and excitation systems", IEEE Transactions, Vol. PAS-92, No.5, 1973, pp.1538-1546.

11. Dandeno, P.L. et al. "Effect of high-speed rectifier excitation systems on generator stability limits", IEEE Transactions, Vol. PAS-87, No.1, 1968, pp.190-196.

12. Watson, M. and Manchur, G. "Experience with supplementary damping signals for generators static excitation system", IEEE Transactions, Vol. PAS-92, No.1, 1973, pp.199-204.

13. Ellis, H.M. et al "Dynamic stability of the Peace River transmission system", IEEE Transactions, Vol. PAS-85, No.3, 1966, pp.586-600.

14. Schielf, F.R. et al "Excitation controls to improve power line stability", IEEE Transactions, Vol. PAS-87, No.3, 1968, pp.1420-1434.

15. Shier, R.M. and Blythe, A.L. "Field tests of dynamic stability analysis using a stabilizing signal and computer program verification", IEEE Transactions, Vol. PAS-87, 1968, No.2, pp.315-322.

16. Marshall, W.K. and Smolinski, W.Y. "Dynamic stability determination by synchronizing and damping torque analysis", IEEE Transactions, Vol. PAS-92, No.4, 1973, pp.1239-1245.

17. Byerly, R.T. et al "Damping of power oscillations in salient-pole machines with static excitors", IEEE Transactions, Vol. PAS-89, No.4, 1970, pp.1009-1021.

18. Gerhart, A.D. et al "Power system stabilizer: Field testing and digital simulation", IEEE Transactions, Vol. PAS-90, No.5, 1971, pp.2095-2100.

19. Keay, F.W., Raczkowski, C. and South, N.M. "Excitation control system complex compensation", IEEE Transactions, Vol. PAS-93, No.5, 1974, pp.1444-1448.

20. Raczkowski, C. "Complex root compensator, a new concept for dynamic stability improvement", IEEE Transactions, Vol. PAS-93, No.6, 1974, pp.1842-1848.

21. Newton, G.C., Gould, L.A. and Kaiser, J.T. "Analytical Design of Linear Feedback Controls", John Wiley, 1957.

22. Molinari, B.P. "Algebraic solution of matrix linear equations in control theory", Proc. IEE, Vol. 116, No. 10, October 1969, pp.1749-1754.

23. Nelder, Y.A. and Mead, R. "A simplex method for function minimization", Computer Journal, Vol. 12, January 1965, pp.308-313.

24. Box, M.J., Davis, D. and Swann, W.H. "Non-linear Optimization technique." Imperial Chemical Industries Monograph No. 5, Oliver and Boyd, Edinburgh, 1969.

25. Lee, T.H., Hanson, O.W. and Fleming, R.J. "Automatic voltage regulator studies", CEA Transactions, Vol. 8, Part 3, 1969, Paper 69-SP-166.

26. IEEE Working group of excitation systems, "Computer representation of excitation systems", IEEE Transactions, Vol. PAS-87, 1968, No.6, pp.1460-1464.

27. Willems, J.L. "Stability Theory of Dynamical Systems", Johm-Wiley, 1970.

28. Hsu, J.C. and Meyer, A.U. "Modern Control Principles and Applications", McGraw-Hill, 1968.

29. Handscwin, H. (Editor), "Real Time Control of Power Systems", Elsevier Publishing Company, 1972.

30. AIEE-ASME Committee Report "Recommended specifications for speed-governing of steam turbines inteded to drive electric generators rated 500 kw and larger", presented at the AIEE fall general meeting, Chicago, October 1957.

31. Malek, N.G., Tan, O.T., Julich, P.M. and Tacker, E.C. "Trajectory sensitivity design of load-frequency control systems", Proc. IEE, Vol. 120, No. 10, October 1973, pp.1273-1277.

32. Cohn, N. "Control of Generation and Power Flow on Interconnected Systems", John Wiley, 1966.

33. Landau, J.D. "Model-reference adaptive system, a survey (MRAS) - what is possible and why", Transactions of the ASME, Journal of Dynamic Systems, Measurements and Control, June 1972, pp.119-132.

34. Whitaker, H.P. "An adaptive system for control of the dynamic performance of aircraft and spacecraft", Institute of Aeronautical Sciences, Paper No. 59-100, June 1959.

35. Donaldson, D.D. and Leondes, C.T. "A model referenced parameter tracking technique for adaptive control systems", IEEE Transactions, Appl. Ind.,September 1963, pp.241-262.

36. Dressler, R.M. " simplified technique for the synthesis of model reference adaptive control systems", 1966, Ph.D. thesis.

37. Price, C.F. "An accelerated gradient method for adaptive control", Proc. 9th IEEE Symp. Adaptive processes decision and control, December 1970, pp.IV.4.1-4.9.

38. Kokotovic, P.V. et al "Sensitivity method in the experimental design of adaptive control systems", Proc. 3rd IFAC Congr. (London), 1966, pp.45B.1-B.12.

39. Medamic, J.V. and Kokotovic, P.V. "Some problems in the development of adaptive systems using the sensitivity operator", Proc. 1965 IFAC Symp. Adaptive Control, ISA, 1966, pp.204-212.

40. Winsor, C.A. "Model reference adaptive design", NASA-CR-98453, November 1968.

41. Green, J.W. "Adaptive control of multiloop speed control systems with particular reference to the Ward-leonard system", Ph.D. dissertation, Dept. Elec. Electron. Eng., Leeds University, September 1969.

42. Butchart, R.L. and Shackcloth, B. "Synthesis of model-reference adaptive control systems by Lyapunov's second method", Proc. of the 2nd IFAC Symp. on theory of self-adaptive control systems, Teddington, Plenum Press, 1966, pp.145-152.

43. Parks, P.C. "Lyapunov redesign of model-reference adaptive control systems", IEEE Transactions on Automatic control, Vol. AC-11, No.3, July 1966, pp.362-367.

44. Phillipson, P.H. "Design methods for model-reference adaptive systems", Mechanical Engineering, 1968-1969, Vol. 183, Part 3, No.35, pp.695-700.

45. Gilbart, J.W. et al "Improved convergence and increased flexibility in the design of model-reference adaptive control systems", Proc. 9th IEEE Symp. Adaptive processes, Decision and Control, December 1970, pp.IV 3.1-3.10.

46. Monopoli, R.V. et al "Model reference adaptive control based on Lyapunor-like techniques", Proc. 2nd IFAC Symp. System sensitivity and adaptivity, August 1968, pp.F24-F36.

47. Currie, M.G. and Stear,E.B. "State space structure of model reference adaptive control for a noisy system", Proc. 2nd Asilomar Conf. Circuits and Systems, 1968, pp.401-405.

48. Osburn, P.V., Whitaker, M.P. and Kezer, A. "New developments in the design of model-reference adaptive control systems", IAS Paper No. G1-39.

49. Porter, B. and Tatnall, M. "Performance characteristics of multivariable model-reference adaptive systems synthesized by Lyapunor's direct method", Int. Y. Control, Vol.10, No.3, pp.241-257.

50. Truxal, T.G. "Control Systems Synthesis", McGraw-Hill, New York, 1955.

Appendix A

PERFORMANCE CRITERION EVALUATION

Consider eqn. A.1

$$A'R + RA = -W \tag{A.1}$$

Denote the characteristic polynomial of A by

$$\Delta(S) = S^n + a_n S^{n-1} + \text{----} + a \tag{A.2}$$

Assume that A is similar to a matrix of companion form, i.e. a non-singular matrix T exists so that

$$TAT^{-1} = C \tag{A.3}$$

where C has the form

$$C = \left[\begin{array}{c|ccccc} 0 & & I & & & \\ \hline -a_1 & -a_2 & -a_3 & \text{----} & -a_n \end{array}\right] \tag{A.4}$$

using eqn. A.3, eqn. A.1 transforms to:

$$C'Y + YC = P \tag{A.5}$$

where $$P = -(T^{-1})' \; W \; T^{-1} \tag{A.6}$$

$$Y = (T^{-1})' \; R \; T^{-1} \tag{A.7}$$

the matrices P and Y are symmetric.

Writing eqn. A.5 as

$$U + V = S \tag{A.8}$$

the matrices U and V take the simple form

$$u_{ij} = \begin{bmatrix} -a_1 y_{nj} & i = 1;\ j = 1, \ldots n \\ y_{i-1,j} - a_i y_{nj} & i = 2, \ldots n\ ;\ j = 1, \ldots n \end{bmatrix} \quad (A.9)$$

$$v_{ij} = \begin{bmatrix} - a_1 y_{in} & i = 1, \ldots n,\ j = 1 \\ y_{i,j-1} - a_j y_{in} & i = 1, \ldots n;\ j = 2, \ldots n \end{bmatrix} \quad (A.10)$$

Eqn. A.8 represent n^2 component equations, these equations are reduced to:

$$\sum_{j=\sigma}^{\theta} (-1)^{j+1}(u_{jk}+v_{jk}) = \sum_{j=\sigma}^{\theta} (-1)^{j+1} s_{jk} \quad i = 1,2 \ldots (2n-1) \quad (A.11)$$

where $k = i - j + 1$. the limits are given by:

$$\sigma = \begin{bmatrix} 1 & 1 \leq n \\ i + 1 - n & i > n \end{bmatrix} \quad (A.12)$$

$$\theta = \begin{bmatrix} i & i \leq n \\ n & i > n \end{bmatrix} \quad (A.13)$$

Denoting the right-hand side of eqn. A.11 by h_i, the equations may be rewritten

$$\begin{aligned} -2a_1 y_{n_1} &= h_1 \quad (A.14) \\ -2a_3 y_{n1} + 2a_2 y_{n2} - 2a_1 y_{n3} &= h_3 \\ \text{----------} & \\ 2(-1)^n (y_{n,n-1} - a_n y_{nn}) &= = h_{2n-1} \end{aligned}$$

this system may be written more concisely by defining an n xn matrix $H(z,n)$ on a general $(n + 1)$-tuple z by

$$H(z,n) = \begin{bmatrix} z_1 & 0 & 0 & 0 & 0 \\ z_3 & z_2 & z_1 & 0 & 0 \\ z_5 & z_4 & z_3 & z_2 & \\ \hline 0 & z_{n+1} & z_n & z_{n-1} & z_{n-2} \\ 0 & 0 & 0 & z_{n+1} & z_n \end{bmatrix} \qquad \text{(A.15)}$$

and by defining $2g_i = h_{2i-1}$ $(i = 1, \ldots n)$ (A.16)

Eqn. A.14 becomes $H(c,n)\lambda = g$ (A.17)

where $c' = (a_1, a_2 \ldots a_n, 1)$ (A.18)

$\lambda' = \{-y_{n1}, y_{n2}, \ldots (-1)^n y_{nn}\}$ (A.19)

Eqn. A.19 yields the last row and the last column of y. i.e. $y_r(n)$ and $y_c(n)$, the remainder may be simply generated from other vector using eqn. A.5

$$y_r(j-1) = p_r(j) + a_j\, y_r(n) - C'\, y_r(j) \quad j = n, \ldots 2 \qquad \text{(A.20)}$$

$$0 = p_r(1) + a_1 y_r(n) - C'\, y_r(1)$$

where $y_r'(i) \rightarrow$ ith row of y

$y_c(j) \rightarrow$ jth col of y.

The last equation provides a check. The matrix y should be symmetric, which provides another consistency check.

Appendix B

OPTIMIZATION TECHNIQUE

This program finds the minimum of a multivariable unconstrained, nonlinear function:

Minimize $F(X_1, X_2, \ldots, X_N)$

The procedure is based on the work by J.A. Nelder and R. Mead[23]. This simplex method adapts itself to the local landscape, using reflected, expanded, and contracted points to locate the minimum. Unimodality is assumed and thus several sets of starting points should be considered. Derivatives are not required. The algorithm proceeds as follows:

1) A starting point, $\underline{X}_1$, is selected.

2) A starting "simplex" is constructed consisting of the starting point and the following additional points:

$$\underline{X}_j = \underline{X}_1 + \underline{\xi}_j \quad , \quad j = 2, 3, \ldots, N+1$$

where $\underline{\xi}_j$ is determined from the following table:

j	$\xi_{1,j}$	$\xi_{2,j}$	...	$\xi_{N-1,j}$	$\xi_{N,j}$
2	p	q	...	q	q
3	q	p	...	q	q
.	.	.		.	.
.	.	.		.	.
.	.	.		.	.
N	q	q	...	p	q
N+1	q	q	...	q	p

N = total number of variables

a = side length of simplex

$$p = \frac{a}{N\sqrt{2}}\left(\sqrt{N+1} + N-1\right)$$

$$q = \frac{a}{N\sqrt{2}}\left(\sqrt{N+1} - 1\right)$$

3) Once the simplex is formed, the objective function is evaluated at each point. The worst point (highest value of objective function) is replaced by a new point. Three operations are used--reflection, contraction, and expansion. A reflected point is located first as follows:

$$X_{i,j}\ (\text{reflected}) = \bar{X}_{i,c} + \alpha(\bar{X}_{i,c} - X_{i,j}\ (\text{worst}))$$

$$i = 1, 2, \ldots, N$$

where α is a positive constant.

$\bar{X}_{i,c}$ are the centroid coordinates of all points excluding the worst point and are calculated from the following:

$$\bar{X}_{i,c} = \frac{1}{K-1}\left|\sum_{j=1}^{K} X_{i,j} - X_{i,j}\ (\text{worst})\right|, \quad i = 1, 2, .., N$$

$$K = N+1$$

4) If the reflected point has the worst objective function value of the current points, a contracted point is located as follows:

$$X_{i,j}\ (\text{contracted}) = \bar{X}_{i,c} - \beta(\bar{X}_{i,c} - X_{i,j}\ (\text{worst}),$$

$$i = 1, 2, \ldots, N$$

where β lies between 0 and 1.

If the reflected point is better than the worst point but is not the best point, a contracted point is calculated from the reflected point as follows:

$$X_{i,j}\ (\text{contracted}) = \overline{X}_{i,c} - \beta(\overline{X}_{i,c} - X_{i,j}\ (\text{reflected})\ ),$$

$$i = 1, 2, \ldots, N$$

The objective function is now evaluated at the contracted point. If an improvement over the current points is achieved, the process is restarted. If an improvement is not achieved, the points are moved one half the distance toward the best point:

$$X_{i,j}\ (\text{new}) = (X_{i,j}\ (\text{best}) + X_{i,j}\ (\text{old})\ )/2$$

$$i = 1, 2, \ldots, N$$

The process is then restarted.

5) If the reflected point calculated in step 3) is the best point, an expansion point is calculated as follows:

$$X_{i,j}\ (\text{expansion}) = \overline{X}_{i,c} + \gamma(X_{i,j}\ (\text{reflected}) - \overline{X}_{i,c})$$

$$i = 1, 2, \ldots, N$$

where γ is a positive constant. If the expansion point is an improvement over the reflected point, the reflected point is replaced by the expansion point and the process restarted. If the expansion point is not an improvement over the reflected point, the reflected point is retained and the process restarted.

6) The procedure is terminated when the convergence criterion is satisfied or a specified number of iterations has been exceeded. A flow sheet illustrating the procedure is given in Figure B.1.

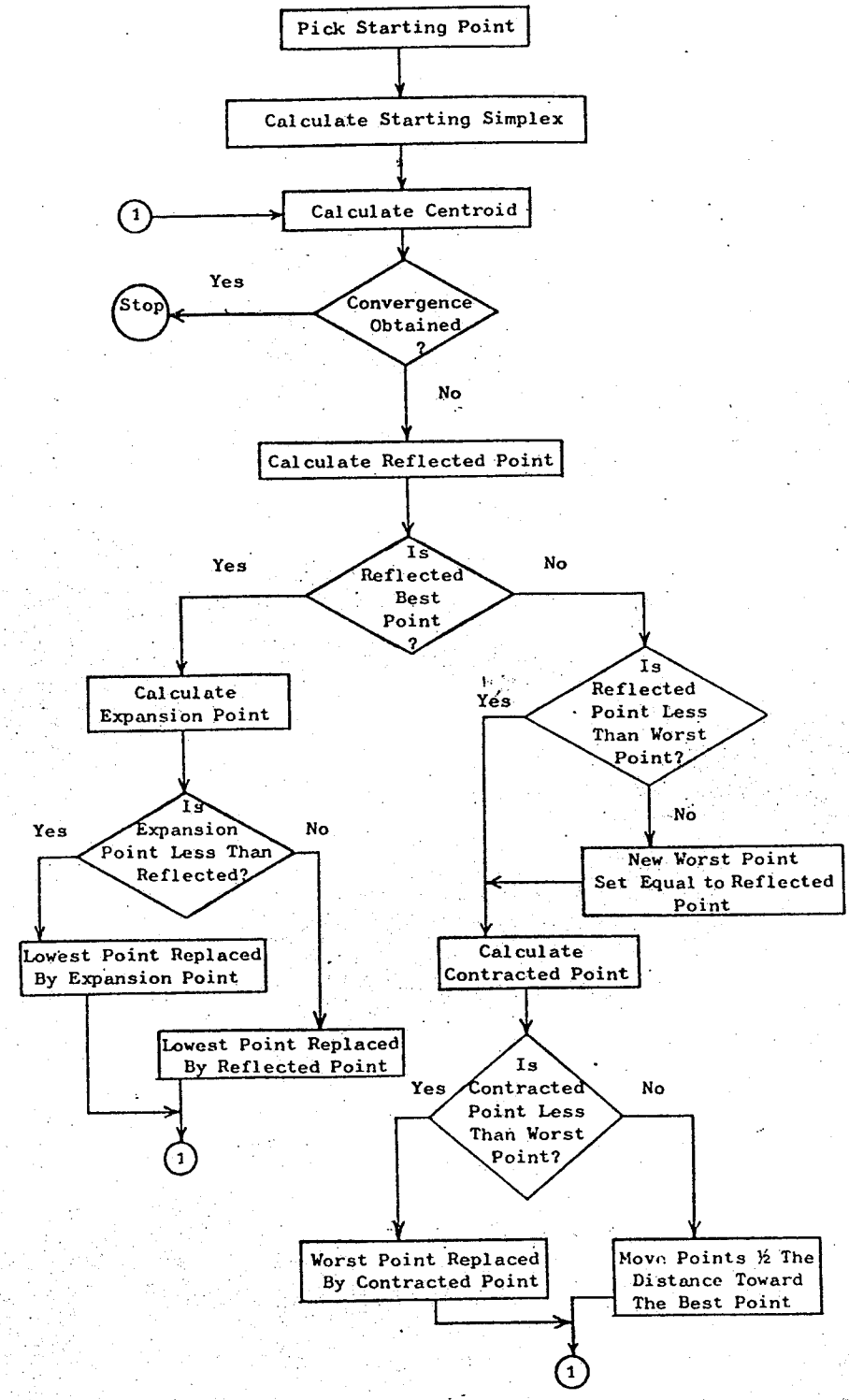

Fig. B.1 Nelder and Mead (Nelder algorithm) logic diagram